Behavior of Aqueous Electrolytes in Steam Cycles

The Final Report on the Solubility and Volatility of Copper(I) and Copper(II) Oxides

Product ID #

Final Report, May 2004

EPRI Project Manager
D.B. Dooley

EPRI • 3412 Hillview Avenue, Palo Alto, California 94304 • PO Box 10412, Palo Alto, California 94303 • USA
800.313.3774 • 650.855.2121 • askepri@epri.com • www.epri.com

DISCLAIMER OF WARRANTIES AND LIMITATION OF LIABILITIES

ORGANIZATION(S) THAT PREPARED THIS DOCUMENT

Research Contractor Company Name (add others on lines below if more than one)

ORDERING INFORMATION

Requests for copies of this report should be directed to the EPRI Distribution Center, 1355 Willow Way, Suite 2478, Concord, CA 94520, Pleasant Hill, CA 94523, (800) 313-3774.

CITATIONS

This report was prepared by

Oak Ridge National Laboratory
P.O. Box 2008
Oak Ridge, TN 37831-6110

Principal Investigator
D. A. Palmer

Authors
D.A. Palmer
P. Bϑnϑzeth
J.M. Simonson

This report describes research sponsored by EPRI

The report is a corporate document that should be cited in the literature in the following manner:

Behavior of Aqueous Electrolytes in Steam Cycles: The Final Report on the Volatility and Solubility of Copper(I) and Copper(II) Oxides, EPRI, Palo Alto, CA: 2004. TR-.

REPORT SUMMARY

Measurements were completed on the solubility of cupric and cuprous oxides in liquid water and steam at controlled pH conditions from 25 to 400°C (77 to 752°F). The results of this study have been combined with those reported from this laboratory in two previous EPRI reports to provide a complete description of the solubility of these oxides and the speciation of copper dissolved in liquid water and steam as a function of oxidation state, temperature, pH, and in the case of steam, pressure. These constitute the first set of reliable data for cuprous oxide solubility over this range of conditions. For the more intensively studied CuO case, agreement was found between our results and those of previous studies of its solubility in steam, whereas only partial agreement was evident for its solubility in liquid water. For both oxides this disagreement often amounted to orders of magnitude. The solubility of cuprous oxide is somewhat lower than that of CuO at ambient conditions, except as very high pH. However, by 350°C (662°F), Cu_2O is the more soluble phase. At 100°C (212°F) and above, the logarithm of the solubility of both phases decreases linearly with increasing pH to a minimum value then sharply increases linearly with pH. In other words, above 100°C the solubility of both oxides become highly pH dependent. In fact at constant pH during startup, very high copper concentrations can be reached in the boiler water, more than an order of magnitude above those at ambient or operating temperatures. The enhancing effect of added ammonia on the solubility of both oxides is most significant at low temperatures and is much greater for cuprous oxide. Consequently, the mobility of copper is affected significantly under AVT startup conditions. The oxidation of copper metal and presumably cuprous oxide by addition of air-saturated makeup water can lead to much higher copper concentrations than equilibrium with cupric oxide would allow, but the presence of both copper metal and cuprous oxide provides an effective scavenger for oxygen, even at room temperature, with copper levels consistent with those in equilibrium with cuprous oxide. The solubilities of Cu_2O and CuO in steam are quite similar and are virtually temperature independent at the 1 to 2 ppb level, respectively, although at supercritical conditions, both solubilities increase with increasing pressure and temperature. The species that partition to the vapor are believed to be the neutrally charged molecules, $Cu(OH)^0$ and $Cu(OH)_2{}^0$, for the reduced and oxidized forms, respectively, and their concentrations in the vapor are therefore independent of the pH of the liquid water phase from which they originate.

Background

Recent analyses of copper alloy corrosion even in high purity feed-water have shown that there is poor scientific understanding of copper corrosion, release and transport. Indeed, under reducing conditions where cuprous oxide is the dominant surface phase on copper condensers and low-pressure heaters, there are no well-documented data on its solubility at any temperature. Thus, in

accordance with the EPRI initiative of Program Copper, the laboratory-scale experimental research project was extended from solubility measurements of cupric oxide to those of cuprous oxide from ambient, or startup, conditions to high temperatures (350°C or 662°F; 400°C or 752°F for steam) over a range of pH and pressures.

Objectives

- The principal objective is to quantify the equilibrium solubility of cuprous and cupric oxides over the range of temperature, pH, and pressure relevant to the water-steam cycle of fossil-fired stream generators.
- A rigorous thermodynamic model will be created that allows prediction of the fate of copper in water and steam under conditions from startup to normal operation, as well as under conditions that mimic departures from normal operating conditions.
- An additional aspect of this work is to identify, where possible, the effects of treatment chemicals and impurities on the transport of copper in the water-steam circuit of fossil-fired units.

Approach

The approach taken in this research is based on experimental knowledge gained in earlier investigations within Program Copper in this laboratory, as well as in other similar solubility studies of other metal oxides, such as ZnO, NiO, Fe_3O_4, $ZnCrO_4$ and $CoCrO_4$. Various experimental techniques that provide complementary information have been applied to this problem, including the use of flow-through cells, batch-style autoclaves and the volatility (liquid water – steam equilibration) apparatus, all of which have inert wetted surfaces to mitigate surface adsorption and trace metal contamination. Most importantly, the water chemistry is strictly controlled and monitored to ensure continuous knowledge of the experimental parameters that influence dissolution. The solubility results are treated based on the experimentally-derived speciation of dissolved copper in solution. Finally, these results are compared, where possible, with previously published experimental and plant data.

Results

The following highlights summarize the experimental conditions, results and conclusions of this project.

- Further measurements of the solubility of Cu_2O were made with a dynamic technique, passing either liquid water or steam containing pH control agents (NH_3, NaOH or CF_3SO_3H) through a bed of cuprite from ambient temperatures to 350°C (662°F) and fixed pressures. Additional pH buffers were employed at low temperatures (25-75°C) where their interactions with dissolved copper are minimal.
- Further flow-cell measurements of the solubility of CuO were carried out to strengthen the database already complied in this research program. The new data also reaffirmed the unusual speciation of copper(II) in solution compared to other divalent transition metals.

- The solubility minimum is only 0.02ppb at 25°C for Cu_2O at a pH of about 9.2 and rising to 0.7ppb at 100°C (pH_t = 8.2), which is still a factor of two less than the corresponding value for CuO. The solubility of Cu_2O reaches 7ppb at the minimum by 350°C where it is four orders of magnitude lower than reported in the only other investigation in the literature (Var'yash, 1989).
- Although the solubility of both oxides in water exhibit broad minima with respect to pH at temperatures ≤ 75°C, at higher temperatures the minima are sharp (V shaped) such that the solubility becomes highly pH dependent. As a consequence, during startup at a fixed pH, the equilibrium concentrations of copper(I) and (II) pass through maxima at about 250 and 200°C (482 and 392°F), respectively, that are up to 100 times higher than the starting concentrations. The maxima decrease with increasing pH.
- The effect of added ammonia on the solubility of CuO and Cu_2O, and the volatility of Cu_2O is greatest at low pH and low temperatures, becoming negligible above 200°C (392°F), but extends to much higher pH than reported elsewhere. The effect on Cu_2O solubility is significantly greater than that for CuO.
- The solubility of Cu(II) in steam, where it exists exclusively as $Cu(OH)_2^0$, is nearly independent of temperature (250 – 350°C, 482 – 662°F) at saturation vapor pressures (580 – 2400psi). However, above 350°C into the supercritical region of water, increasing pressure causes a marked increase in the solubility of CuO. The observed solubilities of CuO in steam are entirely consistent with the reported values for supercritical steam by Stewart and Pocock (1963).
- The solubility of Cu_2O in steam is virtually identical to that of CuO to temperatures up to 350°C (662°F). The average solubility is (2.6 ± 1.2)ppb compared to (1.4 ± 0.6)ppb for CuO. The solubilities for Cu_2O are at least compatible with the limited number of supercritical measurements of Pocock and Stewart (1963).
- The partitioning constant for $Cu(OH)^0$ calculated for a solution in contact with Cu_2O is similar to that of $Cu(OH)_2^0$ at low temperatures, but is significantly smaller at high temperatures.

EPRI Perspective

EPRI Project Manager should compose this section. Apply EPRI RS Text Style.

Keywords

Power plant availability
Power plant reliability
Steam turbines
Copper
Solubility
Volatility
Partitioning

ABSTRACT

The equilibrium solubilities of cuprous and cupric oxides were determined experimentally in liquid water and steam using two flow-through reactor columns. In general, these measurements were carried out at 25, 50 and 75°C (77, 122 and 167°F) in one apparatus and from 100 to 400°C (77 – 662°F) at 50°C intervals in another where pH was buffered by a variety of chemical agents. The solids recovered from the experiments were characterized to ensure that no changes in composition or morphology had occurred during the experiments. In the study of Cu_2O solubility, metallic copper was present to preserve the Cu(I) oxidation state. Qualitative measurements were also made of the solubility-enhancing effects of the pH buffers used, particularly those of ammonia. For ammonia these effects were strongest at low temperatures, and extended to higher pH values than previously recognized. For other buffers in anionic form, such as acetate, phosphate, borate, etc., these form complexes with copper(I) and (II) that become stronger with increasing temperature, as do those with anionic contaminants, such as chloride and sulfate.

The solubilities of both copper(I) and (II) oxides in steam were found to be independent of temperature and pH in the range 200 – 400°C (392 – 662°F), although the solubility did increase with increasing pressure at supercritical conditions. The solubilities of both oxides were on the order of one to several ppb. This behavior is readily understood in that only the neutral hydroxide forms of these metals, $Cu(OH)^0$ and $Cu(OH)_2^0$, respectively, are expected to exist in the vapor phase and their concentrations are independent of pH in the co-existing liquid water phase. On the other hand, the partitioning constants for both species show strong pH dependencies because the solubilities of both oxides in water are strongly pH dependent. The latter effect is attributable to Cu^+ and $Cu(OH)_2^-$ being the dominant forms of copper(I) in solution, whereas for the copper(II) system, $Cu(OH)^+$ and $Cu(OH)_3^-$ are the dominant forms at elevated temperatures (*i.e.*, ≥ 100°C). The solubility of Cu_2O in water is less than that of CuO at low temperatures, except at very high pH, but becomes somewhat higher than that for CuO at high temperatures. Comparison of the current data for Cu_2O with those from the only previously available dataset showed in near-neutral solutions the new results are lower by about four orders of magnitude by 350°C (662°F). Good agreement was found between the CuO solubility results in steam determined in this laboratory with those of Pocock and Stewart (1963). An explanation was found for the higher solubilities reported by Hearn *et al.* in 1969.

Equations describing the solubilities of both oxides in liquid water as a function of temperature and pH have been developed based on the current data. Similar equations have been derived for the solubilities in steam as functions of pressure or water density.

CONTENTS

LIST OF FIGURES

LIST OF TABLES

1
BACKGROUND INFORMATION

The report on the "State of Knowledge of Copper in Fossil Plant Cycles" published in 1997 [1] set the stage for the establishment of "Program Copper" by EPRI. A number of reports have since been published within this program that have advanced understanding of copper chemistry both from the standpoint of the underlying science and its practical applications to plant operations [2-10]. The current work is an extension of the two previous studies [3,10] in this laboratory on the solubility and volatility of copper and includes new data mainly on the cuprous oxide system. The following discussion alludes briefly to the current understanding of copper dissolution, transport and deposition around the water-steam cycle of fossil plants with mixed metallurgy (copper) feedwater systems, and to the status of current scientific literature on aqueous copper chemistry with emphasis on copper(I).

Fossil-fired plants with mixed-metallurgy feedwater systems containing copper have experienced problems associated with deposition in the boiler, superheater and HP turbine blades. The copper limit at the economizer inlet for AVT under normal operating conditions is 2 ppb [4]. Interestingly, 2 ppb corresponds approximately to the minimum solubility of CuO and Cu_2O in water measured in our laboratory studies at near ambient temperatures over the pH range 9-10 [3,10]. Copper enters the cycle with the feedwater [6] and its concentration is largely a function of the ORP (oxidizing-reducing potential). Under reducing conditions (≤ -300mV), copper alloy surfaces are protected by a relatively thin, impervious layer of cuprous oxide [7]. However, ORP values > 0mV correspond to oxidizing conditions and the formation of thicker, more porous layers of cupric oxide [7], which give rise to more rapid dissolution kinetics and the increased likelihood of spallation generating suspended particulates [4]. Shutdowns without nitrogen blanketing also permit oxidation of metallic copper deposited in the boiler and can lead to a surge in copper carryover to the superheater during startup. Copper eventually finds its way from the superheater to the high-pressure turbine blades due to its relatively high solubility in steam, exacerbated by cycling and over-pressurization of units with mixed metallurgy [4]. Shields *et al.* [6] suggested that a synergistic effect exists between the solubility of copper and the presence of oxygen and ammonia at low temperatures due to the formation in solution of cupric amine complexes. However, Stodola *et al.* [11] calculated that the ammonia complexes are too weak to affect the copper concentrations significantly, even at low temperatures where these complexes are known to be strongest. The latter authors concluded that the presence of carbon dioxide in the feedwater and the water in an unprotected boiler during shutdown has the effect of decreasing the pH sufficiently to greatly enhance the solubility of copper oxide. However, the study by Stodola *et al.* considered only ammonia complexes with Cu^{2+}. Our previous solubility study [3] with CuO and the newer data presented here for Cu_2O give strong support for the existence of mixed

hydroxo-ammonia complexes {*e.g.*, $Cu^{II}(OH)_x(NH_3)_y^{2-x}$ and $Cu^{I}(OH)_x(NH_3)_y^{1-x}$} that persist at high pH relevant to boiler start-up conditions. The latter complexes are much stronger than the former, but their effects diminish with increasing temperature.

Plant measurements of copper (particulates and dissolved) levels in steam were shown by Howell and Weisser [12] to be affected by precipitation of copper in the sampling lines, indicating that copper transport might be underestimated when sampling the steam cycle. It should be noted that precipitation of copper oxide was also observed in this study (see discussion below), particularly when sampling copper(I) solutions (liquid and steam phases). As the sampling lines in the experimental rigs used in our study are made from platinum/rhodium alloys, precipitation in this case cannot be due to reduction on the walls of the tubing.

This discussion is focused on the thermodynamics of the dissolution and precipitation of CuO and Cu_2O, and therefore such issues as deposition of copper due to reduction on reducing metal surfaces [1] or adsorption of ionic copper(II) species, particularly copper cations (Cu^{2+}, $Cu(OH)^{+}$ and Cu^{+}) onto metal oxide surfaces [13,14] are not considered here, although these processes provide tangible sinks for copper in fossil plant water/steam cycles. Furthermore, the negative surface charge on metal oxides increases with temperature and persists to lower pH values [15, 16]. Consequently, experiments with Ca^{2+} adsorption on rutile (TiO_2) surfaces confirm that this interaction becomes so strong at elevated temperatures that it even begins at pH values below the pH of zero-net-surface-charge (pH_{zpc}) where the surface would otherwise be positively charged [17]. The interaction of transition metal cations with metal oxides such as magnetite and goethite is stronger than for Ca^{2+}, and is even enhanced by the presence of organic ligands [14]. Therefore, surface adsorption interactions within the boiler at operating conditions could lead to substantial hideout of copper and may provide a path for subsequent reduction of the adsorbed copper by the underlying metal oxide surface.

1.1 Previous Investigations of the Solubility of Copper Oxide

Lvov *et al.* [2] constructed Pourbaix diagrams showing that cupric oxide is the stable form of copper in equilibrium with air-saturated aqueous solutions at least from ambient to 300°C (572°F). The stability of copper(II) extends to deoxygenated aqueous solutions that do not contain added reducing agents. Lvov *et al.* also show, based on available hydrolysis and ammonia complexation constants, that at sub-ppm levels of ammonia, copper(II) amine complexes are not major species at any condition, although again it should be mentioned that complexes of the type $Cu^{II}(OH)_x(NH_3)_y^{2-x}$ were not considered because no corresponding thermodynamic data were available. The stability field of copper(I) with respect to ORP is narrow and in the current experiments it was maintained by using deoxygenated solutions and added copper metal to maintain a controlled, slightly reducing ORP with the Cu/Cu_2O couple.

Two substantial solubility investigations with apparently disparate results were published in the 1960's [18, 19] dealing largely with the solubility of CuO in superheated steam. The latter also provided data on CuO solubility in "pure" water from ambient to the critical temperature of

water. Hearn *et al*. [19] claimed that the small amount of solid oxide exposed to a relatively fast flow of steam in the former experiments [18] may have led to non-equilibrated results. They also sited the presence of corrosion in the reactor used by Pocock and Stewart [17] as providing a possible sink for copper deposition. Pocock and Stewart also reported limited data for the solubility of Cu_2O in superheated steam. Two more recent studies of CuO solubility in liquid water at sub-critical conditions [20, 21] also led to different solubilities as a function of temperature and pH (*i.e.*, different speciation schemes for the soluble hydrolyzed copper(II) species). Var'yash [22] also reported the only comprehensive study of Cu_2O solubility over a wide range of pH to 350°C (662°F). Petrov [23] summarized the extensive, if somewhat fragmented, experimental studies of copper solubility performed in the former Soviet Union since the early 1960's, almost all of which involved cupric oxide and hydroxide. Most of these investigations used dynamic, flow-through techniques. Finally, the computer codes used extensively in the nuclear power industry, MULTEQ [24], and in geothermal applications, SUPCRT97 [25] provide predictions of CuO solubility over a wide range of pH to high temperatures. However, MULTEQ only gives estimates of the solubility of Cu_2O in acidic solutions, presumably due to the lack of reliable experimental data on which to base their extrapolations.

Previous reviews of aqueous copper chemistry indicated that the solubility-enhancing effect of complexing ligands that may be present in boiler water as impurities (*e.g.*, chloride, and acetate) would not be significant, even at elevated temperatures under oxidizing conditions [11, 26]. The formation constants for these $CuCl_n^{2-n}$ and $Cu(CH_3COO)_n^{2-n}$ complexes are not large enough even at ppm levels of these impurities in neutral pH to basic solutions. New measurements of the analogous copper(I) complexes, which are relatively strong [27, 28], also show that these do not contribute significantly to the level of dissolved copper in solution under reducing conditions.

1.1.1 Solubility of Cu_2O in liquid water

The equilibria involved in the dissolution of cuprous oxide in aqueous solutions are:

$$0.5\ Cu_2O + H^+ \Leftrightarrow Cu^+ + 0.5\ H_2O \qquad (1\text{-}1)$$

$$0.5\ Cu_2O + 0.5\ H_2O \Leftrightarrow Cu(OH)^0 \qquad (1\text{-}2)$$

$$0.5\ Cu_2O + 1.5\ H_2O \Leftrightarrow Cu(OH)_2^- + H^+ \qquad (1\text{-}3)$$

The solubility constants associated with these reactions are as follows:

$$K_{s0} = m\{Cu^+\}\gamma\{Cu^+\}/(m\{H^+\}\gamma\{H^+\} \qquad (1\text{-}4)$$

$$K_{s1} = m\{Cu(OH)^0\}\gamma\{Cu(OH)^0\} \quad (1\text{-}5)$$

$$K_{s2} = m\{Cu(OH)_2^-\}\gamma\{Cu(OH)_2^-\}m\{H^+\}\gamma\{H^+\} \quad (1\text{-}6)$$

where $m\{X\}$ represents the molality of species X (moles $kg^{-1}(H_2O)$). The symbol $\gamma\{X\}$ refers to the activity coefficient of species X and is assumed to be unity for neutral molecules such as $Cu(OH)^0$. The activity of water is also assumed to be unity in these expressions due to the relatively low concentrations of solutes employed and taking into account the overall accuracy of the measurements. From equations (1-4) to (1-6) the total copper(I) in solution in molal units, $(Cu^I,molal)_{total}$, is defined as:

$$(Cu^I,molal)_{total} = m\{Cu^+\} + m\{Cu(OH)^0\} + m\{Cu(OH)_2^-\} \quad (1\text{-}7)$$

$$= K_{s0}(m\{H^+\}\gamma\{H^+\})/\gamma\{Cu^+\} + K_{s1} + K_{s2}(\gamma\{Cu(OH)_2^-\})/(m\{H^+\}\gamma\{H^+\}) \quad (1\text{-}8)$$

From the definition of $pH_t \equiv m\{H^+\}$ at temperature, t °C, it follows that the solubility constants can be used to calculate the total dissolved copper(I) in solution as a function of pH_t using calculated values of the activity coefficients. Calculation of activity coefficients is described in the following section. The isothermal solubility profiles shown below were constructed using equation (1-8).

The solubility profile for Cu_2O given by Var'yash [22] is shown in Figure 1-1. In that study, pH_t was apparently measured directly, although no indication was given as to the technique used to make this difficult, but crucial, measurement. Moreover, there is no description of the means used to control the oxidation state of copper, nor were any analyses given of the solid copper oxide recovered after completion of the experiments. Nevertheless, this remains the only complete experimental investigation of this system and is an indication of the inherent difficulty in making these measurements.

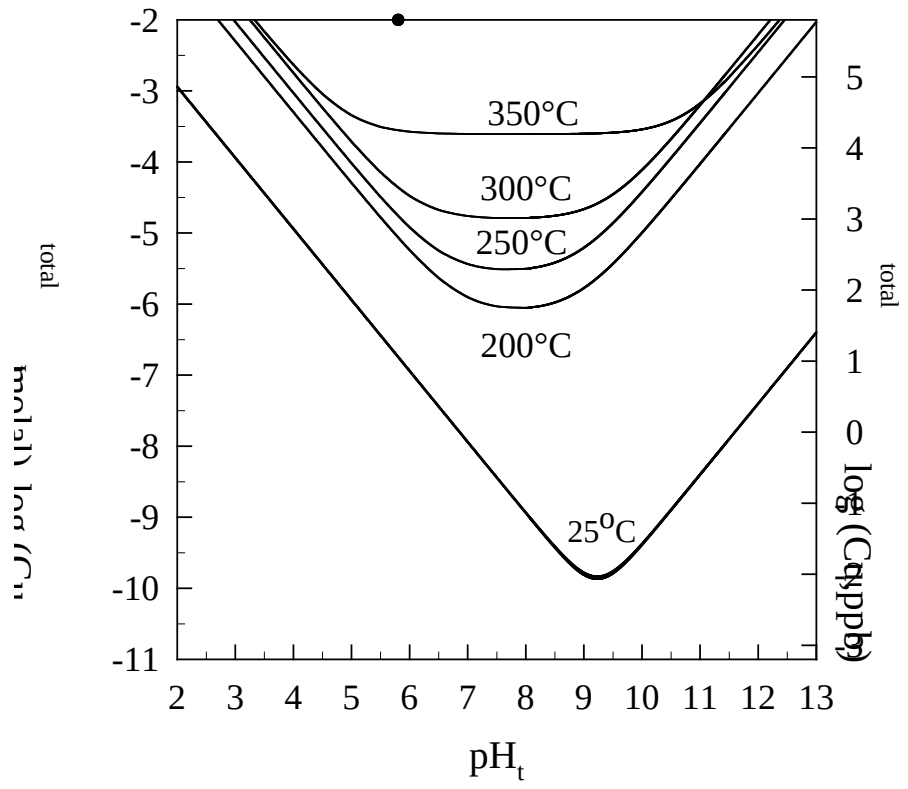

Figure 1-1
Solubility profile for cuprous oxide calculated from the solubility constants reported by Var'yash [22].

Fortunately, the speciation of cuprous ion as a function of pH_t is simple in accordance with equations (1-1) to (1-3) and accordingly there are fewer ambiguities in the interpretation of the data. It can be seen from Figure 1-1 that these date predict that there is a dramatic increase in solubility of Cu_2O with increasing temperature, such that by 350°C (662°F), the solubility minimum, which extends over the range of pH of boiler water, reaches 16 ppm. Such a high solubility is completely incompatible with observed copper levels found in fossil-fired plants. Moreover, as it is the neutrally charged species, $Cu(OH)^0$, that partitions to the vapor [29] and is dominant over the broad solubility minimum predicted by Var'yash [22] at 350°C (662°F), vaporous carryover on the ppm scale would be expected. Copper levels in steam from drum boiler units are generally about 2 ppb, which is in agreement with the measured solubility levels for CuO in steam [3].

Other systematic solubility data for Cu_2O are available only for the equilibrium reaction in acidic solutions, namely for equation (1-1), from the correlations in MULTEQ and SUPCRT97. The predicted log K_{s0} values are compared with those reported by Var'yash in Figure 1-2. The two

computer codes are based on solubility data at 25°C, and use different semi-empirical approximations to extrapolate to higher temperatures with virtually the same results.

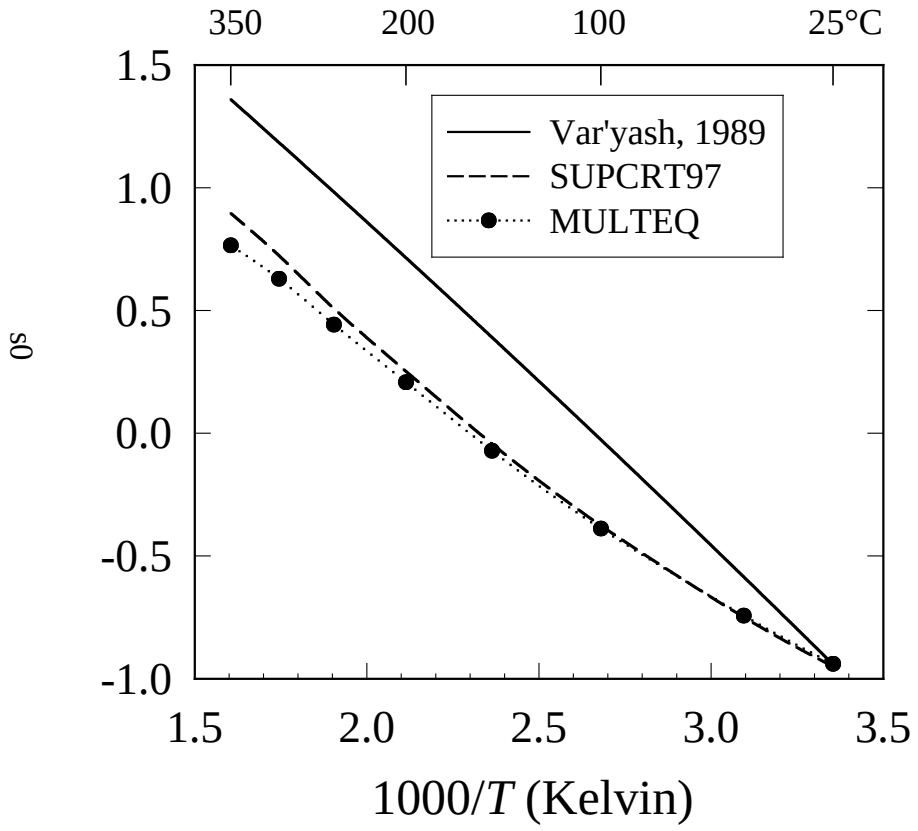

Figure 1-2
Comparison of the log K_{s0} values predicted by the codes MULTEQ [24] and SUPCRT97 [25], and the measured values of Var'yash [22].

However, the calculated solubility of Cu_2O in acidic solutions is about 0.7 log units lower than claimed by Var'yash [22]. Clearly new data are required and more recent innovations in equipment and analytical techniques should allow improvements to be made to the pioneering work of Var'yash.

1.1.2 Solubility of Cu_2O in steam

Pocock and Stewart [18] reported solubility data at 1150°F (621°C) and pressures between 2700 and 4500 psi (186 and 310 bar) with copper(I) concentrations ranging from 0.3ppb to (9.6 ±

1.7)ppb, respectively. The experiments were performed at two pH values, but as mentioned previously and verified for a wide range of systems [3, 29], the solubility in steam is not expected to depend on pH. In this case the copper(I) species dissolved in steam would be the neutral molecule, $Cu(OH)^0$. Moreover, pH is a very difficult variable to define at low density, supercritical conditions. As determined in our previous report on cupric oxide solubility [3], and generally acknowledged, solubility increases with increasing steam density and within the usual accuracy of such data is usually described adequately by the equation of the type:

$$\log (Cu^I, ppb) = a + b \log (\rho_s) \quad (1\text{-}9)$$

where ρ_s represents the density of pure steam. More terms have been included for other systems where the accuracy warrants [30] and more empirical equations are considered for the copper data where lower temperature data have been obtained for the first time. However, in terms of equation (1-9), the density of steam can be varied over a wide range in the supercritical region compared to subcritical conditions where condensation limits the maximum density that can be achieved. The values measured by Pocock and Stewart [18] at supercritical conditions fit this trend.

1.1.3 Solubility of CuO in liquid water

The equilibria involved in the dissolution of cupric oxide in aqueous solutions are as follows:

$$CuO(cr) + 2H^+ \Leftrightarrow Cu^{2+} + H_2O \quad (1\text{-}10)$$

$$CuO(cr) + H^+ \Leftrightarrow Cu(OH)^+ \quad (1\text{-}11)$$

$$CuO(cr) + H_2O \Leftrightarrow Cu(OH)_2{}^0 \quad (1\text{-}12)$$

$$CuO(cr) + 2H_2O \Leftrightarrow Cu(OH)_3{}^- + H^+ \quad (1\text{-}13)$$

$$CuO(cr) + 3H_2O \Leftrightarrow Cu(OH)_4{}^{2-} + 2H^+ \quad (1\text{-}14)$$

The solubility constants associated with each of these equilibria in very dilute solutions are given by the following equations, which are analogues of those given above for Cu_2O:

$$K_{s0} = m\{Cu^{2+}\}\gamma\{Cu^{2+}\}m\{H^+\}\gamma\{H^+\})^2 \quad (1\text{-}15)$$

$$K_{s1} = m\{Cu(OH)^+\}\gamma\{Cu(OH)^+\}(m\{H^+\}\gamma\{H^+\}) \quad (1\text{-}16)$$

$$K_{s2} = m\{Cu(OH)_2{}^0\} \quad (1\text{-}17)$$

$$K_{s3} = (m\{Cu(OH)_3{}^-\}\gamma\{Cu(OH)_3{}^-\})(m\{H^+\}\gamma\{H^+\}) \quad (1\text{-}18)$$

$$K_{s4} = (m\{Cu(OH)_4^{2-}\}\gamma\{Cu(OH)_4^{2-}\})(m\{H^+\}\gamma\{H^+\})^2 \quad (1\text{-}19)$$

where $m\{CuX\}$ represents the molality of the CuX species in solution. The presence of multinuclear copper ions, such as $Cu_2(OH)_2^{2+}$, $Cu_3(OH)_4^{2+}$, *etc*. [31], can be ignored here due to the low concentrations of copper in solution. From equations (1-15) to (1-19) the total copper in solution in molal units, $(Cu^{II},molal)_{total}$, is defined as:

$$(Cu^{II},molal)_{total} = m\{Cu^{2+}\} + m\{Cu(OH)^+\} + m\{Cu(OH)_2^0\} + m\{Cu(OH)_3^-\} + m\{Cu(OH)_4^{2-}\} \quad (1\text{-}20)$$

$$= K_{s0}(m\{H^+\}\gamma\{H^+\})^2 + K_{s1}(m\{H^+\}\gamma\{H^+\}) + K_{s2} + K_{s3}/(m\{H^+\}\gamma\{H^+\})$$

$$+ K_{s4}/(m\{H^+\}\gamma\{H^+\})^2 \quad (1\text{-}21)$$

The previous studies in this laboratory concerned mainly the solubility of CuO in water as a function of pH and temperature [3,10]. Over the temperature range covered in this work, 100 – 350°C (212 – 662°F) the dominant species in solution were $Cu(OH)^+$ and $Cu(OH)_3^-$. A typical solubility profile is shown in Figure 1-3 in which comparisons are also made with other data gathered from the literature. The large discrepancies between the various experimental and computational solubility curves are obvious, amounting to three orders of magnitude in copper concentration and leading to very different speciation schemes. Var'yash [21] only includes the species $Cu(OH)^+$, $Cu(OH)_2^0$ and $Cu(OH)_4^{2-}$ with the neutral species dominating over a wide range of pH. Ziemniak *et al*. [20] reworked the data from Hearn *et al*. [19] to extract the stability of $Cu(OH)^+$, which they assumed to be the dominant copper(II) species in solution; an assumption that was not made by the original investigators. Ziemniak *et al*. [20] reported new experimental results obtained in phosphate solutions and proposed that only $Cu(OH)_3^-$ and copper phosphate complexes were present. MUTLEQ [24] does not include data for the anionic copper hydroxides and is therefore only valid for acidic to near neutral pH solutions. It is clear that our earlier results [3,10] predict the lowest solubility at pH values of interest to the power industry. As mentioned previously, these early results did not include a rigorous treatment of activity coefficients, nor where accurate low temperature data available. The current report remedies this situation, although the basic differences between our results and those obtained by others, as depicted in Figure 1-3 at the maximum temperature studied in our laboratory (350°C), remain. Most of the previous investigations were carried out at lower temperatures.

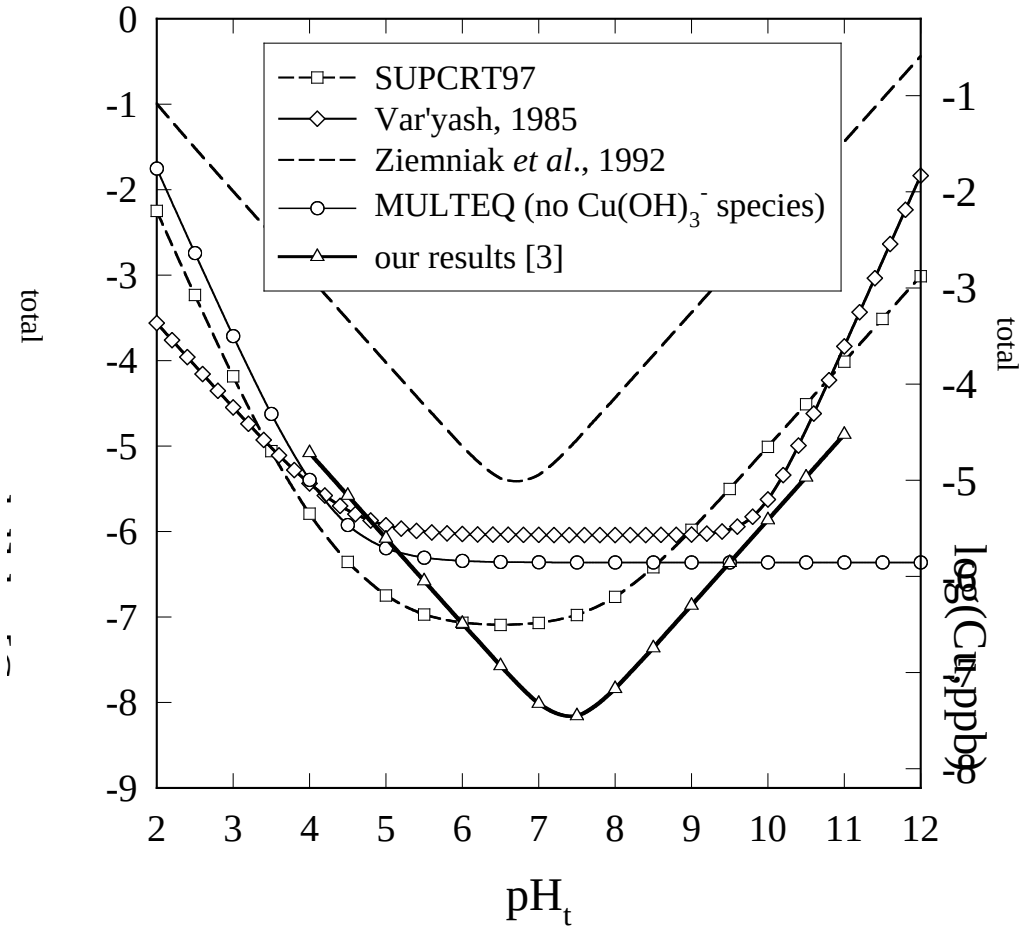

Figure 1-3
Solubility profile for CuO at 350°C (662°F) and saturation vapor pressure, featuring curves generated from SUPCRT97 [25], Var'yash [21], Ziemniak *et al.* [20], MULTEQ [24], and early study [3].

1.1.4 Solubility of CuO in steam

There were two major studies of the solubility of CuO in superheated steam [18, 19] carried out in the 1960's. Hearn *et al.* [19] contended that the small mass of CuO used by Pocock and Stewart [18] compounded by the appearance of corrosion in the vessel used in this previous study, led to lower solubilities being reported. The set of results from the Hearn *et al.* study obtained in water at subcritical conditions were also more than an order of magnitude higher than our corresponding results (see previous section). In the same decade, Martynova *et al.* [32] reported copper levels in steam of 0.1 to 1.6 ppb at 357°C (680°F) using a large-scale water-steam experimental loop. Recently, Sue *et al.* [33] reported four measurements made at supercritical conditions while Daucik and Jensen [34] performed two series of supercritical

experiments also with a laboratory-scale, flow-through apparatus. These results, together with those from our laboratory [3,10] are combined in Figure 1-4 in the form of a plot of the logarithm of the copper concentration in ppb as a function of the logarithm of the density of steam calculated from the IAPWS 95 code [35]. There is obviously a large degree of scatter in these results and there is also uncertainty as to the copper phase used by Hearn et al. [19]. Further discussion of these results is given in Section 4.3.3.

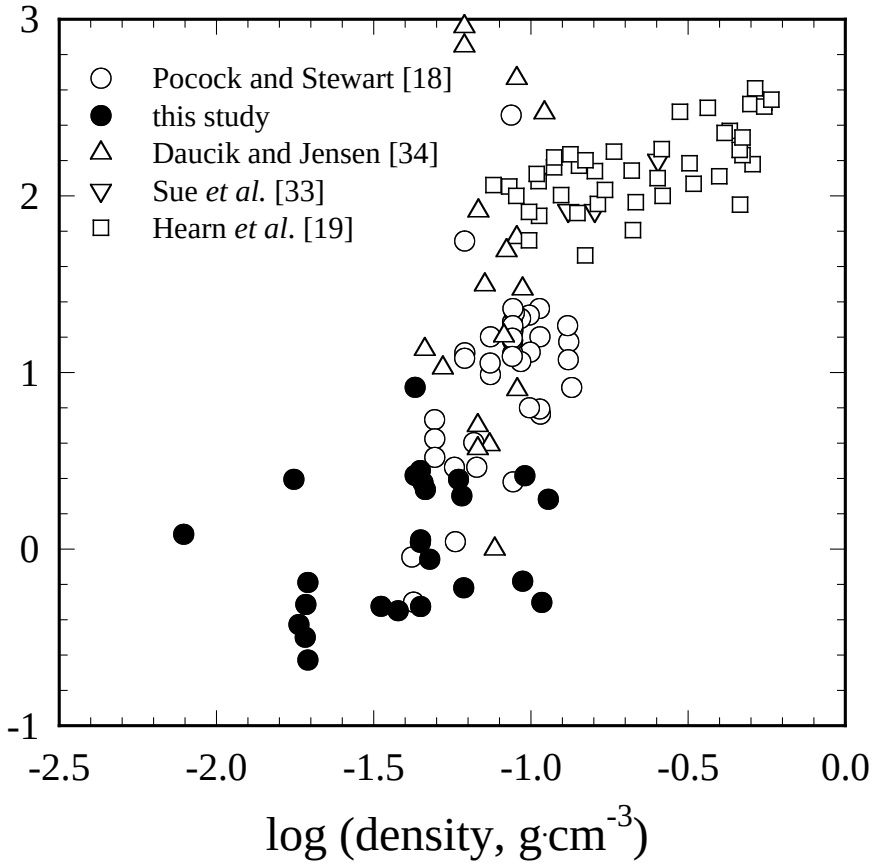

Figure 1-4
Summary of the existing experimental data on the solubility of CuO in steam.

1.2 References

1. R.B. Dooley, B.C. Syrett, T.H. McCloskey, J. Lsou, K.J. Shields, and D.D. Macdonald, "State-of Knowledge of Copper in Fossil Plant Cycles." EPRI Final Report, September 1997, TR-108460.

2. S.N. Lvov, A.V. Bandura, S.M. Ulyanov, X.Y. Zhou, and K. Osseo-Asare, "Corrosion of Cu-Ni-Zn Alloys in Water-Ammonia Power Plant Environments." EPRI Final Report, November 1999, TR-113697.

3. D.A. Palmer, P. Bénézeth, A.Y. Petrov, L.M. Anovitz and J.M. Simonson, "Behavior of Electrolytes in Steam: The Solubility and Volatility of Cupric Oxide." EPRI Report TR-1000455. Palo Alto, CA, Electric Power Research Institute (2000).

4. R.B. Dooley, "Fossil Plant Cycle Chemistry and Steam." *PowerPlant Chemistry*. Vol. 1, No. 6, pp. 5-11 (1999).

5. R.B. Dooley, "Fossil Plant Cycle Chemistry and Steam." in Steam, Water, and Hydrothermal Systems: Physics and Chemistry, Meeting the Needs of Industry. P.R. Tremaine, P.G. Hill, D.E. Irish, and P.V. Balakrisknan, Eds. pp. 35 - 49, Toronto, Canada, September, 1999.

6. K.J Shields, B. Dooley, T.H. McCloskey, B.C. Syrett, and J. Tsou, "Copper Transport in Fossil Units." *PowerPlant Chemistry*. Vol. 1, No. 4, pp. 8-16 (1999).

7. J.E. Castle and P.A. Zhdan, "Copper Alloy Corrosion in High Purity Feedwater." EPRI Report TR-1000456. Palo Alto, CA, Electric Power Research Institute (2000).

8. R.B. Dooley and D.E. Douglas, "Latest Development in Fossil Plant Cycle Chemistry." PowerP*lant Chemistry*. Vol. 2, No. 71, pp. 389-359 (2000).

9. R.B. Dooley, A. Aschoff, K.J. Shields and B.C. Syrett, "Guidelines for Copper in Fossil Plants." EPRI Report TR-1000457. Palo Alto, CA, Electric Power Research Institute (2000).

10. D.A. Palmer, P. Bénézeth, A.Y. Petrov, L.M. Anovitz, and J.M. Simonson. *Behavior of Aqueous Electrolytes in Steam Cycles, The Solubility and Volatility of Copper(I) and Copper(II) Oxides*, EPRI, Palo Alto, CA: December 2001. TR-1003993.

11. J. Stodola, P. Tremaine, V. Binette, and L. Trevani, "Volatility of Copper Corrosion Products in Reactor Primary Conditions." *PowerPlant Chemistry*. Vol. 2, No. 1, pp. 9-13 (2000).

12. D.A. Howell and K. Weisser, "Loss of Copper Sampled from Main Steam." *PowerPlant Chemistry*. Vol. 2, No. 4, pp. 211-212 (2000).

13. K.G. Karthikeyan and H.A. Elliott, "Surface Complexation Modeling of Copper Sorption by Hydrous Oxides of Iron and Aluminum." *Journal of Colloid and Interface Science*. Vol. 220, No. 1, pp. 88-95 (1999).

14. M.A. Ali and D.A. Dzombak, "Effects of Simple Organic Acids on Sorption of Cu^{2+} and Ca^{2+} on Goethite." *Geochimica et Cosmochimica Acta*. Vol. 60, No. 2, pp. 291-304 (1996).

15. M.L. Machesky, D.J. Wesolowski, D.A. Palmer and K. Ichiro-Hayashi, "A Potentiometric Titrations of Rutile Suspensions in NaCl Media to 295°C." *Journal of Colloidal and Interface Science*. Vol. 200, pp. 298-309 (1998).

16. D.J. Wesolowski, M.L. Machesky, D.A. Palmer and L.M. Anovitz "Magnetite Surface Charge Studies to 290°C from in situ pH Titrations." *Geochimica et Cosmochimica Acta.* Vol. 63, pp. 3087-3096 (1999).

17. M.K. Ridley, M.L. Machesky, D.J. Wesolowski, and D.A. Palmer. "Ca(II) Adsorption at the Rutile-Water Interface: A Potentiometric Study in NaCl Media to 250°C." *Geochimica Cosmochimica et Acta.* Vol. 63, 3087-3096 (1999).

18. F.J. Pocock and J.F. Stewart, "The Solubility of Copper and Its Oxides in Supercritical Steam." *Journal of Engineering for Power*. pp. 33-45 (1963).

19. B. Hearn, M.R. Hunt, and A. Hayward, "Solubility of Cupric Oxide in Pure Subcritical and Supercritical Water," *Journal of Chemical and Engineering Data.* Vol 14, pp. 442- 447 (1969).

20. S.E. Ziemniak, M.E. Jones and K.E.S. Combs, "Copper(II) Oxide Solubility Behavior in Aqueous Sodium Phosphate Solutions at Elevated Temperatures." *Journal of Solution Chemistry*. Vol. 29, No. 2, pp. 179-200 (1992).

21. L. Var'yash, "Hydrolysis of Cu(II) at 25-350°C." *Geokhimiya*. No. 7, pp. 1003-1013 (1985).

22. L.N. Var'yash, "Equilibria in the Cu-Cu_2O-H_2O System at 150-450°C." *Geochemistry International*. Vol. 26, pp. 80-90 (1989).

23. A.Y. Petrov, "Copper Solubility and Volatility. Former USSR Studies." International Association for the Properties of Water and Steam Report. 1998.

24. J.H. Alexander and F.H. Howard, "MULTEQ: Equation of an Electrolytic Solution with Vapor-Liquid Partitioning and Precipitation, Volume 2: The Database (Revision 3)." EPRI Final Report, April 1992, NP-5561-CCML.

25. E.L. Shock, D.C. Sassani, M. Willis, and D.A. Sverjensky, "Inorganic Species in Geologic Fluids: Correlations among Standard Molal Thermodynamic Properties of Aqueous Ions and Hydroxide Complexes." G*eochimica et Cosmochimica Acta.* Vol. 61, pp. 907-950 (1997).

26. D.A. Palmer, J.M. Simonson, and D.B. Joyce, "Volatility of Copper." in Interaction of Non-Iron-Based Materials with Water and Steam. B. Dooley and A. Bursik, Eds. pp. 7-1 - 7-17, Piacenza, Italy, June, 1996.

27. Z. Xiao, C.H. Gammons and A.E. Williams-Jones, "Experimental Study of Copper(I) Complexing in Hydrothermal Solutions at 40 to 300°C and Saturation Water Vapor Pressure." *Geochimica et Cosmochimica Acta*. Vol. 62, No. 17, pp. 2949-2964 (1998).

28. W. Liu, D.C. McPhail and J. Brugger "An Experimental Study of Copper(I)-Chloride and Copper(I)-Acetate Complexing in Hydrothermal Solutions between 50 to 250°C and Vapor-

Saturated Pressure." *Geochimica et Cosmochimica Acta*. Vol. 65, No. 17, pp. 2937-2948 (2001).

29. M. Ball, A. Bursik, R.B. Dooley, M. Gruszkiewicz, D.A. Palmer, K.J. Shields and J.M. Simonson, "The Volatility of Impurities in Water/Steam Cycles." EPRI Report TR-1001042. Palo Alto, CA, Electric Power Research Institute (2001).

30. D.A. Palmer, J.P. Jensen and J.M. Simonson, "Partitioning of Electrolytes to Steam and Their Solubility in Superheated Steam", in The Physical and Chemical Properties if Aqueous Systems at Elevated Temperatures and Pressures: Water, Steam and Hydrothermal Solutions. D.A. Palmer, R. Fernandez-Prini and A.H. Harvey, Eds., Elsevier, in press.

31. C.F. Baes and R.E. Mesmer, "The Hydrolysis of Cations." Wiley-Interscience, 1976.

32. O.I. Martynova, Y.F. Samoilov and T.I. Petrova, "The Effect of Ammonia on the Distribution Ratio of Copper Corrosion Products between Water and Steam." *Teploenergetika*. Vol. 16, No. 5, pp. 101-104 (1969).

33. K. Sue, Y. Hakuta, R.L. Smith, Jr., T. Adschiri and K. Arai, "Solubility of Lead(II) Oxide and Copper(II) Oxide in Subcritical and Supercritical Water." *Journal of Chemical and Engineering Data*. Vol. 44, pp. 1422-1426 (1999).

34. K. Daucik and J.P. Jensen, "Solubility of Salts in Superheated Steam: International Collaboration Project 1996-2001." Final Report, November 2001.

35. W. Wagner and A. Pruss, "The IAPWS Formulation 1995 for the Thermodynamic Properties of Ordinary Water Substance for General and Scientific Use." *Journal of Chemical Reference Data*, Vol. 31, No. 2, 387–535 (2002).

2
TEST RIGS AND ANALYTICAL PROCEDURES

2.1 Test Rigs

Four types of experiments have been performed in the past during the complete study of cupric and cuprous oxide solubilities. Three of these apparatus were described in the first EPRI report [1], which focused on cupric oxide, namely, the "high-temperature" flow-through apparatus, the stirred batch reactor and the volatility apparatus. The fourth apparatus consists of a series of three flow-through columns for use at low temperatures (< 100°C) was described in the second EPRI report [2]. Only the flow-through cells were used in the current report, but these will not be described further here.

2.2 Analytical Procedures

In this final phase of the study only two analytical techniques were required for routine analyses of copper, namely, flame atomic absorption (AA) and graphite furnace atomic absorption (GFAA) spectrophotometry. The former technique was described in detail in the last EPRI report [2]. The GFAA technique involved either a single injection of the sample solution with a non-linear calibration curve over the range of standards 25ppb Cu, whereas an almost linear response was obtained with four injections per analysis over the range 13ppb Cu. The latter gave more precise analyses for low ppb samples, but required much longer analysis times and resulted in more rapid degradation of the graphite sample tubes. The GFAA instrument used previously was replaced with a Perkin Elmer Analyst 600 model, which gave more consistent results during each suite of analyses and has a marginally lower detection limit.

2.3 Chemicals

The dilute nitric acid solution (0.2% HNO_3) that was used to stabilize the sample solution and prepare the copper standards was obtained from J.T. Baker (ULTRX II Ultrapure reagent) and was diluted with distilled, deionized (Barnstead, NANOpure four stage system) water and stored in acid-washed polypropylene containers. Pure trifluoromethanesulfonic acid (commonly known as "Triflic acid", CF_3SO_3H) was prepared by vacuum distillation of commercial (Alfa Aesar, 99%) reagent and diluted with distilled, deionized water. Note that this acid was used in the cuprous oxide solubility measurements because it has little, if any, tendency to complex metal ions and is a strong acid that is thermally stable to high temperatures in dilute solutions. The copper standards were prepared from two 1000 ppm AA/ICP calibration solutions (Aldrich

Chemical Co.) by dilution with 0.2% HNO_3. The pH buffers, ammonia (J.T.Baker, ULTREX Ultrapure reagent), sodium monohydrogenphosphate (99.999%, Aldrich Chemical Co.), tris(hydroxymethyl)-aminomethane or "Tris" and 2,2-bis-(hydroxymethyl)-2,2',2"-nitrilotriethanol or "Bis-Tris" (Aldrich Chemical Co.), and boric acid (US Borax) were used without further purification.

All dilutions and solution preparations were performed on a mass basis. The copper sample solutions were collected either in disposable polypropylene/polyethylene syringes or disposable polypropylene sampling containers fitted with polyethylene lids (Aldrich Chemical Co.). Blank tests, in which the containers were exposed to 0.2 % HNO_3 over extended periods of time, showed that no detectable copper release was observed. The NaOH stock solutions were prepared from 50% (by weight) NaOH, stored under argon, and standardized by weight titrations against potassium hydrogenphthalate.

2.4 Characterization of the Solid Oxide Material

The characterization of the original cupric and cuprous oxides used throughout this research was described in the earlier EPRI reports [1,2], which also include similar details on the treated material and run products. One batch of Cu_2O that was treated hydrothermally [2], apparently contained traces of CuCl that could not be detected by XRD, and this solid gave consistently high copper levels that could not be leached out though constant flushing with an acidic feed solution. The resulting solution had a different color to that normally obtained with this feed solution and also gave a white AgCl precipitate when a few drops of silver nitrate solution were added. A subsequent batch from the same manufacturer, but with a different lot number, was free of such highly soluble contaminants.

Cuprous and cupric oxide samples taken from the flow-through reactors after completion of each series of experiment in the current research showed no evidence of any other copper phase that was not present initially.

2.5 References

1. D.A. Palmer, P. Bénézeth, A.Y. Petrov, L.M. Anovitz, and J.M. Simonson. *Behavior of Aqueous Electrolytes in Steam Cycles, The Solubility and Volatility of Cupric Oxide*, EPRI, Palo Alto, CA: November 2000. TR-1000455.

2. D.A. Palmer, P. Bénézeth, A.Y. Petrov, L.M. Anovitz, and J.M. Simonson. *Behavior of Aqueous Electrolytes in Steam Cycles, The Solubility and Volatility of Copper(I) and Copper(II) Oxides*, EPRI, Palo Alto, CA: December 2001. TR-1003993.

3
CUPROUS OXIDE: EXPERIMENTAL RESULTS

The most recent experimental solubility data for cuprous oxide are summarized in Appendices A and B. Listed in these tables are the dates on which the samples were collected, temperature, inlet and outlet pressures, composition and concentration of the feed solution and the corresponding flow rate, and the measured concentrations in parts per million (ppm) or parts per billion (ppb) of copper (after correction for dilution). In all of the high temperature experiments either dilute HNO_3, HCl or NaOH were injected into the flow at the outlet of the tubular reactor at rates that were generally one tenth or less of that of the main inlet feed solution, but this was always sufficient to prevent precipitation of copper in the exit sampling line.

3.1 Thermodynamics of Copper(I) in Solution

The equilibria involved in the dissolution of cuprous oxide in aqueous solutions are:

$$0.5\ Cu_2O + H^+ \Leftrightarrow Cu^+ + 0.5\ H_2O \qquad (3\text{-}1)$$

$$0.5\ Cu_2O + 0.5\ H_2O \Leftrightarrow Cu(OH)^0 \qquad (3\text{-}2)$$

$$0.5\ Cu_2O + 1.5\ H_2O \Leftrightarrow Cu(OH)_2^- + H^+ \qquad (3\text{-}3)$$

The solubility constants associated with these reactions are:

$$K_{s0} = m\{Cu^+\}\gamma\{Cu^+\}/(m\{H^+\}\gamma\{H^+\} \qquad (3\text{-}4)$$

$$K_{s1} = m\{Cu(OH)^0\}\gamma\{Cu(OH)^0\} \qquad (3\text{-}5)$$

$$K_{s2} = m\{Cu(OH)_2^-\}\gamma\{Cu(OH_2)\}m\{H^+\}\gamma\{H^+\} \qquad (3\text{-}6)$$

where $m\{X\}$ represents the molality of species X ($moles \cdot kg^{-1}(H_2O)$). The symbol $\gamma\{X\}$ refers to the activity coefficient of species X and is assumed to be unity for neutral molecules such as $Cu(OH)^0$.

3.2 Calculation of pH

The equilibrium constant for the dissociation of water, K_w, in the MULTEQ code is based solely on the equation of Marshall and Franck [1].

$$H_2O \Leftrightarrow H^+ + OH^- \quad (3\text{-}7)$$

$$K_w = m_{H+}\gamma_{H+}m_{OH-}\gamma_{OH-} \quad (3\text{-}8)$$

Although this equation is not recommended at water densities of $<0.4 cm^3 g^{-1}$, this condition is not reached until 373°C (703°F) at saturation vapor pressure. Furthermore, this equation is in very good agreement with the precise experimental data of Busey and Mesmer [2] to 250°C (482°F), after which the relationship of Busey and Mesmer becomes less reliable and is not usable above 300°C (572°F). The Marshall and Franck equation provides estimates of K_w at finite temperatures (T in Kelvin) and pressures (water densities, ρ_w):

$$\log K_w = -4.098 - 3245.2/T + 223620/T^2 - 39840000/T^3 + (13.957 - 1262.3/T + 856410/T^2)\log \rho_w \quad (3\text{-}9)$$

The ionic strength of solutions containing either a strong acid or a strong base is simply equal to the molality of that base, because the dissolved copper(I) species are either singly-charged cations or anions (Eqns. 3-1 and 3-3), respectively, and consequently their presence does not alter the ionic strength. The ionic activity coefficient product, $\gamma_{H+}\gamma_{OH-}$ can be approximated by the mean stoichiometric activity coefficient of NaCl as determined by Archer [3] (this routine requires only knowledge of the ionic strength, pressure and temperature to define the activity coefficient, $\gamma_{H+} = \gamma_{OH-} = \{\gamma_{\pm\,NaCl}^2\}^{½}$). This assumption involving the use of NaCl as the standard electrolyte forms the basis of the MULTEQ code in calculations of all activity coefficients and is particularly relevant here where low concentrations of 1:1 electrolytes are employed.

In the case of solutions containing strong acid, F_3CSO_3H, and strong base, NaOH, at pressures above the saturation vapor pressure of water, the stoichiometric concentration of each acid or base (as given in Appendices A and B) was first corrected for consumption of hydrogen ions caused by Cu_2O dissolution, then in the former case the activity of hydrogen ion was calculated. In the latter case, the value of Q_w (= $m_{H+}m_{OH-}$) was calculated at the ionic strength of feed solution using the appropriate γ_{NaCl}^2 value from Archer [3] so that the free hydroxide concentration was converted to the corresponding pH_t value which in turn was corrected to infinite dilution $pH_t°$ with the same γ_{NaCl} value. For pressures below the saturation vapor pressure of water, all electrolytes can be considered to be strongly associated and hence activity coefficients are set to unity and hence pH_t is considered as only approximate.

For solutions containing ammonia at pressures above the saturation vapor pressure, hydrolysis of aqueous ammonia must be considered.

$$NH_4^+ \Leftrightarrow NH_3 + H^+ \quad (3\text{-}10)$$

The corresponding hydrolysis constant is defined as:

$$K_{NH4} = m_{NH3}\gamma_{NH3}m_{H+}\gamma_{H+}/m_{NH4+}\gamma_{NH4+} \quad (3\text{-}11)$$

The temperature dependence of the hydrolysis constant, K_{NH4}, was given by the expression (t in °C) in MULTEQ that is based largely on the experimental work of Hitch and Mesmer [4].

$$\log K_{Eqn.\ (3\text{-}10)} = -10.0106 + 0.0329798\,t - 7.86471\cdot10^{-5}\,t^2 + 9.68690\cdot10^{-8}\,t^3 \quad (3\text{-}12)$$

The ammonia concentrations in these solutions were then corrected for copper dissolution with the activity coefficients [3] again being used to derive the final $pH_t°$ value.

3.3 Solubility Data for Cuprous Oxide in Water and Steam

3.3.1 Solubility of Cu_2O in water

The solubility data for cuprous oxide in water (containing various pH buffering agents) obtained using the high- and low-temperature, flow-through cells are listed in detail in Appendices A and B, respectively. The results from the previous EPRI report [7] are summarized in Table 3-1 where corrections for the activity coefficients were made. The more recent experimental results from Appendices A and B are given in Table 3-2.

The molal copper concentrations listed in Tables 3-1 and 3-2 were calculated from the mean values at each condition given in Appendices A and B in ppb (parts per million) or ppm (parts per billion) units. The activity coefficients, $\gamma_{\pm}$, in Table 3-1 are values for NaCl taken from the correlations of Archer [4] as described in the previous section. The activity coefficients for the solutes in the steam phase are taken as unity because of the low concentrations involved, the fact that these solutes are considered to be uncharged and there are no reliable activity coefficient measurements or models at these conditions. The $pH_t°$ values refer to the state of infinite dilution (see discussion in section 3-2).

As indicated in the previous report [7] and confirmed later in this section, the Cu_2O solubilities recorded in CF_3SO_3H solutions are all associated with Cu^+ being the dominant form of copper in those solutions. Therefore, according to equation (3-4), values of K_{s0} can be calculated from the $pH_t°$ values, which were corrected for the formation of Cu^+ using the measured molalities of copper and the corresponding activity coefficients. For the experiments carried out at 25 and 50°C (Table 3-2), the solubility at the minimum was below the detection limits of the GFAA apparatus so that the depth of these minima cannot be accessed and hence the possible appearance of $Cu(OH)^0$ as a significant species at low temperatures is not known. At 100°C and above, the concentration at the minimum was measurable and there was no evidence for a "flat" region that would indicate the presence of this uncharged species. Thus, only Cu^+ and $Cu(OH)_2^-$ are detectable species over the range of conditions investigated.

The log $m_{Cu}°$ versus $pH_t°$ isothermal datasets were treated with the ORGLS least-squares fitting routine [8] using Eqns. (3-4) and (3-6) to give values of these two constants at each temperature. These constants are given in Table 3-3. Figures 3-1 to 3-8 depict the experimental results at each temperature and the fits to these data based on the constants in Table 3-3.

Table 3-1
Summary of Previous Results for the Solubility of Cuprous Oxide in Water

T °C	P bar	Ionic Strength molal	$\gamma_{\pm}$	pH_t	$pH_t°$	log m_{Cu}	log $m_{Cu}°$	Sample Series Cu_2O
22	19	0.000993	0.966	3.230	3.237	-3.405±0.013	-3.420	22-1
50	5	0.001005	0.963	3.006	3.022	-3.367±0.008	-3.383	50-1
50	19	0.002645	0.955	2.827	2.847	-2.951±0.019	-2.971	50-2
50	14	0.000980	0.994	3.225	3.228	-3.417±0.007	-3.417	50-3
52	11	0.000191	0.984	3.999	4.006	-4.054±0.023	-4.047	s-50-2
52	10	0.001036	0.963	3.186	3.202	-3.429±0.007	-3.446	s-50-3
100	55	0.00103	0.960	9.248	9.266	-7.011±0.358	-7.028	100-2
100	55	0.00107	0.959	9.365	9.383	-6.991±0.136	-7.010	100-3
100	53	0.000115	0.986	8.304	8.310	-6.785±0.239	-6.791	100-4
100	53	0.000035	0.992	7.791	7.794	-7.502±0.301	-7.505	100-5
100	5	0.000035	0.992	7.801	7.804	-7.664±0.134	-7.667	100-6
100	4	0.001218	0.955	3.245	3.265	-3.196±0.013	-3.216	100-7
100	11	0.001000	0.959	3.159	3.177	-3.535±0.051	-3.553	100-8
100	46	0.002645	0.938	2.789	2.817	-3.015±0.008	-3.043	100-9
100	14	0.000982	0.960	3.233	3.251	-3.416±0.009	-3.434	100-10
100	18	0.000982	0.960	3.254	3.272	-3.386±0.005	-3.404	100-11
102	10	0.03500	0.817	10.715	10.803	-5.724±0.101	-5.812	s-100-1
102	14	0.000191	0.982	3.957	3.965	-4.099±0.050	-4.107	s-100-2
102	20	0.001036	0.959	3.187	3.205	-3.590±0.070	-3.608	s-100-3
150	18	0.000982	0.954	3.449	3.469	-3.209±0.007	-3.229	150-1

Table 3-1
Continued

T °C	P bar	Ionic Strength molal	$\gamma_{\pm}$	pH_t	$pH_t°$	log m_{Cu}	log $m_{Cu}°$	Sample Series Cu_2O
150	21	0.001001	0.954	3.416	3.436	-3.215±0.004	-3.235	150-2
200	53	0.001003	0.949	8.256	8.279	-6.879±0.090	-6.902	200-3
200	53	0.03147	0.587	9.648	9.879	-5.228±0.124	-5.228	200-4
200	53	0.01006	0.858	9.236	9.303	-6.215±0.382	-6.282	200-5
200	53	0.01052	0.856	9.255	9.323	-5.839±0.091	-5.839	200-6
200	53	0.01007	0.858	9.236	9.303	-5.735±0.392	-5.735	200-7
200	25	0.001001	0.947	3.556	3.580	-3.146±0.015	-3.169	200-9
200	37	0.002638	0.919	3.191	3.227	-2.706±0.013	-2.743	200-10
202	35	0.001036	0.947	3.321	3.345	-3.264±0.022	-3.287	200-12
250	53	0.000100	0.981	7.183	7.191	-7.648±0.062	-7.648	250-1
250	53	0.000105	0.980	7.109	7.118	-7.561±0.375	-7.561	250-2
250	53	0.000100	0.981	7.183	7.126	-7.356±0.288	-7.356	250-3
250	54	0.000028	0.988	6.621	6.626	-7.058±0.150	-7.058	250-6
250	55	0.000099	0.980	7.168	7.177	-7.421±0.389	-7.421	250-6
250	42	0.001001	0.939	3.714	3.741	-3.094±0.070	-3.121	250-8
300	97	0.000012	0.990	6.485	6.489	-6.680±0.192	-6.680	300-2
300	93	0.001006	0.934	8.380	8.410	-6.674±0.091	-6.703	300-4
300	94	0.01038	0.816	9.362	9.450	-6.042±0.095	-6.130	300-5
300	100	0.000103	0.972	7.383	7.395	-7.353±0.166	-7.365	300-6
350	170	0.000093	0.960	8.212	8.230	-7.279±0.191	-7.297	350-1

Table 3-2
Summary of New Results for the Solubility of Cuprous Oxide in Water

T °C	P bar	Ionic Strength molal	$\gamma_{\pm}$	pH_t	$pH_t°$	log m_{Cu}	log $m_{Cu}°$	Sample Series Cu_2O
25	1	0.001213	0.962	3.185	3.202	-3.251±0.002	-3.268	25-3
25	1	0.000150	0.986	4.040	4.046	-4.227±0.007	-4.234	25-4
25	1	0.01201	0.895	11.979	12.027	-6.289±0.060	-6.337	25-5
25	1	0.001339	0.960	11.083	11.101	-7.372±0.258	-7.389	25-6
25	1	0.1085	0.772	12.810	12.922	-5.491±0.057	-5.604	25-7
25	1	0.000135	0.987	10.136	10.142	-7.761±0.103	-7.767	25-8
25	1	0.001899	0.953	6.805	6.826	-7.114±0.086	-7.134	25-9
25	1	0.000149	0.986	8.074	8.080	-7.784±0.032	-7.784	25-10
25	1	0.001656	0.956	9.681	9.681	-8.126±0.202	-8.126	25-11
25	1	0.000575	0.972	4.769	4.782	-5.019±0.020	-5.032	25-12
25	1	0.001017	0.965	10.972	10.987	-7.141±0.052	-7.141	25-13
25	1	0.001863	0.953	8.114	8.132	-6.383±0.014	-6.404	25-14
25	1	0.005811	0.812	8.214	8.305	-5.337±0.021	-5.428	25-15
25	1	0.001014	0.965	9.305	9.320	-7.852±0.277	-7.852	25-16
25	1	0.001014	0.965	9.305	9.320	-8.159±0.234	-8.159	25-17
25	1	0.000853	0.968	8.107	8.121	-6.974±0.021	-6.974	25-18
50	1	0.001213	0.960	3.144	3.162	-3.305±0.006	-3.323	50-1
50	1	0.01098	0.894	11.316	11.365	-6.884±0.084	-6.933	50-3
50	1	0.09625	0.772	12.259	12.371	-5.758±0.032	-5.870	50-4
50	1	0.03215	0.840	11.631	11.707	-6.573±0.067	-6.649	50-6
50	1	0.000111	0.987	9.308	9.313	-7.760±0.170	-7.760	50-7

Table 3-2
Continued

T °C	P bar	Ionic Strength molal	$\gamma_{\pm}$	pH_t	$pH_t°$	log m_{Cu}	log $m_{Cu}°$	Sample Series Cu_2O
50	1	0.000965	0.964	10.228	10.244	-7.633±0.076	-7.633	50-8
50	1	0.000149	0.985	7.928	7.934	-7.771±0.132	-7.771	50-9
50	1	0.000853	0.966	7.418	7.433	-6.736±0.028	-6.736	50-13
75	1	0.001014	0.961	9.075	9.092	-7.392±0.034	-7.397	75-1
75	1	0.000109	0.987	8.736	8.742	-7.450±0.047	-7.450	75-2
75	1	0.001090	0.960	9.713	9.731	-7.270±0.126	-7.270	75-3
75	1	0.01067	0.890	10.638	10.688	-6.877±0.032	-6.877	75-4
75	1	0.07621	0.777	11.374	11.483	-5.803±0.095	-5.912	75-5
75	1	0.03608	0.825	11.101	11.185	-6.098±0.088	-6.182	75-6
75	1	0.00023	0.981	8.110	8.118	-7.364±0.126	-7.364	75-7
75	1	0.001025	0.961	3.202	3.219	-3.402±0.008	-3.419	75-8
75	1	0.00034	0.988	3.628	3.633	-4.086±0.013	-4.091	75-9
75	1	0.004783	0.922	2.564	2.599	-2.687±0.048	-2.722	75-10
75	1	0.001689	0.951	6.858	6.880	-6.024±0.174	-6.046	75-11
75	1	0.002412	0.942	2.847	2.873	-3.005±0.007	-3.031	75-12
200	55	0.000996	0.946	8.261	8.285	-6.781±0.071	-6.805	200-1
200	51	0.000125	0.980	7.392	7.401	-6.347±0.061	-6.355	200-2
250	41	0.001089	0.932	8.207	8.237	-7.118±0.179	-7.149	250-9
250	41	0.000051	0.984	8.207	8.214	-5.494±0.123	-5.501	250-10
250	54	0.001205	0.929	8.248	8.280	-6.709±0.052	-6.741	250-3

Table 3-2
Continued

T °C	P bar	Ionic Strength molal	$\gamma_{\pm}$	pH_t	$pH_t°$	log m_{Cu}	log $m_{Cu}°$	Sample Series Cu_2O
250	55	0.000310	0.962	4.060	4.076	-3.651±0.062	-3.668	250-4
250	56	0.001072	0.939	5.186	5.213	-4.456±0.096	-4.483	250-5
250	54	0.001118	0.931	8.217	8.248	-6.731±0.048	-6.763	250-6
250	54	0.01002	0.820	9.054	9.140	-5.450±0.016	-5.536	250-7
300	94	0.000977	0.917	3.702	3.740	-3.109±0.003	-3.146	300-8
300	94	0.000196	0.961	4.203	4.220	-3.876±0.007	-3.893	300-9
300	96	0.00002	0.988	6.322	6.327	-6.770±0.220	-6.775	300-10
300	119	0.000959	0.919	3.661	3.698	-3.130±0.003	-3.167	300-12
300	121[b]	0.000946	0.920	4.628	4.664	-5.658±0.044	-5.694	300-13
350	183	0.001124	0.874	9.520	9.578	-6.161±0.053	-6.219	350-15
350	184	0.01261	0.658	10.313	10.495	-5.085±0.009	-5.267	350-15’
350	182	0.000528	0.911	4.956	4.996	-4.672±0.030	-4.713	350-16
350	182	0.001950	0.840	3.750	3.826	-3.241±0.030	-3.317	350-17

[a] For unknown reasons these results are too high and were ignored
[b] Feed solution saturated with an Ar/H_2 gas mixture to create a reducing environment

Note that in experiment number 300-17 summarized in the table above, a strongly reducing condition was applied through by saturating the ammonia buffer feed solution with a hydrogen/argon gas mixture. This resulted in a measured solubility approximately 1.5 log units below that calculated for the Cu_2O crystals with which the column was packed (see Figure 3.7). This implies that the solubility of copper metal is at least 1.5 log units lower at this condition and could well be even lower as a residual amount of unreduced Cu^+ in solution could account for the measured concentration.

Table 3-3
Values of log K_{s0} and log K_{s2} for Cuprous Oxide

T °C	log K_{s0}	log K_{s1}	log K_{s2}
25.0	-0.079±0.012	-8.0±0.3	-18.38±0.22
50.0	-0.218±0.026	-7.9±0.7	-18.28±0.22
75.0	-0.215±0.036	-7.5±0.2	-17.61±0.24
100.0	-0.148±0.025	-	-16.59±0.70
150.0	0.211±0.017	-	-
200.0	0.397±0.061	-	-15.11±0.31
250.0	0.521±0.197	-	-14.74±0.07
300.0	0.542±0.030	-	-15.38±1.03
350.0	0.490±0.036	-	-15.76±0.04

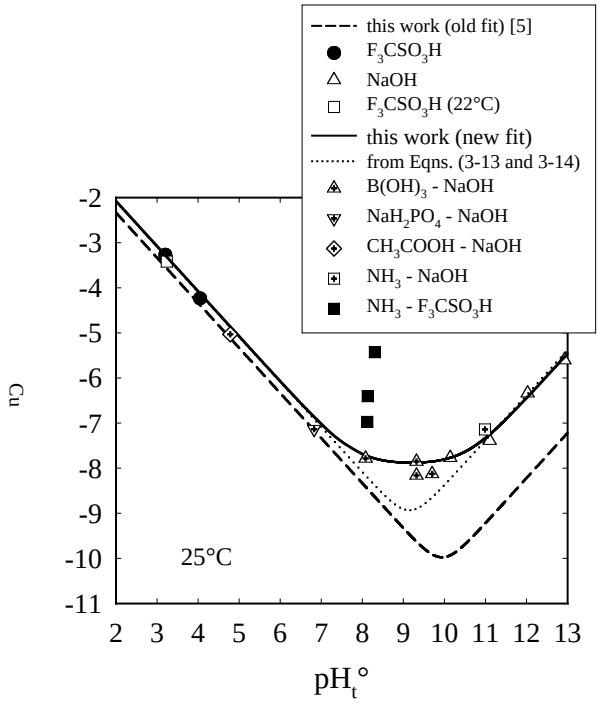

Figure 3-1
Solubility profile for Cu_2O at 25°C (77°F) showing the curve representing the logarithm of the total copper(I) molality versus $pH_t°$ for an infinitely dilute solution.

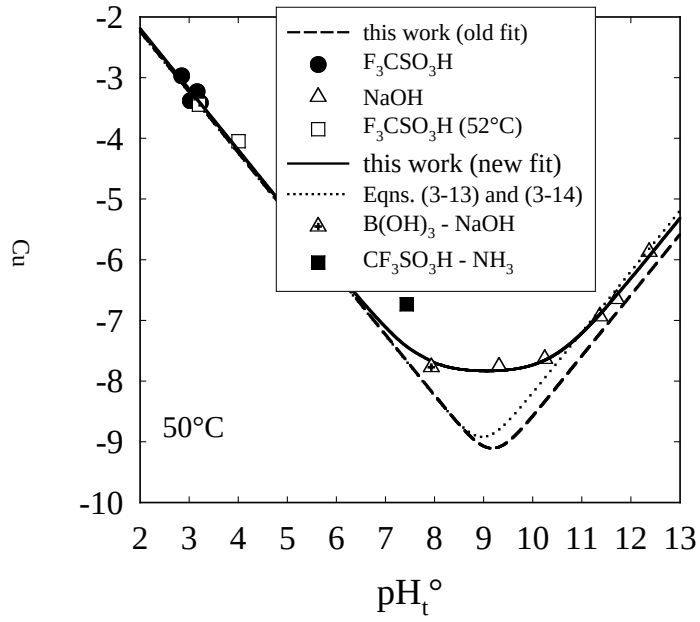

Figure 3-2
Solubility profile for Cu_2O at 50°C (122°F) showing the curve representing the logarithm of the total copper(I) molality versus $pH_t°$ for an infinitely dilute solution.

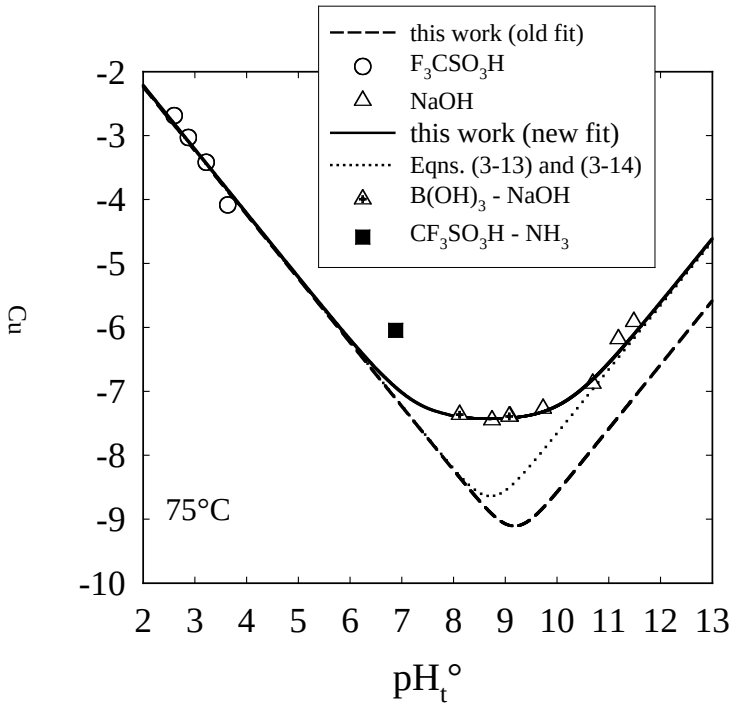

Figure 3-3
Solubility profile for Cu_2O at 75°C (167°F) showing the curve representing the logarithm of the total copper(I) molality versus $pH_t°$ for an infinitely dilute solution.

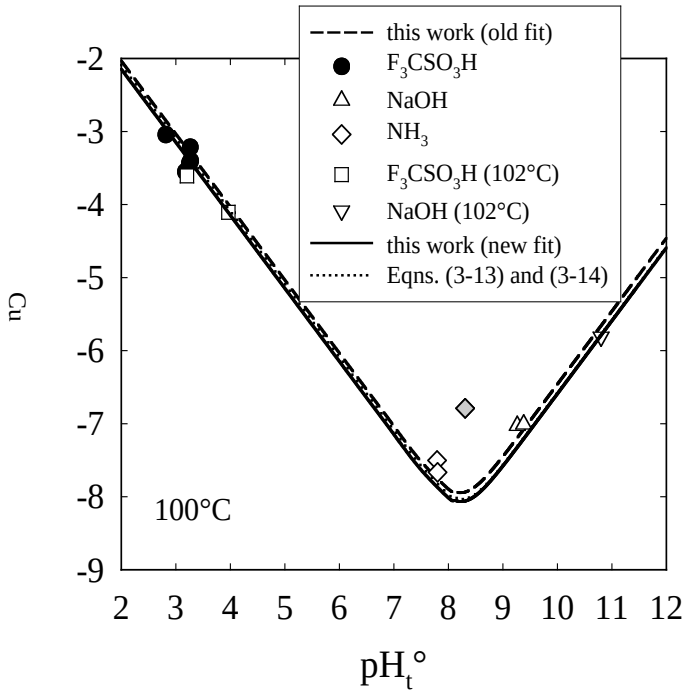

Figure 3-4
Solubility profile for Cu_2O at 100°C (212°F) showing the curve representing the logarithm of the total copper(I) molality versus $pH_t°$ for an infinitely dilute solution. The grey diamond was not included in the fit.

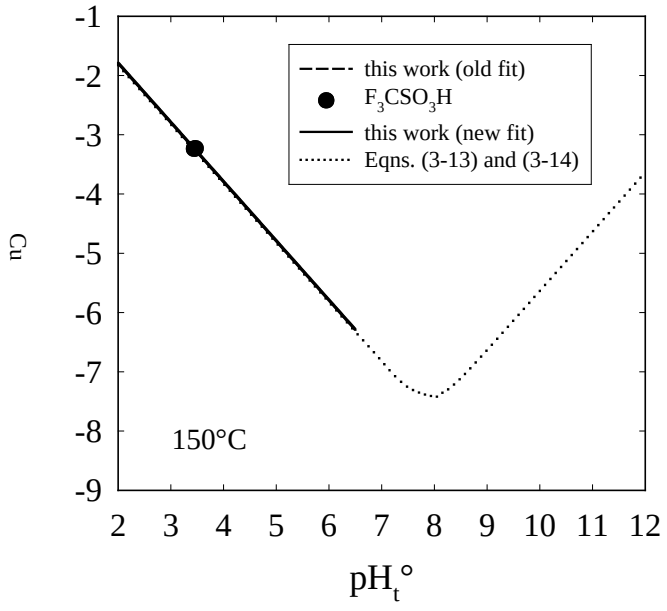

Figure 3-5
Solubility profile for Cu_2O at 150°C (302°F) showing the curve representing the logarithm of the total copper(I) molality versus $pH_t°$ for an infinitely dilute solution.

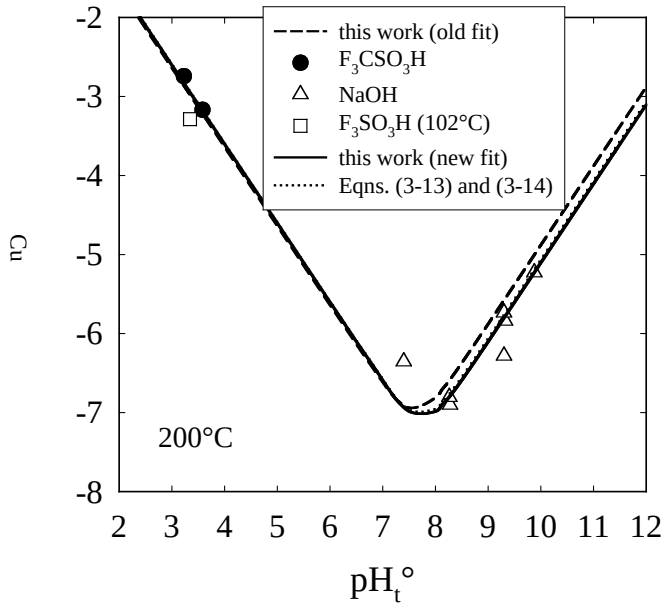

Figure 3-6
Solubility profile for Cu_2O at 200°C (392°F) showing the curve representing the logarithm of the total copper(I) molality versus $pH_t°$ for an infinitely dilute solution.

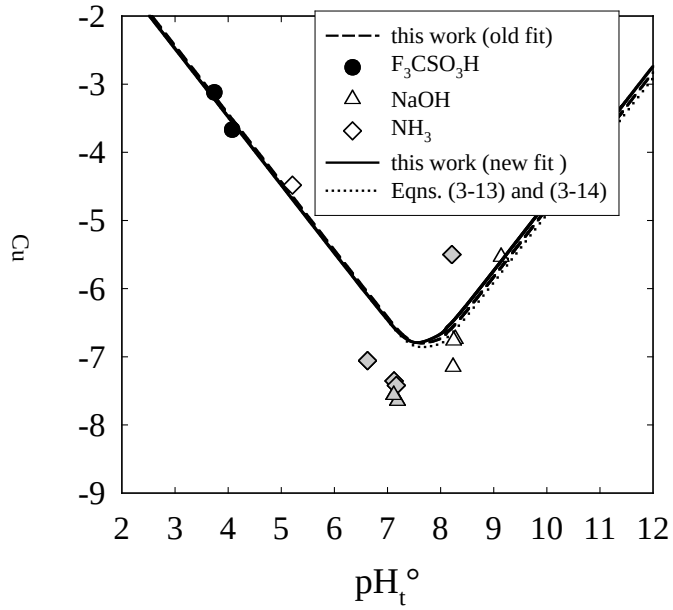

Figure 3-7
Solubility profile for Cu_2O at 250°C (482°F) showing the curve representing the logarithm of the total copper(I) molality versus $pH_t°$ for an infinitely dilute solution. The grey symbols were not included in the fit.

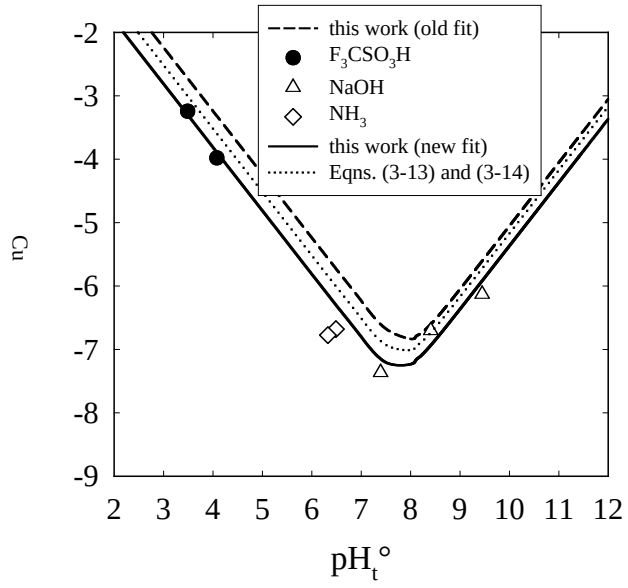

Figure 3-8
Solubility profile for Cu_2O at 300°C (572°F) showing the curve representing the logarithm of the total copper(I) molality versus $pH_t°$ for an infinitely dilute solution.

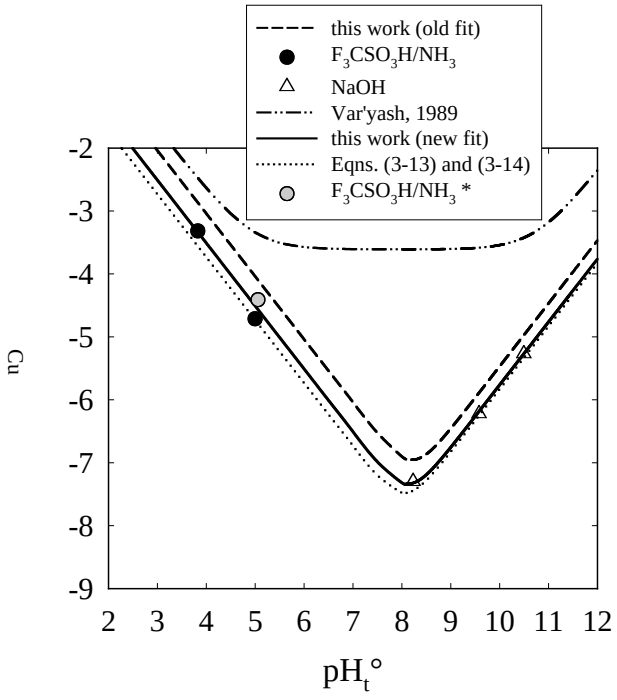

Figure 3-9
Solubility profile for Cu_2O at 350°C (662°F) showing the curve representing the logarithm of the total copper(I) molality versus $pH_t°$ for an infinitely dilute solution. The gray value (also indicated by an asterisk in the legend) was not included in the fit and stems from a series of experiments with CuO (see Figure 4-7) where reduction of the surface layer of the CuO particles apparently occurred and solubilities compatible with Cu_2O were obtained.

The two sets of log K_{s0} and log K_{s2} values were then fitted to various functions of temperature to determine which combinations of temperature terms gave the best fit to these values with the minimum number of terms. Another version of the ORGLS [6] program was used for this purpose. Eqns. (3-13) and (3-14) were the equations of choice.

$$\log K_{s0} = -1522.946 + 42552.24/T + 267.400\ln(T) - 0.531237T + 1.68742\cdot10^{-4}T^2 \quad (3\text{-}13)$$

$$\log K_{s2} = -3287.305 + 90564.36/T + 572.468\ln(T) - 1.086369T + 3.07670\cdot10^{-4}T^2 \quad (3\text{-}14)$$

where T is the temperature in kelvin. These equations are far more reliable than those reported previously [7], because of the much larger dataset that could now be evaluated and because of some improvements in the quality of these data. These fits are shown in Figures 3-10 and 3-11. The downturn at temperatures approaching 300°C is in keeping with the change in heat capacity of ions as the critical temperature of water is approached and was also seen for the solubility constants for CuO (following chapter). The average value of log K_{s0} at 300°C appears to be too low and experimental clarification is called for, but considering the results in Figure 3-7, it is difficult to understand how both sets of data could be in error.

The dotted curves in Figures 3-1 to 3-9 were included to illustrate that at temperatures of 100°C and higher, only two Cu(I) species dominate the liquid phase, or, conversely, below 100°C the neutral $Cu(OH)^0$ species is significant in the pH range of general interest to power plant start-up operation. The inclusion of the latter species at low temperatures gives rise to higher copper concentrations by more than a log unit at the solubility minimum.

The form of these equations with the sharp change in these functions (Eqns. 3-13 and 3-14) at temperatures approaching the operating conditions in a fossil-fired boiler, underscore the importance of making measurements at these extreme conditions, rather than rely on extrapolation of low temperature results.

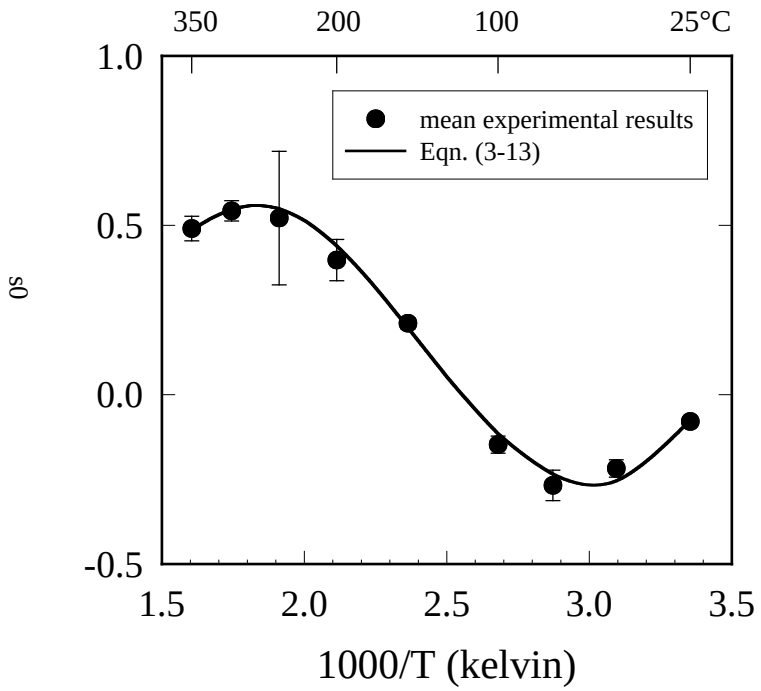

Figure 3-10
The temperature dependence of log K_{s0} for Cu_2O in water.

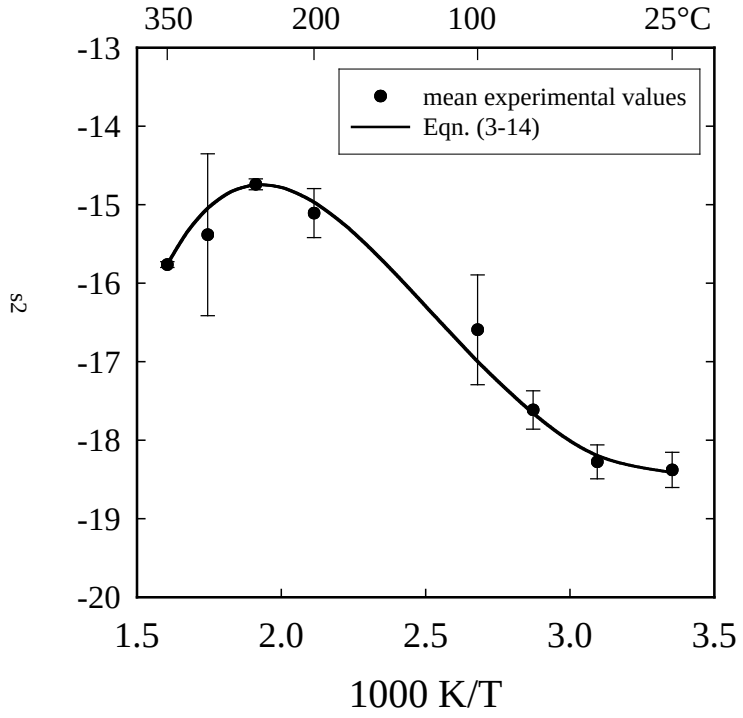

Figure 3-11
The temperature dependence of log K_{s2} for Cu_2O in water.

3.3.2 Solubility of Cu_2O in steam

The experimental data contained in Appendix A for the solubility of Cu_2O in steam are summarized in Table 3-4, including the results obtained during the last segment of this program that had not been available previously [5,8]. It was established in these previous reports that high concentrations of ammonia enhance the volatility of copper(I) at low temperatures, presumably through the formation of amine complexes of Cu(I), such as, $Cu(NH_3)_n(OH)^0$ (n = 1-4). However, ammonia concentrations of about 0.5 ppm commonly used in fossil-fired units under AVT conditions are too low to cause enhanced vaporous carryover of copper(I) to steam.

Much of the new data were obtained at 350 and 400°C. The latter condition, which exceeds the critical temperature of water, allows the pressure of the system to be varied over a wide range without the possibility of condensation. These results are depicted in Figure 3-12 from which it is immediately clear that the solubility in steam decreases with increasing temperature. Moreover, as expected, the solubility increases with increasing pressure, and within the relatively large experimental scatter in the data, these results are very compatible with those published at (620±1) °C (1148 °F) at 186 to 310 bar (2697 – 4495 psi) [9]. This combined data set was fitted to a function of temperature (t, °C) and pressure (p, bar) to yield Eqn. (3-15). Although such equations are more commonly given in terms of temperature in Kelvin and logarithm of the density of water, the form of Eqn. (3-15) is hopefully of more immediate practical application, and resulted in a fit that represents the data virtually to the same precision as the more thermodynamically-rigorous form.

$$\log (\text{Cu(I), ppb}) = 1.232 - 5.683 \cdot 10^{-3}\, t + 1.048 \cdot 10^{-2}\, p \qquad (3\text{-}15)$$

These results and their implications to actual power plant conditions are discussed in Chapter 4 in conjunction with the corresponding data for cupric oxide.

Table 3-4
Summary of All Data for the Solubility of Cuprous Oxide in Steam

T °C	P bar	P_{sat} bar	Buffer	Buffer Conc'n molal	Buffer Conc'n ppm	log m_{Cu°	Copper Conc'n ppb
200	12	15.5	NaOH	0.000099	4.0	-7.167±0.143	4.3
250	33	39.7	NH_3	0.01034	176	-5.538±0.082	184
250	33	39.7	NH_3	0.000826	14.1	-7.369±0.274	2.7
250	36	39.7	NaOH	0.000099	4.2	-7.421±0.150	2.4
250	36	39.7	NaOH	0.000106	4.0	-7.488±0.196	2.1
300	76	85.8	NH_3	0.000987	16.8	-6.210±0.158	39.2
300	74	85.8	NH_3	0.00102	17.5	-6.974±0.067	6.7
300	80	85.8	NaOH	0.000106	4.2	-7.554±0.178	1.8
300*	81	85.8	NH_3	0.000994	16.9	-7.399±0.078	2.5
350	158	165.2	NaOH	0.000093	3.7	-7.522±0.115	1.9
350*	155	165.2	NH_3	0.000994	16.9	-7.719±0.040	1.2
350*	81	165.2	NaOH	0.000099	3.7	-7.782±0.236	1.1
350*	144	165.2	NaOH	0.000193	7.7	-7.639±0.120	1.5
400*	159	-	NaOH	0.000137	5.5	-6.918±0.037	7.7
400*	198	-	NaOH	0.000137	5.5	-6.361±0.035	27.7
400*	93	-	NaOH	0.000137	5.5	-8.362±0.300	0.3
400*	120	-	NaOH	0.000137	5.5	-7.899±0.718	0.8

* recent values obtained after publication of the previous report

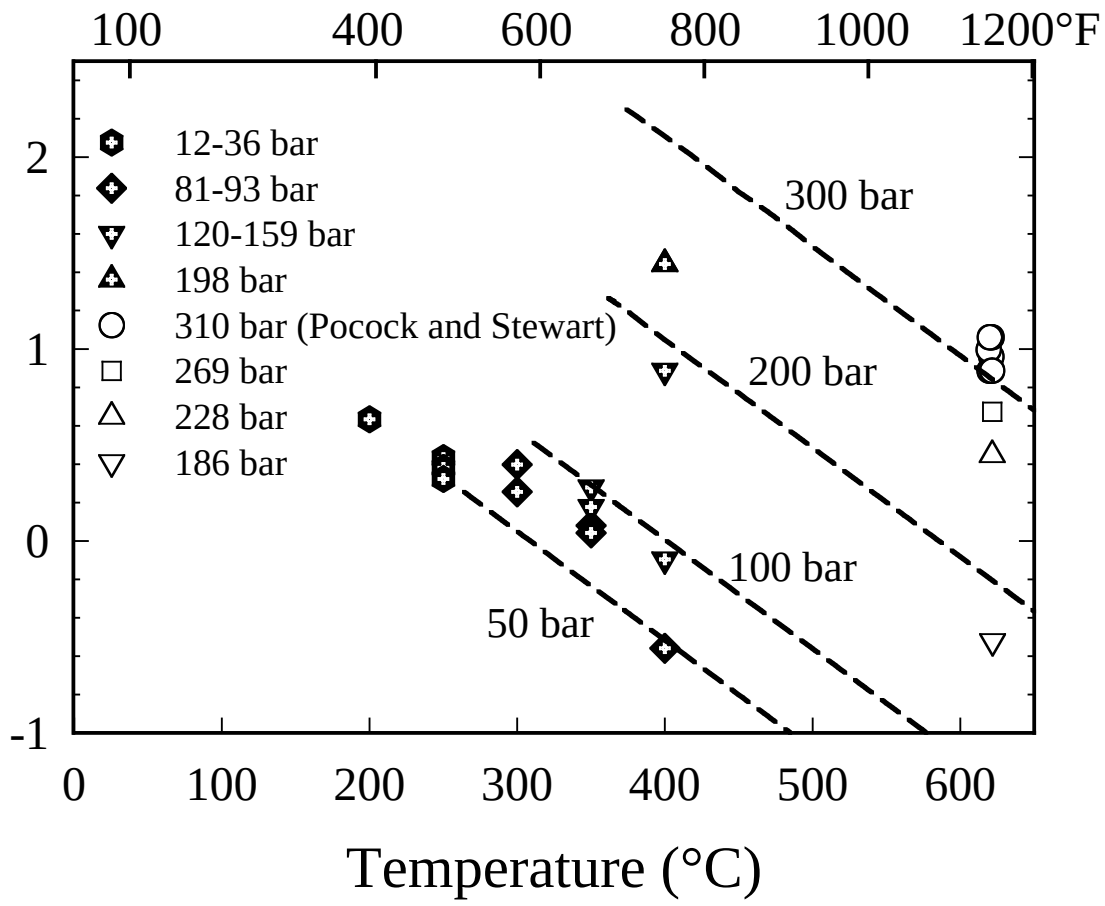

Figure 3-12
The solubility of Cu_2O in steam at different pressures as a function of temperature, including the results of Pocock and Stewart. The dashed lines were generated from Eqn. (3-15).

In order to present these results in terms of the partitioning constants of cuprous hydroxide the following equilibria must be considered. First, the partitioning equilibrium can be written in terms of basic solutions:

$$Cu(OH)_2^- \text{ (liq)} + H^+ \text{ (liq)} \Leftrightarrow Cu(OH)^0 \text{ (vap)} + H_2O \text{ (liq)} \qquad (3\text{-}16)$$

The partitioning constant as defined by reaction (3-16) is then given by:

$$K_D^* = m\{Cu(OH)^0\}_{vap}/(m\{Cu(OH)_2^-\}\gamma\{Cu(OH)_2^-\}m\{H^+\}_{liq}\gamma\{H^+\}) \qquad (3\text{-}17)$$

Under the condition that the solutions are saturated with respect to Cu_2O, it follows by combining equations (3-6) and (3-17):

$$K_D^*(Cu_2O,sat) = m\{Cu(OH)^0\}_{vap}/K_{s2} \quad (3\text{-}18)$$

As in all previous cases, the activity coefficient of the neutral species in the vapor phase is assumed to be unity.

The second approach is to consider the partitioning equilibrium in terms of Cu^+ in acidic solutions:

$$Cu^+ (liq) + OH^- (liq) \Leftrightarrow Cu(OH)^0 (vap) \quad (3\text{-}19)$$

The partitioning constant is then given by the expression:

$$K_D = m\{Cu(OH)^0\}_{vap}/(m\{Cu^+\}\gamma\{Cu^+\}m\{OH^-\}_{liq}\{OH^-\}) \quad (3\text{-}20)$$

Combination of Eqn. (3-20) under saturation conditions with respect to Cu_2O with Eqns. (3-4) and (3-7) gives:

$$K_D(Cu_2O,sat) = m\{Cu(OH)^0\}_{vap}/(K_{s0}K_w) \quad (3\text{-}21)$$

The concentration of $Cu(OH)^0$ in the vapor is derived from Eqn. (3-15). The values of K_{s0} and K_w can be calculated at various temperatures from Eqns. (3-15) and (3-9), respectively. The plot of log K_D versus temperature is shown in the next section and a comparison id given to the corresponding results for CuO.

3.4 References

1. W.L. Marshall and E.U. Franck, "Ion Product of Water Substance, 0-1000°C, 1-10,000 bars. New International Formulation and Its Background." *Journal of Physical and Chemical Reference Data,* Vol. 10, No. 2, pp. 295-304 (1981).

2. R.H Busey and R.E. Mesmer, "Thermodynamic Quantities for the Ionization of Water in Sodium Chloride Media to 300 °C", *Journal of Chemical and Engineering Data,* Vol. 23, No. 2, pp. 175-176 (1978).

3. D.G. Archer, "Thermodynamic Properties of the NaCl + H_2O System. II. Thermodynamic Properties of NaCl(aq), NaCl.2H_2O(cr), and Phase Equilibria." *Journal of Physical and Reference Data.* Vol. 21, No. 4, pp.793-829 (1992).

4. B.F Hitch and R.E. Mesmer, "The Ionization of Aqueous Ammonia to 300°C in KCl Media", *Journal of Solution Chemistry,* Vol. 5, No. 10, pp. 667-680 (1976).

5. D.A. Palmer, P. Bénézeth, A.Y. Petrov, L.M. Anovitz and J.M. Simonson, "Behavior of Electrolytes in Steam: The Solubility and Volatility of Cupric Oxide." EPRI Report TR-1000455. Palo Alto, CA, Electric Power Research Institute (2000).

6. L.N. Var'yash, "Equilibria in the Cu-Cu_2O-H_2O System at 150-450°C." *Geochemistry International*. Vol. 26, pp. 80-90 (1989).

7. M. Ball, A. Bursik, R.B. Dooley, M. Gruszkiewicz, D.A. Palmer, K.J. Shields and J.M. Simonson, "The Volatility of Impurities in Water/Steam Cycles." EPRI Report TR-1001042. Palo Alto, CA, Electric Power Research Institute (2001).

8. D.A. Palmer, P. Bénézeth, A.Y. Petrov, L.M. Anovitz, and J.M. Simonson. *Behavior of Aqueous Electrolytes in Steam Cycles, The Solubility and Volatility of Copper(I) and Copper(II) Oxides*, EPRI, Palo Alto, CA: December 2001. TR-1003993.

9. F.J. Pocock and J.F. Stewart, "The Solubility of Copper and Its Oxides in Supercritical Steam." *Journal of Engineering for Power*. pp. 33-45 (1963).

4
CUPRIC OXIDE: EXPERIMENTAL RESULTS

The final cupric oxide experimental solubility data derived in our laboratory for the EPRI sponsored "Program Copper" are summarized in Appendices C and D, and complement data provided in two previous reports [1,2]. The current experiments were all completed using the high-temperature flow-through cell. The earlier results obtained in liquid water are summarized in Table 4-1 with similar headings as given in Table 3-1. Whereas in the previous reports activity coefficients had been essentially ignored due to the uncertainty in speciation and the general magnitude of the experimental uncertainties, activity coefficients have now been derived as outlined in Chapter 3 for the corresponding cuprous case (*i.e.*, the Meissner treatment used in MULTEQ was employed to calculate activity coefficients to be consistent with the MULTEQ code as described in the previous chapter [3]). The results obtained during this final stage of the project are summarized in Table 4-2.

The corresponding results for the solubility of cupric oxide in steam are combined in Table 4-5. In this case activity coefficients are assumed to be unity for the copper species dissolved in steam because these species are believed to be uncharged and no experimental activity coefficient measurements are available.

4.1 Thermodynamics of Copper(II) in Solution

The equilibria involved in the dissolution of cupric oxide in aqueous solutions are:

$$CuO(cr) + 2H^+ \Leftrightarrow Cu^{2+} + H_2O \quad (4\text{-}1)$$

$$CuO(cr) + H^+ \Leftrightarrow Cu(OH)^+ \quad (4\text{-}2)$$

$$CuO(cr) + H_2O \Leftrightarrow Cu(OH)_2^0 \quad (4\text{-}3)$$

$$CuO(cr) + 2H_2O \Leftrightarrow Cu(OH)_3^- + H^+ \quad (4\text{-}4)$$

$$CuO(cr) + 3H_2O \Leftrightarrow Cu(OH)_4^{2-} + 2H^+ \quad (4\text{-}5)$$

The solubility constants associated with these reactions are:

$$K_{s0} = m\{Cu^{2+}\}\gamma\{Cu^{2+}\}/(m\{H^+\}\gamma\{H^+\})^2 \quad (4\text{-}6)$$

$$K_{s1} = m\{Cu(OH)^+\}\,\gamma\{Cu(OH)^+\}/(m\{H^+\}\gamma\{H^+\}) \quad (4\text{-}7)$$

$$K_{s2} = m\{Cu(OH)_2^0\}\gamma\{Cu(OH)_2^0\} \quad (4\text{-}8)$$

$$K_{s3} = m\{Cu(OH)_3^-\}\gamma\{Cu(OH)_3^-\}m\{H^+\}\gamma\{H^+\} \quad (4\text{-}9)$$

$$K_{s4} = m\{Cu(OH)_4^{2-}\}\gamma\{Cu(OH)_4^{2-}\}(m\{H^+\}\gamma\{H^+\})^2 \quad (4\text{-}10)$$

where $m\{X\}$ and $\gamma\{X\}$ represent the molality and activity coefficient of species X, respectively. Note that the $Cu(OH)_4^{2-}$ species, which would be expected to appear at high pH_m, was not observed in any of these studies and is therefore not included in the subsequent calculations.

4.2 Calculation of pH

Treatment of these results in terms of calculating the pH_t of the solutions at temperature t (°C) was described in the previous reports [1,2] and in the previous chapter (section 3.2), including the use of ammonia as a pH buffer. Two additional buffer systems were used in the study of CuO solubility, because the speciation in solution is more complex than that of Cu_2O at low temperatures and hence more data were needed over the whole pH_t range under these conditions.

The boric acid, sodium borate buffer (in fact, solid boric acid and sodium hydroxide solutions were mixed to make these buffer mixtures) was used only at low temperatures to fix the pH_t as at higher temperatures complexation of borate with copper(II) in solution may become significant. Nevertheless, there is a possibility that boric acid could complex the hydrolyzed copper(II) species even at low temperatures (25 and 50°C), but by varying the total boric acid – sodium hydroxide concentration (*i.e.*, keeping pH_m constant) it was established that no corresponding variation in copper concentration was observed, thus ruling out the presence of significant complexation.

The hydrogen ion dissociation of aqueous boric acid is described by the equation:

$$B(OH)_3 \Leftrightarrow B(OH)_4^- + H^+ \quad (4\text{-}11)$$

Polymeric borate species do not need to be considered at the low concentrations of total borate employed in these studies. The equation describing the temperature dependence of this dissociation reaction was reported recently [4] as:

$$\log K_{Eqn.\,(4\text{-}11)} = -36.2605 + 3645.18/T + 11.6402 \log(T) + (16.4914 - 0.023917\,T)\log \rho_w \quad (4\text{-}12)$$

where T is in Kelvin and ρ_w is the density of pure water ($g\cdot cm^{-3}$) taken from the formulation of Wagner and Pruss [5].

The mono- and di-hydrogen phosphate buffer was used at 25 and 50°C:

$$H_2PO_4^- + OH^- \Leftrightarrow HPO_4^{2-} + H_2O \quad (4\text{-}13)$$

where the equilibrium is written in this pseudo-isocoulombic form to minimize the temperature dependence of the equilibrium constant allowing more accurate fitting of the experimental data to be carried out. These experiments were performed by Mesmer and Baes [6] who derived the following expression for the base hydrolysis constant at infinite dilution,

$$\log K_{Eqn.\ (4\text{-}13)} = -246.045 + 17156.9/T + 37.7345 \ln(T) - 0.0322082\, T - 897579/T^2 \quad (4\text{-}14)$$

The Meissner [3] model for activity coefficients, γ_{NaCl}, based on the NaCl model substance concept was again used to correct this equilibrium constant to the ionic strength of the experiments, as was done for the previous boric acid case, and as described in the previous chapter (section 3.2). The dissociation constant for water, Q_w, was then used to convert Eqn. (4-14) to its protolytic form, which corresponds to reaction (4-15) and provides for the calculation of pH_t, which is the pH_m value at temperature, t°C. The pH_t value was then converted to pH_t° (pH_m at t°C and infinite dilution) with the same γ_{NaCl} value.

$$H_2PO_4^- \Leftrightarrow HPO_4^{2-} + H^+ \quad (4\text{-}15)$$

The acetic acid – sodium acetate buffer was used at low temperatures where pH could not be controlled to a predictable level by acid alone, due the high solubility of CuO at low pH. The pH_m value for each buffer mixture was calculated from the acid dissociation constant for acetic acid as measured by Mesmer *et al*. [7], namely,

$$CH_3COOH \Leftrightarrow CH_3COO^- + H^+ \quad (4\text{-}16)$$

$$\log K_{Eqn.\ (4\text{-}16)} = -350.02 + 18325/T + 55.3275 \ln(T) - 0.063513\, T - 1105000/T^2 \quad (4\text{-}17)$$

Again the corresponding equilibrium constants at the ionic strength of the experiments were calculated from the value of $\log K_{Eqn.\ (4\text{-}16)}$ and the activity coefficients from the Meissner model .

For the Tris buffer the equilibrium and relevant dissociation constant [8] are,

$$(HOCH_2)_3NH_3^+ \Leftrightarrow (HOCH_2)_3NH_2 + H^+ \quad (4\text{-}18)$$

$$\log K_{Eqn.\ (4\text{-}18)} = 235.33 - 14876/T - 37.504 \ln(T) - 0.038824\, T + 660680/T^2 \quad (4\text{-}19)$$

whereas for Bis-Tris [9] these are:

$$(HOCH_2)_3N(CH_2CH_2OH)_2H^+ \Leftrightarrow (HOCH_2)_3N(CH_2CH_2OH)_2 + H^+ \quad (4\text{-}20)$$

$$\log K_{Eqn.\ (4\text{-}20)} = -2.2541 - 1329.07/T + 2.5356 \cdot 10^{-6}\, T^2 \quad (4\text{-}21)$$

4.3 Solubility Data for Cupric Oxide in Water and Steam

4.3.1 Solubility of CuO in water

The new solubility data for cupric oxide in water (containing various pH buffering agents) obtained using the high-temperature, flow-through cell are listed in detail in Appendix C, whereas the low-temperature data are given in Appendix D. All the solubility data for cupric oxide are summarized in Tables 4-1 and 4-2. The solubility profile diagrams (plots of the logarithm of the total copper(II) molality versus $pH_t°$) generated from these results and calculated to a consistent standard state of infinite dilution at the experimental temperatures of 25, 50, 100, 200, 250, 300 and 350°C (77 – 662°F), are shown in Figures 4-1 to 4-7, respectively.

The majority of the new data are shown in Figures 4-1 to 4-2 corresponding to experiments at 25 and 50°C, respectively. As indicated in previous reports, and the discussion earlier in this report, pH_t is generally the critical variable in determining the solubility of metal oxide phases and hence it must be known as accurately as possible. In moderately acidic and basic solutions either CF_3SO_3H or NaOH can be added to control pH_t, provided that their concentrations exceed that of the total copper present in solution, because the copper species under these conditions consume H^+ and OH^-, respectively, according to Eqns. (4-1), (4-2) and (4-4). In other words, pH_t can only be calculated by subtracting the contributions of the copper species' concentrations from the known total acid or base concentration, also implying that the speciation of copper in solution must be know as each species contributes differently to this correction. Although in basic media the concentration of copper was significantly less than that of total added NaOH, in many cases the copper concentration in CF_3SO_3H solutions was so large that it consumed virtually all the hydrogen ions in solution and thereby rendered the calculation of pH_t very inaccurate or even unfeasible. However, in the low temperature regime many pH buffers exist that can be utilized to fix the pH_t, provided they do not interact, or complex, the dissolved copper and thereby enhance the solubility of CuO. As interactions, or complex formation reactions, between metal ions and anionic ligands become stronger with increasing temperature, a number of standard pH buffers were investigated for the low-temperature (25 and 50°C) experiments. The effect of some of these buffers, in particular ammonia, in raising the solubility of CuO will be discussed in the following section, noting that as also observed for copper(I) in section 3, ammonia complexes with copper(II) are strongest at low temperatures.

Table 4-1
Summary of Previous Results for the Solubility of Cupric Oxide in Water

T °C	P bar	Ionic Strength molal	pH_t	$\gamma_{\pm(NaCl)}$	$pH_t°$	log m_{Cu}	log $m_{Cu}°$	Sample Series CuO-
100	6	0.0106	10.181	0.884	10.234	-7.445±0.145	-7.499	Batch
100	12	0.0276	10.542	0.832	10.622	-7.032±0.058	-7.112	Batch
100	7	0.0397	10.677	0.809	10.769	-7.198±0.077	-7.290	Batch
100	116	0.00055	8.944	0.969	8.958	-4.577±0.097	-4.591	Flow
100	101	0.00124	9.283	0.955	9.303	-7.689±0.103	-7.709	Flow
100	99	0.00026	8.626	0.979	8.636	-8.047±0.187	-8.056	Flow
100	99	0.00033	8.728	0.976	8.738	-8.025±0.099	-8.036	Flow
100	98	0.00007	8.066	0.989	8.071	-7.952±0.078	-7.957	Flow
100	96	0.00007	8.087	0.988	8.093	-7.303±0.141	-7.308	Flow
100	98	0.00007	8.048	0.989	8.053	-7.457±0.202	-7.462	Flow
100	82	0.00006	8.009	0.990	8.014	-6.125±0.213	-6.130	Flow
100	83	0.00006	8.003	0.989	8.008	-5.820±0.084	-5.825	Flow
150	13	0.01056	9.553	0.868	9.615	-7.639±0.017	-7.701	Batch
200	24	0.01056	9.162	0.846	9.234	-7.306±0.188	-7.378	Batch
200	22	0.0834	9.874	0.684	10.039	-6.073±0.340	-6.238	Batch
200	85	0.00118	8.344	0.942	8.344	-7.074±0.122	-7.074	Flow
200	30	0.00010	4.418	0.982	4.426	-4.215±0.043	-4.223	Batch
200	28	0.00010	4.627	0.982	4.635	-4.121±0.061	-4.129	Batch
200	29	0.00010	4.245	0.982	4.253	-4.374±0.119	-4.382	Batch

Table 4-1
Continued

T °C	P bar	Ionic Strength molal	pH_t	$\gamma_{\pm(NaCl)}$	$pH_t°$	log m_{Cu}	log $m_{Cu}°$	Sample Series CuO-
200	22	0.00010	4.190	0.982	4.198	-4.462±0.010	-4.470	Batch
200	15	0.00019	4.011	0.975	4.022	-4.038±0.024	-4.049	Batch
250	113	0.00012	7.185	0.977	7.185	-8.138±0.374	-8.138	Flow
250	38	0.0144	9.151	0.792	9.252	-6.081±0.170	-6.183	Volatility
250	37	0.00798	8.940	0.835	9.018	-6.465±0.191	-6.543	Volatility
250	36	0.00016	7.373	0.973	7.373	-7.854±0.400	-7.854	Volatility
250	37	0.1260	9.820	0.579	10.057	-5.205±0.140	-5.443	Volatility
250	54	0.00010	4.189	0.978	4.199	-4.462±0.143	-4.472	Batch
250	57	0.00010	4.215	0.978	4.224	-4.418±0.033	-4.428	Batch
250	75	0.00019	3.891	0.970	3.905	-4.217±0.016	-4.230	Batch
300	98	0.00013	7.470	0.968	7.470	-7.758±0.643	-7.758	Flow
300	187	0.00014	7.351	0.969	7.351	-7.254±0.615	-7.254	Flow
300	103	0.00118	8.364	0.910	8.405	-6.895±0.104	-6.936	Flow
300	85	0.00005	7.065	0.980	7.074	-7.978±0.253	-7.987	Volatility
300	83	0.0066	9.047	0.807	9.140	-6.720±0.162	-6.813	Volatility
300	84	0.0106	9.206	0.767	9.321	-6.026±0.319	-6.141	Volatility
300	84	0.0026	8.706	0.871	8.766	-6.544±0.319	-6.604	Volatility
300	84	0.0089	9.148	0.783	9.254	-6.523±0.074	-6.629	Volatility

Table 4-1
Continued

T °C	P bar	Ionic Strength molal	pH_t	$\gamma_{\pm(NaCl)}$	$pH_t°$	log m_{Cu}	log $m_{Cu}°$	Sample Series CuO-
300	82	0.00019	7.660	0.962	7.660	-7.555±0.077	-7.555	Volatility
300	83	0.00094	8.312	0.918	8.349	-7.527±0.305	-7.564	Volatility
300	99	0.00010	4.122	0.972	4.134	-4.623±0.017	-4.635	Batch
300	116	0.00019	3.824	0.962	3.840	-4.408±0.025	-4.425	Batch
350	203	0.00014	8.110	0.954	8.110	-7.248±0.260	-7.248	Flow
350	170	0.00071	9.001	0.895	9.050	-7.310±0.295	-7.358	Flow
350	176	0.00234	9.394	0.823	9.478	-7.377±0.309	-7.462	Flow
350	185	0.00104	8.615	0.879	9.084	-7.746±0.616	-7.802	Flow
350	156	0.0168	10.178	0.598	10.401	-6.226±0.200	-6.449	Volatility
350	154	0.0120	10.130	0.641	10.317	-5.955±0.420	-6.142	Volatility
350	161	0.00078	9.127	0.887	9.179	-7.175±0.354	-7.227	Volatility
20	20	0.00171	5.524	0.956	5.544	-3.405±0.010	-3.484	20-2
20	45	0.00148	5.944	0.959	5.962	-3.666±0.023	-3.739	20-3
21	3	0.00230	5.251	0.948	5.274	-3.510±0.023	-3.603	20-4
20	4	0.00338	5.438	0.939	5.465	-3.115±0.007	-3.224	20-5
100	7	0.00225	4.932	0.941	4.959	-4.177±0.028	-4.284	100-12
100	3	0.00167	5.386	0.948	5.409	-5.062±0.133	-5.155	100-14
100	5	0.00198	6.813	0.944	6.838	-5.275±0.090	-5.300	100-15
200	21	0.00198	5.237	0.925	5.270	-4.455±0.002	-4.489	200-10
200	20	0.00100	5.728	0.945	5.753	-5.011±0.097	-5.035	200-11

Table 4-1
Continued

T °C	P bar	Ionic Strength molal	pH_t	$\gamma_{\pm(NaCl)}$	$pH_t°$	log m_{Cu}	log $m_{Cu}°$	Sample Series CuO-
200	20	0.000102	7.291	0.982	7.291	-6.656±0.094	-6.656	200-12
200	19	0.00100	8.252	0.845	8.252	-7.368±0.142	-7.368	200-13
250	50	0.00100	5.171	0.934	5.200	-4.836±0.091	-4.866	250-6
250	52	0.000106	7.194	0.978	7.194	-5.833±0.062	-5.833	250-7[a]
250	53	0.00114	8.061	0.930	8.092	-6.385±0.051	-6.416	250-8 [a]
250	52	0.000030	6.666	0.988	6.671	-5.205±0.092	-5.205	250-9
250	53	0.000031	6.674	0.988	6.679	-6.427±0.047	-6.427	250-9’
250	53	0.000319	7.658	0.962	7.658	-5.337±0.089	-5.337	250-10 [a]
250	50	0.000496	5.671	0.953	5.692	-5.094±0.027	-5.115	250-11
250	53	0.000192	4.085	0.970	4.098	-3.963±0.008	-3.976	250-12
300	93	0.00197	2.838	0.886	2.890	-3.289±0.026	-3.342	300-2
300	93	0.000207	3.820	0.960	3.837	-4.262±0.002	-4.280	300-3
300	93	0.000289	7.718	0.953	7.739	-7.387±0.429	-7.408	300-4
350	177	0.000192	8.575	0.944	8.600	-7.523±0.220	-7.548	350-5

[a] the results of these experiments cannot be rationalized and have been ignored in the subsequent data analyses.

Table 4-2
Summary of Recent Results for the Solubility of Cupric Oxide in Water

T °C	P bar	Ionic Strength molal	pH_t	$\gamma_{\pm(NaCl)}$	pH_t°	log m_{Cu}	log m_{Cu}°	Sample Series CuO-
25	1	0.002998	4.727	0.942	4.753	-3.003±0.003	-3.107	25-1
25	1	0.00088	4.929	0.967	4.944	-3.539±0.001	-3.597	25-2
25	1	0.00095	7.3[a]	0.966	7.3[a]	-3.098±0.002	-3.098	25-4
25	1	0.001034	10.978	0.965	10.994	-7.412±0.143	-7.427	25-5
25	1	0.009901	11.902	0.903	11.946	-7.018±0.339	-7.062	25-6
25	1	0.001800	7.12[b]	0.954	7.14[b]	-4.994±0.025	-5.014	25-7
25	1	0.00014	-[c]	-	-	-3.838	-	25-8
25	1	0.000101	9.989	0.988	9.994	-7.595±0.093	-7.595	25-9
25	1	0.000943	9.128	0.966	9.143	-7.590±0.197	-7.590	25-10
25	1	0.000120	8.024	0.987	8.030	-7.093±0.099	-7.099	25-11
25	1	0.000966	10.949	0.966	10.965	-7.591±0.152	-7.606	25-12
25	1	0.09736	12.766	0.779	12.875	-6.185±0.088	-6.294	25-13
25	1	0.001965	7.134	0.952	7.155	-6.187±0.203	-6.208	25-14
25	1	0.000310	7.141	0.980	7.149	-6.115±0.017	-6.123	25-15
50	1	0.000310	6.818	0.979	6.827	-6.164±0.069	-6.169	50-1
50	1	0.000120	7.858	0.987	7.864	-7.354±0.182	-7.360	50-2
50	1	0.000176	9.507	0.984	9.514	-7.836±0.268	-7.843	50-3
50	1	0.001077	10.274	0.962	10.291	-7.856±0.274	-7.873	50-4
50	1	0.01156	11.239	0.892	11.288	-7.531±0.075	-7.581	50-5
50	1	0.1022	12.056	0.768	12.170	-6.353±0.032	-6.468	50-6
50	1	0.002005	-[c]	-	-	-2.993±0.007		50-7

Table 4-2
Continued

T °C	P bar	Ionic Strength molal	pH_t	$\gamma_{\pm(NaCl)}$	pH°_t	log m_{Cu}	log m_{Cu}°	Sample Series CuO-
50	1	0.001965	6.812	0.950	6.834	-6.265±0.034	-6.287	50-8
50	1	0.001060	5.176	0.964	5.192	-3.496±0.018	-3.560	50-9
50	1	0.003430	5.186	0.936	5.215	-3.050±0.003	-3.164	50-10
50	1	0.000693	5.542	0.969	5.555	-4.434±0.014	-4.489	50-11
50	1	0.000017	6.463	0.995	6.465	-5.238±0.043	-5.245	50-12
100	12	0.00096	3.342	0.960	3.360	-3.296±0.004	-3.314	100-16
100	13	0.00021	4.176	0.981	4.184	-3.856±0.015	-3.865	100-17
200	21	0.00021	-[d]	0.974	-	-3.571±0.022	-	200-2
200	22	0.00031	4.823[e]	0.969	4.837[e]	-3.531±0.013	-3.545	200-3
350	179	0.00053	3.332	0.911	3.373	-4.219±0.014	-4.260	350-6
350	174	0.00102	4.044	0.877	4.101	-5.158±0.036	-5.215	350-7
350	176	0.00025	5.057	0.937	5.085	-4.382±0.027	-4.410	350-8
350	175	0.00013	5.615	0.954	5.636	-6.540±0.062	-6.561	350-9
350	176	0.00196	9.331	0.836	9.409	-6.891±0.083	-6.969	350-10
350	175	0.00205	9.354	0.833	9.433	-7.971[f]	-8.050	350-15
350	173	0.00011	8.226	0.957	8.245	-6.494±0.062	-6.513	350-16
350	177	0.00019	8.415	0.944	8.440	-7.520±0.223	-7.545	350-5
350	175	0.00011	8.216	0.957	8.235	-7.379±0.104	-7.398	350-11
350	175	0.00076	3.119	0.893	3.168	-4.726±0.019	-4.775	350-12
350	175	0.00047	3.330	0.914	3.369	-4.705±0.041	-4.744	350-13

350	156	0.00110	2.989	0.866	3.052	-4.150±0.010	-4.212	350-17

Table 4-2
Continued

T °C	P bar	Ionic Strength molal	pH_t	$\gamma_{\pm(NaCl)}$	pH°_t	log m_{Cu}	log m_{Cu}°	Sample Series CuO-
350	175	0.00018	5.029	0.946	5.053	-5.926±0.043	-5.950	350-14
350	175	0.00020	4.946	0.943	4.972	-5.956±0.022	-5.982	350-15

[a] calculation of pH_t relies on an assumption as to the stoichiometry of the Cu(I)-Bis-Tris complex formed in solution (see discussion, section)
[b] calculation of pH_t relies on an assumption as to the stoichiometry of the Cu(I)-Tris complex formed in solution (see discussion, section)
[c] calculation of pH_t relies on an assumption as to the stoichiometry of the Cu(I)-Tris complex formed in solution, but the correction for dissolved copper exceeded the stoichiometric concentration of H^+ rendering this experiment uncalculable
[d] correction for dissolved copper exceeded the stoichiometric concentration of H^+ rendering this experiment un-calculable
[e] correction for dissolved copper was almost equal to the stoichiometric concentration of H^+ rendering this experiment un-calculable
[f] only one value

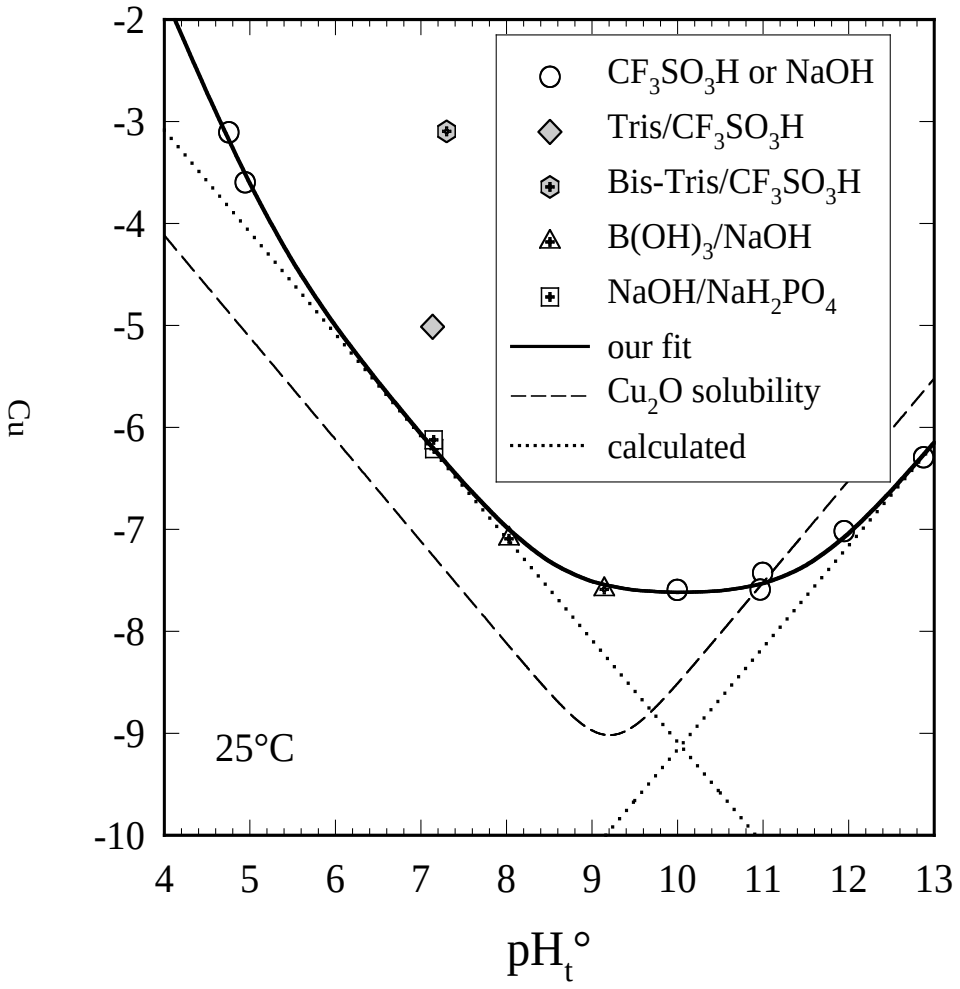

Figure 4-1
Solubility profile for CuO at 25°C (77°F) showing the curve representing the logarithm of the total copper(II) molality versus pH_t° for an infinitely dilute solution. The gray values were not included in the fit. The dotted lines (referred to as calculated) were derived from Eqns. (4-22) and (4-23).

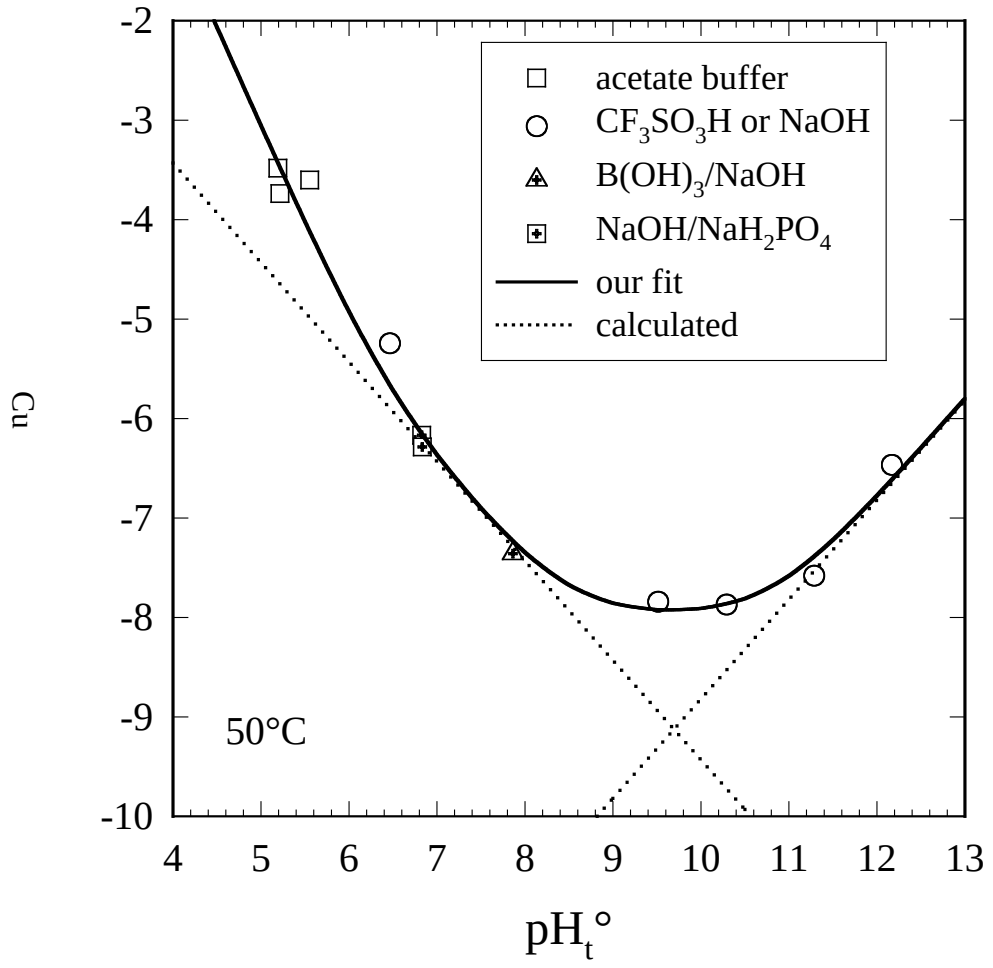

Figure 4-2
Solubility profile for CuO at 50°C (122°F) showing the curve representing the logarithm of the total copper(II) molality versus $pH_t°$ for an infinitely dilute solution. The dotted lines (referred to as calculated) were derived from Eqns. (4-22) and (4-23).

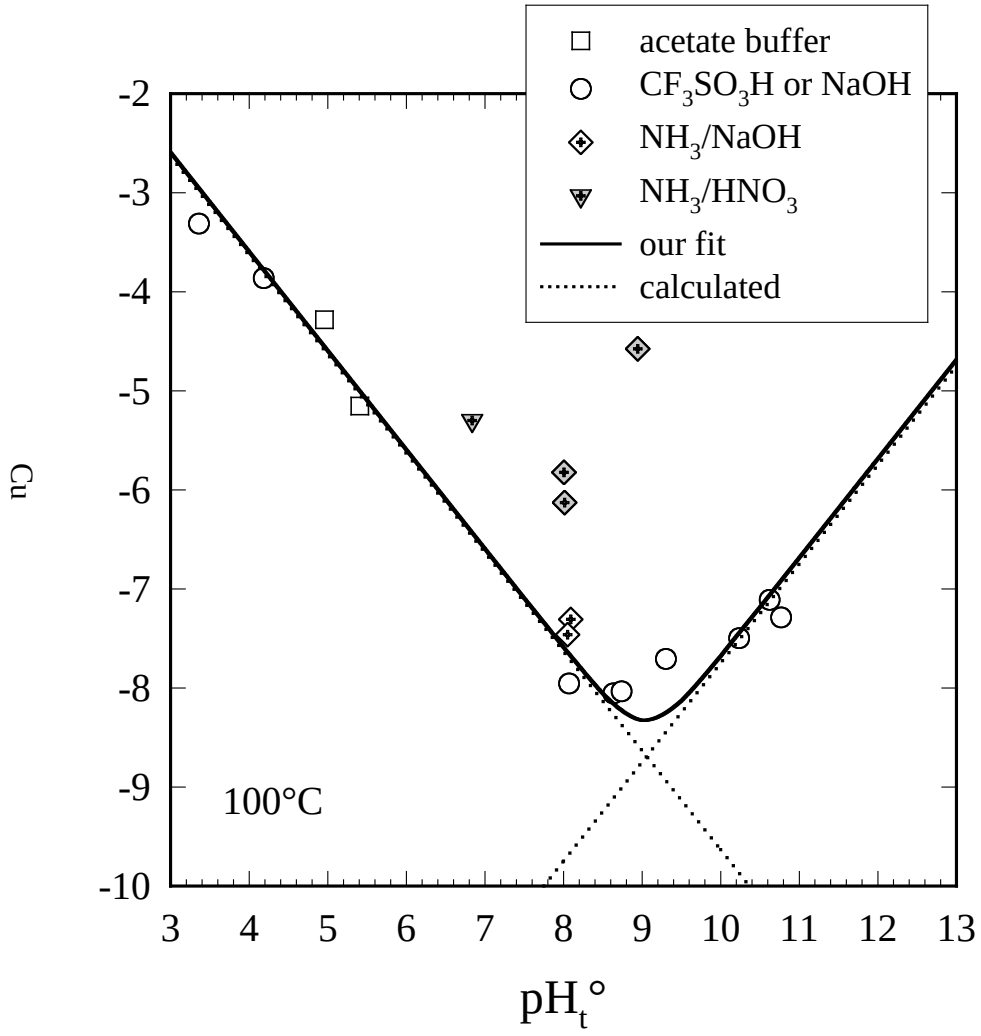

Figure 4-3
Solubility profile for CuO at 100°C (212°F) showing the curve representing the logarithm of the total copper(II) molality versus $pH_t°$ for an infinitely dilute solution. The gray values were not included in the fit. The dotted lines (referred to as calculated) were derived from Eqns. (4-22) and (4-23).

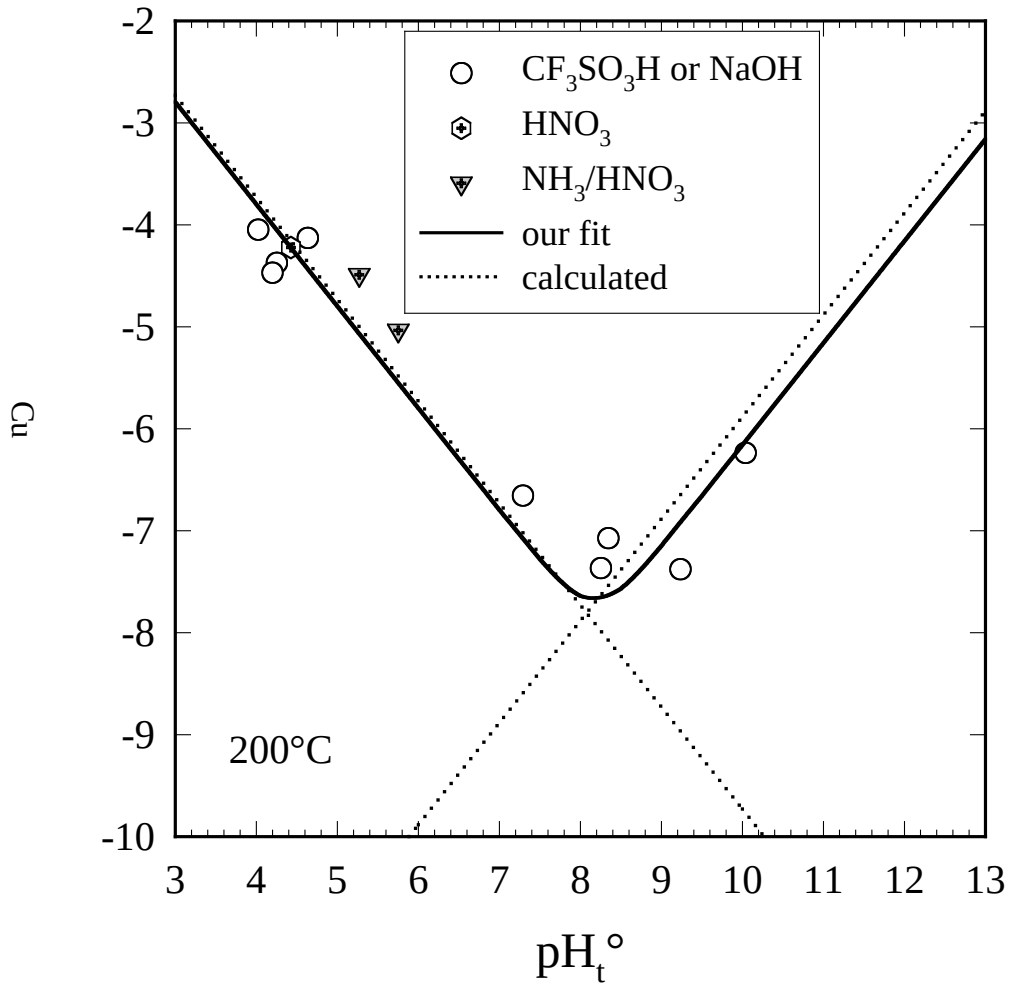

Figure 4-4
Solubility profile for CuO at 200°C (392°F) showing the curve representing the logarithm of the total copper(II) molality versus $pH_t°$ for an infinitely dilute solution. The gray values were not included in the fit. The dotted lines (referred to as calculated) were derived from Eqns. (4-22) and (4-23).

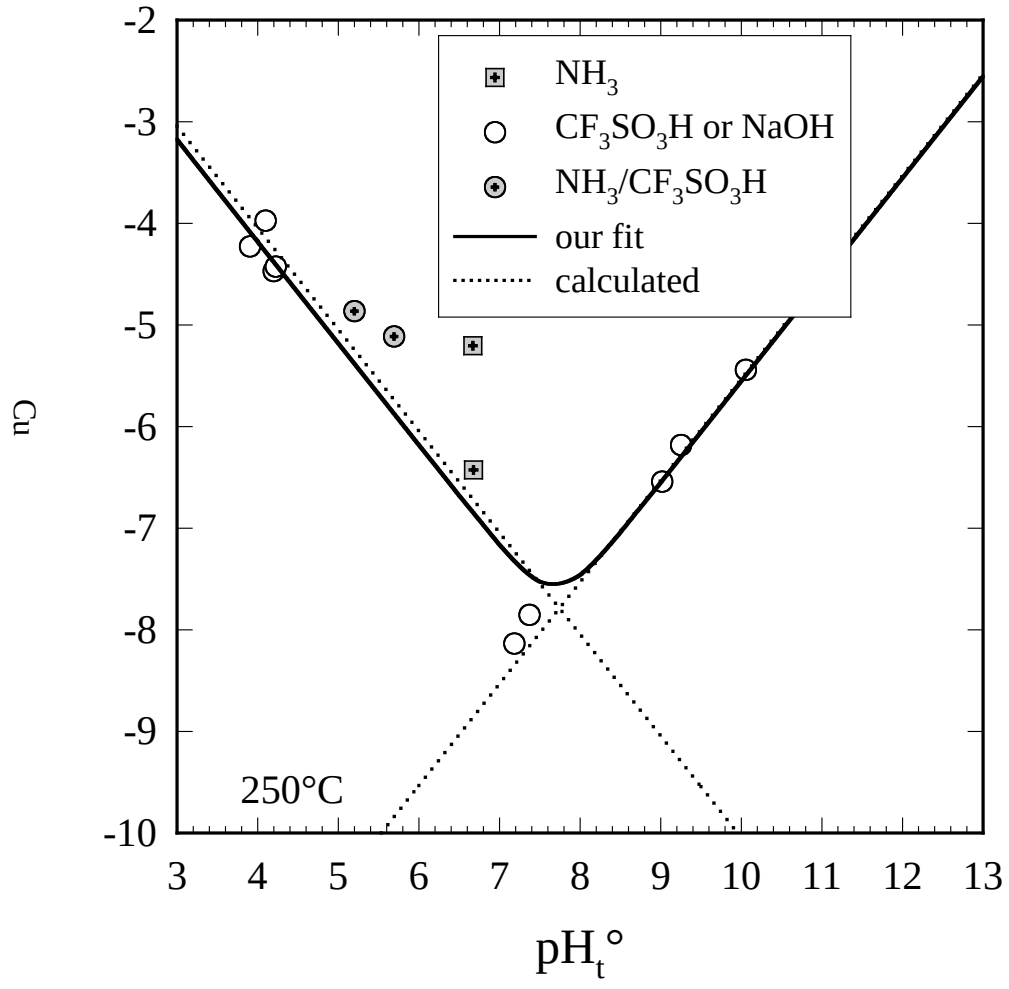

Figure 4-5
Solubility profile for CuO at 250°C (482°F) showing the curve representing the logarithm of the total copper(II) molality versus $pH_t°$ for an infinitely dilute solution. The gray values were not included in the fit. The dotted lines (referred to as calculated) were derived from Eqns. (4-22) and (4-23).

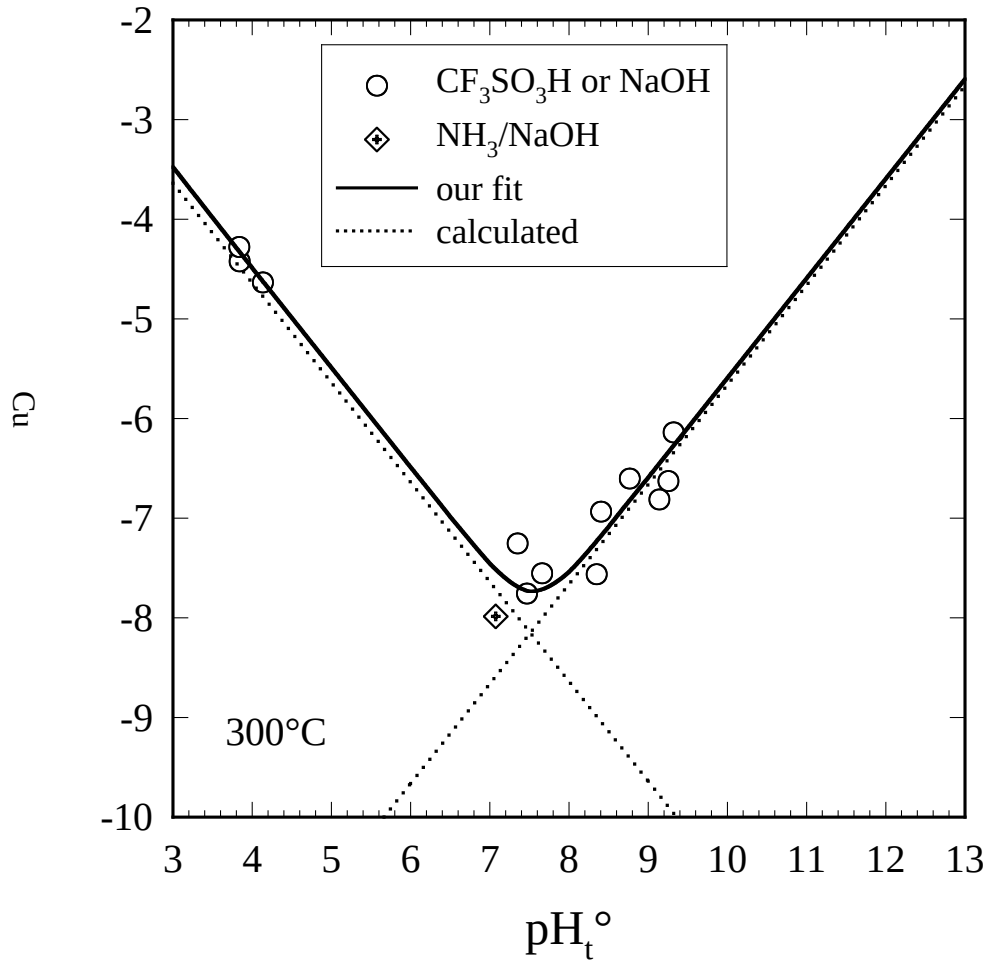

Figure 4-6
Solubility profile for CuO at 300°C (572°F) showing the curve representing the logarithm of the total copper(II) molality versus $pH_t°$ for an infinitely dilute solution. The dotted lines (referred to as calculated) were derived from Eqns. (4-22) and (4-23).

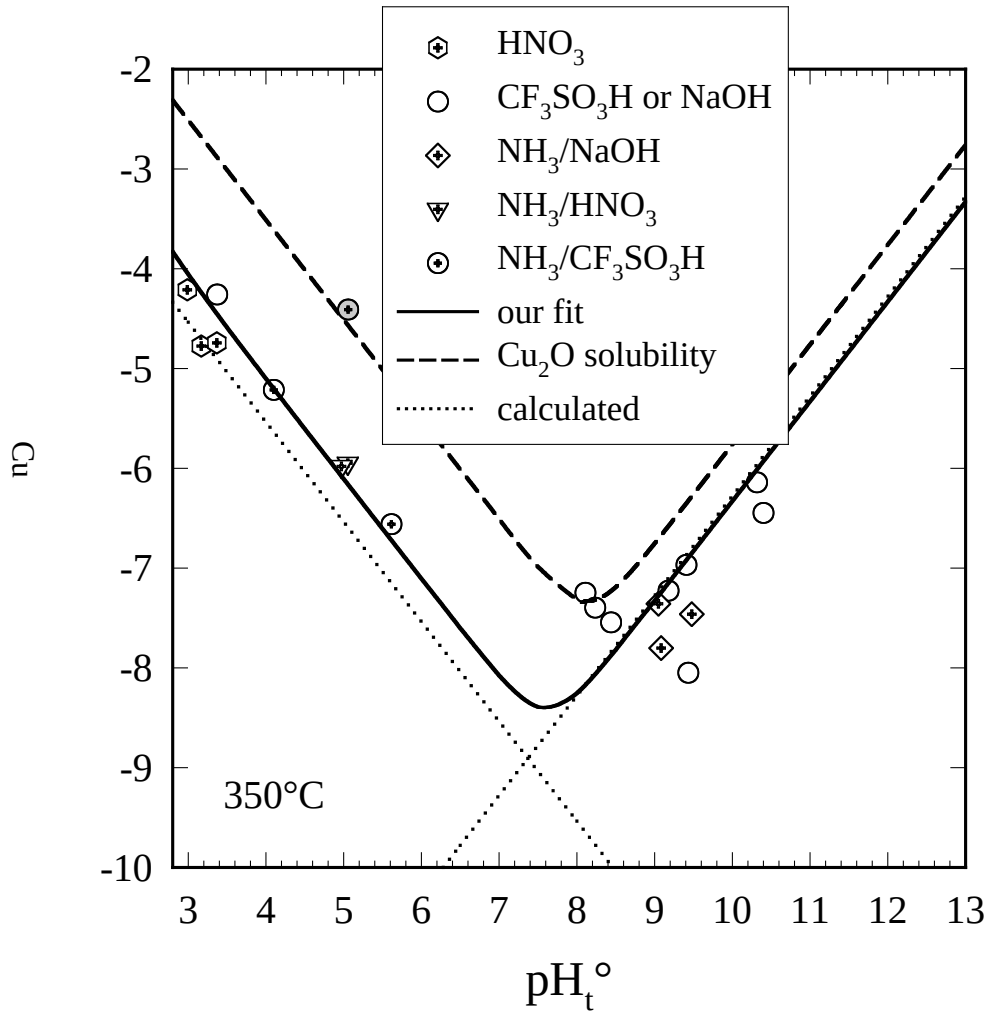

Figure 4-7
Solubility profile for CuO at 350°C (662°F) showing the curve representing the logarithm of the total copper(II) molality versus $pH_t°$ for an infinitely dilute solution. The gray value was not included in the fit. The dotted lines (referred to as calculated) were derived from Eqns. (4-22) and (4-23).

The results in Figure 4-1 show that both Tris and Bis-Tris, which are ternary and quaternary substituted amines, greatly enhance the solubility of CuO, as to a lesser extend does ammonia. However, ammonia was not even tried as a pH buffer at these low temperatures based on our experiences at higher temperatures, see Figure 4-3 for example. The simpler form of Tris and Bis-Tris is triethanolamine, which is an inexpensive stable chemical that would have a similar strong tendency to complex copper(II) and would therefore be a potential cleaning agent for removing copper oxide deposits at low temperature. Obviously as pH buffers in this research, these substituted amines are not suitable.

Two concentrations of the $NaOH/NaH_2PO_4$ buffer were investigated to give assurance that the HPO_4^{2-} species in particular did not form a complex with either the Cu^{2+} or $Cu(OH)^+$ species to a measurable extent. A similar precaution was taken with the $NaOH/CH_3COOH$ buffer at 50°C (Figure 4-2). Regression of the results in Figures 4-1 and 4-2, omitting the two values in gray in the former figure, using the ORGLS program [10] lead to derivation of four solubility constants corresponding to the solubility equilibria in Eqns. (4-1) to (4-4). The values of these constants are listed in Table 4-3 and the solid curves denoted as "our fit" in Figures 4-1 and 4-2, result from this fitting procedure. Clearly, the fit to the experimental points obtained in these various media is very good and provide strong evidence for the existence of four copper species over this range of pH_t.

Table 4-3
Experimental Solubility Constants for Cupric Oxide in Water at 25 and 50°C

T °C	log K_{s0}	log K_{s1}	log K_{s2}	log K_{s3}
25	6.22±0.08	0.92±0.05	-7.65±0.05	-19.16±0.07
50	6.93±017	0.53±0.02	-7.98±0.24	-18.81±0.23

For the higher temperature data represented in Figures 4-3 to 4-7, the same regression analysis yielded only two species in solution, namely $Cu(OH)^+$ and $Cu(OH)_3^-$, as indicated in the two previous reports [1,2]. Furthermore, as also mentioned previously, this behavior is quite different from that observed for ZnO and NiO [11,12] where at high temperatures the M^{2+} species is dominant from acidic to near neutral pH_t conditions and the $M(OH)^+$ species is almost insignificant for NiO and shows only a very narrow stability field for ZnO. However, this speciation of copper(II) results in solubility profiles that are similar in shape to those of Cu_2O described above and the absence of any measurable $Cu(OH)_2^0$ means that the solubility of CuO is highly dependent on pH_t over the full range of plant operating temperatures and pressures.

The values of log K_{s1} and log K_{s3} extracted from the regression of the data in Figures 4-3 to 4-7 are given in Table 4-4. In regressing each isothermal dataset it was found necessary to use unit weights rather than the weights based on the experimental uncertainties in each measurement in order not to bias the fits with one or two values that showed exceptional precision.

Table 4-4
Experimental Solubility Constants for Cupric Oxide in Water from 100 to 350°C

T °C	log K_{s1}	log K_{s3}
100	4.05±0.11	-17.69±0.17
200	0.20±0.16	-16.16±0.24
250	-0.18±0.15	-15.55±0.27
300	-0.49±0.12	-15.59±0.11
350	-1.11±0.12	-16.33±0.13

The values of log K_{s1} and log K_{s3} were then fitted to various combinations of temperature (T in Kelvin) terms using a version of the ORGLS routine [10]. The simplest fits that gave the best representations of each series of constants in Tables 4-3 and 4-4 are shown in Eqns. (4-22) and (4-23) where the fits were weighted according to the uncertainties given in these tables.

$$\log K_{s1} = -792.651 + 26487.41/T + 132.3301 \ln(T) - 0.1651388\ T \qquad (4\text{-}22)$$

$$\log K_{s3} = -1101.960 + 33720.94/T + 181.8137 \ln(T) - 0.2220438\ T \qquad (4\text{-}23)$$

These fits are displayed in Figures 4-8 and 4-9 as functions of reciprocal temperature in Kelvin. The turnover for both constants at high temperatures towards smaller values is consistent with the dramatic change in heat capacity of ions at the approach of the critical temperature of water. These same trends were exhibited by the corresponding log Ks0 and log Ks2 values for copper(I) in Figures 3-9 and 3-10. In Figures 4-1 to 4-7 the dotted lines were generated from application of Eqns. (4-22) and (4-23) to show how this global fit of all the data for each species compares to the individual experimental values. The largest deviation occurs at 350°C in the acidic region and can be traced to the limitations of the function form of Eqn. (4-22) that generated the curve in Figure 4-8 as it does not exhibit enough curvature to match the sharp downturn in the data at this

extreme condition. As mentioned earlier in this section, other combinations of temperature terms gave poorer fits and extra terms were statistically unjustified.

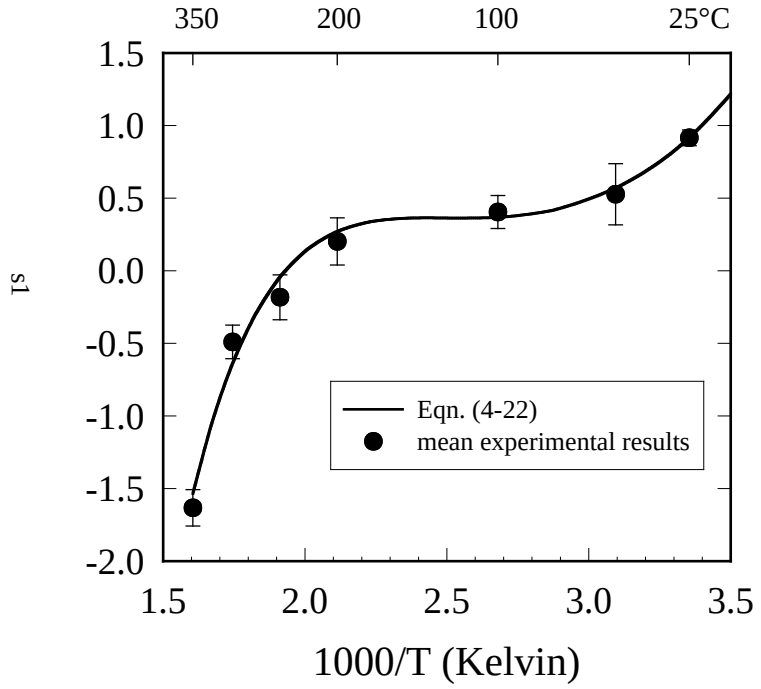

Figure 4-8
The temperature dependence of log K_{s1} for CuO in water.

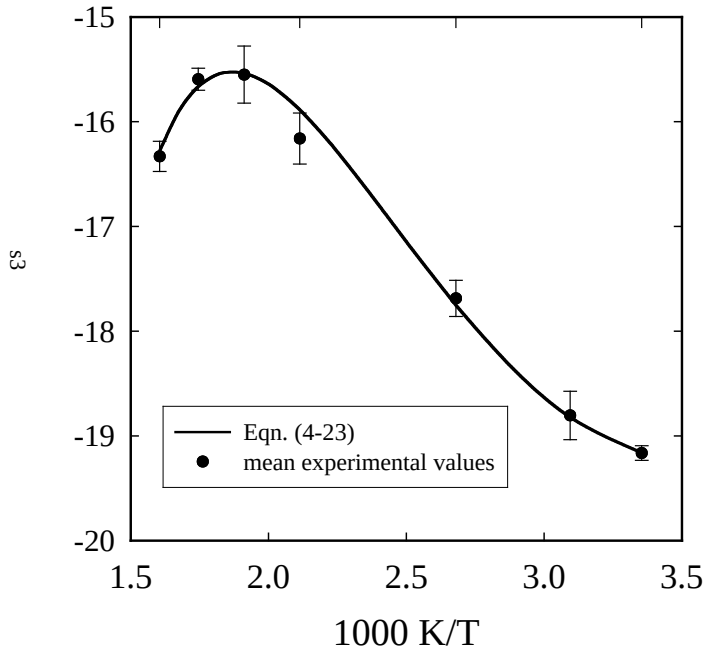

Figure 4-9
The temperature dependence of log K_{s3} for CuO in water.

The regions of pH_t where these dotted lines follow the solid curves in Figures 4-1 to 4-7 illustrated the stability fields of $Cu(OH)^+$ and $Cu(OH)_3^-$. Thus, except for 25 and 50°C where for pH_t regions of 8.6 – 11.5 and 8.6 –10.8, respectively, the $Cu(OH)_2^0$ species dominates the copper speciation in solution, the remaining pH_t space in near neutral to basic conditions at higher temperatures is dominated by $Cu(OH)^+$ and $Cu(OH)_3^-$ as indicated in previous reports. It is interesting, however, that the uncharged $Cu(OH)_2^0$ species will dominate speciation at cold startup conditions in the boiler. Although this species may be less likely to adsorb on the boiler tubing walls by electrostatic interactions, its presence will probably lead to more rapid precipitation from solutions supersaturated with copper(II). Note also that the log K_{s2} values in Table 4-3 decrease with increasing temperature thereby accounting for the decreasing influence of this species at higher temperatures.

On the other hand the log K_{s0} values appear to increase with increasing temperature which runs counter to the observation that Cu^{2+} was not even detected at $pH_t = 3$ at temperatures ≥ 100°C. The value at 25°C of 6.22 for this constant is in very poor agreement with the value quoted by Baes and Mesmer in 1976 [13] of 7.62. The value of log K_{s0} at 50°C of 6.93 is significantly larger than that 25°C, but would be expected to decrease at higher temperatures to be consistent with the behavior of other divalent transition metal ions and to account for the abrupt disappearance of Cu^{2+} by 100°C over the range of pH_t investigated here. Nevertheless, these lower pH_t conditions are of little relevance to fossil plants, except perhaps during chemical cleaning.

A comparison of the solubility of CuO and Cu_2O at 25 (77°F) and 350°C (662°F) in Figures 4-1 and 4-7 shows that the latter is less soluble by more than an order of magnitude below a $pH_t°$ of 10 at 25°C, whereas the reverse is true below a $pH_t°$ of 8 at 350°C.

It is highly significant that while carrying out series of measurements at 350°C using F_3CSO_3H and F_3CSO_3H/NH_3 buffers that one series showed abnormally high solubilities, which in fact corresponded exactly to the solubility anticipated for Cu_2O. Subsequently, a HNO_3/NH_3 buffer combination was used to provide an oxidizing medium and the solubilities reverted to those of CuO (see Figure 4-7). The water used to make up the feed solutions prior to this series had been purged with helium to remove any trace of CO_2 impurities and presumably dissolved oxygen as well. Although this behavior was not observed at other temperatures, it does indicate that reduction of CuO to Cu_2O is readily accomplished under benign reducing conditions, at least at very high temperatures and is presumably only a surface coating that is readily removed under oxidizing conditions. This single result also helps to confirm the results obtained for the pure Cu_2O phase as outline in Chapter 3.

4.3.2 Effects of added dissolved chemicals on the solubility of CuO in water

The borate and phosphate buffers used at relatively low temperatures (25 and 50°C) had no observable effect on the solubility of either copper oxide phase, although Ziemniak *et al.* [14] have demonstrated that copper(II) phosphate complexes are formed at high temperatures. Similarly, low concentrations of acetate has little or nor effect as shown in Figure 4-2, but by

analogy of other transition metal oxide systems, copper(II) acetate complexes must become important at higher temperatures [15]. For these reasons, these buffers were not employed above 50°C, although at the low levels of these anions in power plants operating under chemistries other than phosphate treatment, trace levels of acetate and phosphate (*e.g.*, a few ppb) would have negligible effects on copper transport.

Figure 4-1 clearly shows that substituted amines have an enormous (orders of magnitude) effect on the solubility of CuO at 25°C that probably extends to high pH_t values, whereas the effects of acetate for example are more restricted to low pH_t values [15]. This effect is somewhat surprising; although Bis-Tris is know to form strong complexes with aluminum at ambient conditions [16]. This result can best serve as a warning that some potential chemical additives to boiler/feed water in power plants may have very undesirable effects on copper levels in mixed metallurgy plants.

The most relevant result in terms of the effect of conditioning chemicals on the solubility of copper oxides (CuO and Cu_2O) concerns addition of ammonia as a pH_t control. The papers by Strodola *et al*. [17], Solis *et al.* [18] and many others consider that only those complexes are formed between Cu^{2+} and NH_3. The data shown in Figure 4-3 for CuO solubility at 100°C prove that ammonia complexes with the hydrolyzed forms of Cu^{2+}, most likely $Cu(OH)(NH_3)_n^+$, exist at much higher pHs that are more relevant to power plant operation. Considering the results shown in Figure 4-3 where ammonia was added to a constant concentration of NaOH in the feed solution (*i.e.*, pH_t was approximately held constant), an equilibrium constant derived from these results for the formation of $Cu(OH)(NH_3)^+$ would imply that for 1 ppm NH_3, less than 1% of the total copper in solution would be complexed in this form. Therefore, although these complexes are stronger at lower temperatures, the effect of added ammonia on copper(II) solubility under AVT chemistry would be negligible at the startup at concentrations of ammonia near the ppm level.

4.3.3 Solubility of CuO in steam

The results of all the CuO solubility measurements in steam are summarized in Table 4-5 and illustrated in Figure 4-10. These measurements were made using the flow-through cell with acid injection so that deposition in the sampling lines could not account for these low solubilities in steam. These data are also consistent with the pioneering results of Pocock and Stewart [19] obtained in supercritical steam. A revised equation (Eqn. 4-24), which has the same form as used to fit the solubility data for Cu_2O in steam (Section 3.3.2), is presented below that represents the solubility of CuO in steam as a function of temperature and pressure.

$$\log (\text{Cu(II), ppb}) = -0.613 + 7.296 \cdot 10^{-4}\, t + 4.337 \cdot 10^{-3}\, p \qquad (4\text{-}24)$$

where temperature (t) and pressure (p) are given in units of °C and bars, respectively. This equation was revised to include new data and simplified from that given in an earlier report [1]. Strictly it would be more thermodynamically rigorous to use temperature in Kelvin and replace pressure with the density of water. However, given that this is a very approximate equation due to the experimental uncertainties in the data, the current form is user-friendlier.

The fundamental conclusion remains that the solubility of CuO in steam is only slightly dependent on temperature, but increases with pressure. The latter effect is only distinct at supercritical temperatures where higher steam densities can be attained with increasing pressure without the limit of condensation.

The compatibility of the current results with those of Pocock and Stewart [19] is clearly apparent from the combined results shown in Figure 4-10. As discussed in the previous chapter, the later results of Hearn *et al.* [20], who found much higher solubilities than reported by Pocock and Stewart, appear more in line with our results for Cu_2O in liquid water, but are still much higher than found in this report for either solid in the steam phase. Hearn *et al.* outlined possible experimental flaws in the data of Pocock and Stewart, but these concerns appear groundless and indeed some reduction of the charge of CuO must have occurred in the experiments of Hearn *et al.* and the sensitivity of CuO to reduction has already been mentioned in section 4.3.1 based on our experience at high temperatures.

Table 4-5
Summary of All Data for the Solubility of Cupric Oxide in Steam

T °C	P bar	P_{sat} bar	Buffer	NaOH ppm	NH_3 ppm	log $m_{Cu}°$	Cu ppb
200	14	15.5	NaOH	3336	-	-7.444±0.273	2.3
250	34	39.7	NaOH	41	-	-7.560±0.102	1.9
250	39	39.7	NaOH	576	-	-7.560±0.461	1.9
250	37	39.7	NaOH	319	-	-7.717±0.470	1.2
250	37	39.7	NaOH	45.6	-	-7.958±0.353	0.7
250	36	39.7	NaOH	4.0	-	-7.588±0.380	1.9
250	36	39.7	NaOH	3276	-	-8.241±0.466	0.4
300	86	85.8	NaOH/NH_3	2.0	173	-7.515±0.186	1.9
300	84	85.8	NaOH	4092	-	-7.524±0.186	1.9
300	84	85.8	NaOH	26.4	-	-7.623±0.267	1.5
300	85	85.8	NaOH	424	-	-7.591±0.361	1.6

300	84	85.8	NaOH	113	-	-7.290±0.137	3.3

Table 4-5
Continued

T °C	P bar	P_{sat} bar	Buffer	NaOH ppm	NH_3 ppm	log m_{Cu}°	Cu ppb
303	84	89.5	NaOH	37.6	-	-7.801±0.720	1.0
350	100	165.2	NaOH/NH_3	8.8	14.3	-7.590±0.773	1.6
350	124	165.2	NaOH/NH_3	28.4	156	-7.554±0.635	1.8
350	121	165.2	NaOH/NH_3	93.6	1685	-7.394±0.303	2.6
350	105	165.2	NaOH/NH_3	41.6	332	-7.529±0.608	1.9
350	80	165.2	NaOH/NH_3	41.6	332	-7.736±0.630	1.2
350	48	165.2	NaOH/NH_3	8.4	13.3	-7.896±0.367	0.8
350	156	165.2	NaOH	672	-	-7.461±0.238	3.5
350	155	165.2	NaOH	48.0	-	-7.950±0.282	0.7
350	161	165.2	NaOH	31.2	-	-7.976±0.678	0.7
400	100	-	NH_3	-	9.0	-7.865±0.645	0.9
400	144	-	NH_3	-	10.7	-7.345±0.318	2.9

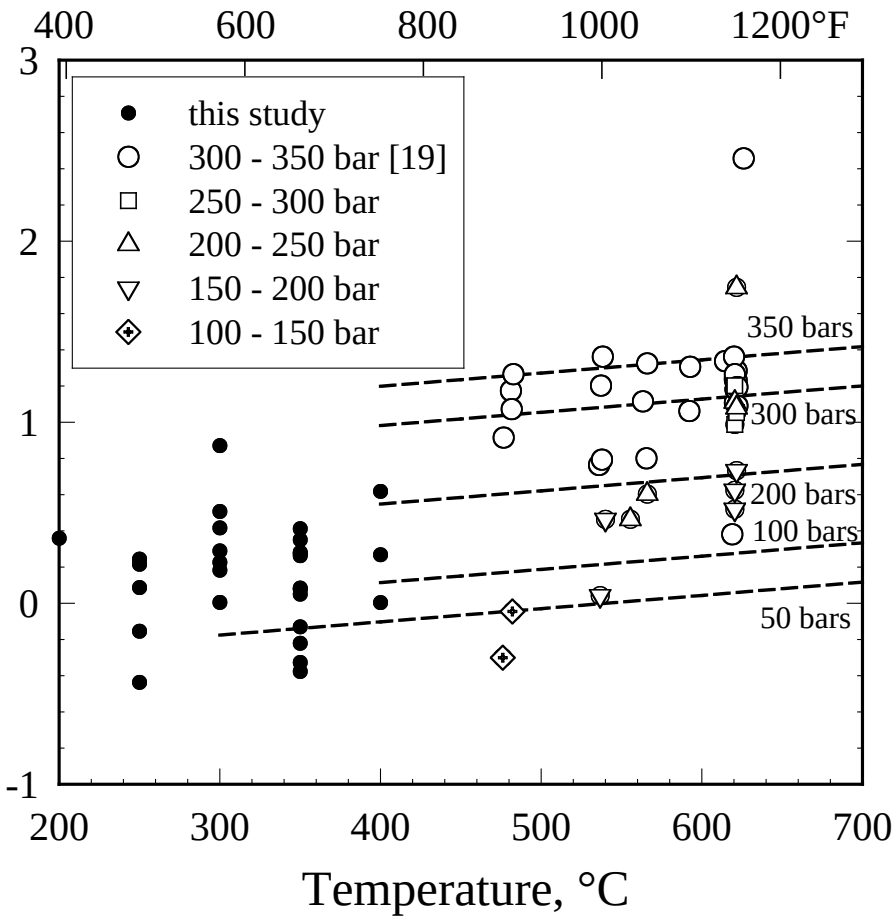

Figure 4-10
Logarithm of the copper(II) concentration in ppb as a function of temperature. The solid points are from this study (Table 4-5) whereas the open symbols represent the data of Pocock and Stewart [19]. The dashed lines were derived from Eqn. (4-24), which is valid at pressures and temperatures corresponding to the steam phase.

A comparison of the calculated solubilities of CuO and Cu_2O is illustrated in Figure 4-11. It must be remembered that the fit of the experimental data for the former oxide is based on a much larger data set than the latter. Given the experimental uncertainties, the general conclusion is that the solubilities are similar over most sub- and super-critical conditions with an apparent higher solubility of Cu_2O at higher pressures in the near super-critical region and a lower solubility at higher temperatures and low pressures.

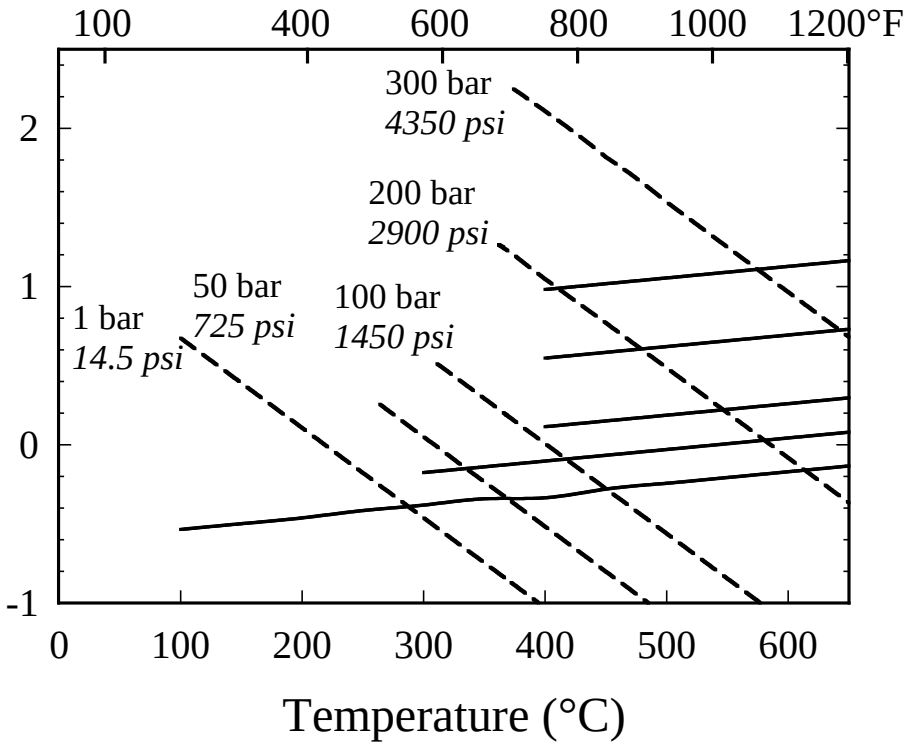

Figure 4-11
Comparison of the solubilities of CuO and Cu_2O is steam as a function of temperature, represented at arbitrarily chosen pressures by solid and dashed lines, respectively.

In order to present these results in terms of the partitioning constants of cuprous hydroxide the following equilibria must be considered. First, the partitioning equilibrium can be written in terms of basic solutions:

$$Cu(OH)_3^- \text{ (liq)} + H^+ \text{ (liq)} \Leftrightarrow Cu(OH)_2^0 \text{ (vap)} + H_2O \text{ (liq)} \qquad (4\text{-}25)$$

The partitioning constant as defined by reaction (4-25) is then given by:

$$K_D^* = m\{Cu(OH)_2^0\}_{vap}/(m\{Cu(OH)_3^-\}\gamma\{Cu(OH)_3^-\}m\{H^+\}_{liq}\gamma\{H^+\}) \qquad (4\text{-}26)$$

Under the condition that the solutions are saturated with respect to Cu_2O, it follows by combining equations (4-9) and (4-26):

$$K_D^*(CuO,sat) = m\{Cu(OH)_2^0\}_{vap}/K_{s3} \qquad (4\text{-}27)$$

As in all previous cases, the activity coefficient of the neutral species in the vapor phase is assumed to be unity.

The second approach is to consider the partitioning equilibrium in terms of $Cu(OH)^+$ in acidic solutions:

$$Cu(OH)^{+}(liq) + OH^{-}(liq) \Leftrightarrow Cu(OH)_2^{0}(vap) \quad (4\text{-}28)$$

The partitioning constant is then given by the expression:

$$K_D = m\{Cu(OH)_2^{0}\}_{vap}/(m\{Cu(OH)^{+}\}\gamma\{Cu(OH)^{+}\}m\{OH^{-}\}_{liq}\{OH^{-}\}) \quad (4\text{-}29)$$

Combination of Eqn. (3-20) under saturation conditions with respect to Cu_2O with Eqns. (4-7) and (4-29) gives:

$$K_D(CuO,sat) = m\{Cu(OH)_2^{0}\}_{vap}/(K_{s1}K_w) \quad (4\text{-}30)$$

The temperature dependencies of the partitioning constants, K_D and K_D*, for saturated solutions in contact with CuO and Cu_2O are displayed in Figure 4-12 with a comparison to the data for aqueous solutions containing HCl and NaOH. Note that the partitioning equilibria associated with the two copper oxides (Eqs. 3-19 and 4-28) are directly analogous to the partitioning of NaOH according to the thermodynamic concept used in throughout this program, *viz.*,

$$Na^{+}(liq) + OH^{-}(liq) \Leftrightarrow NaOH^{0}(vap) \quad (4\text{-}31)$$

Therefore, the partitioning constants for these three reactions can be compared directly. Clearly the copper(I) and (II) species can be considered as being highly volatile from this comparison. The caveat being that the concentrations of copper(I) and (II) cations are extremely low at high pH as dictated by the solubilities of the oxides, whereas NaOH is highly soluble so that high concentrations of both its composite ions can be reached in caustic solutions. Nevertheless, for most power plant applications where the concentration of sodium ions in the boiler may be on the order of a few ppb or less and the concentration of hydroxide ions is only on the order of 1 ppm, the dissolved copper(I) and (II) can be considered as being very volatile, even comparable to, or exceeding, that of HCl which is generally thought of as being a volatile acid at high temperatures.

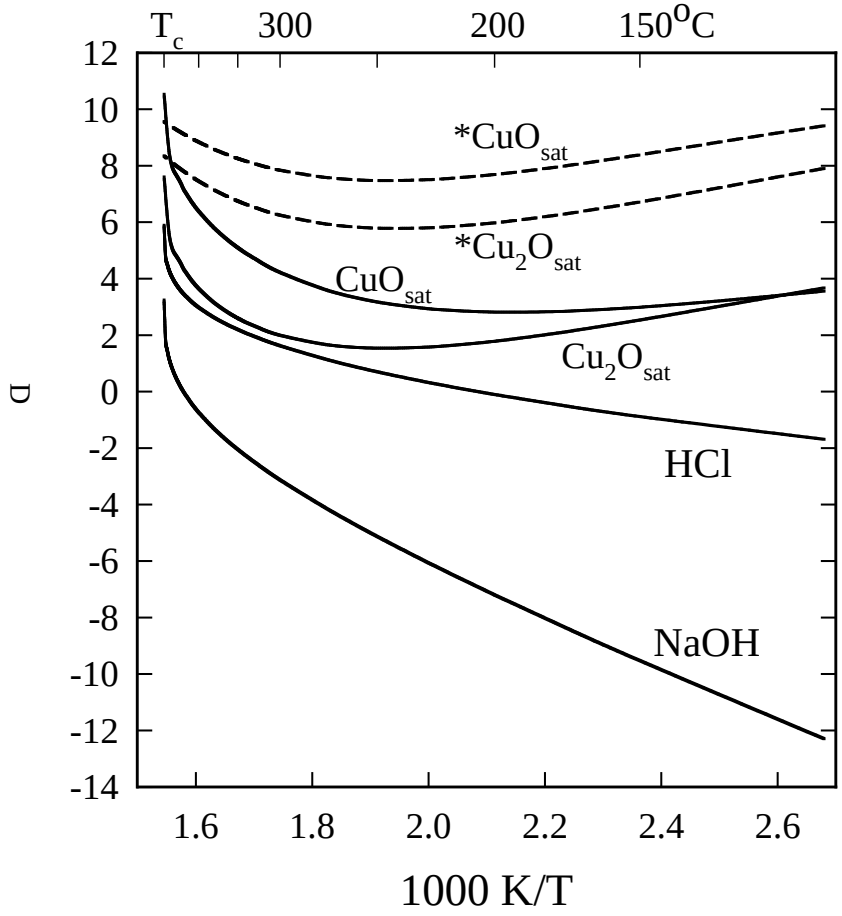

Figure 4-12
Logarithm of the partitioning constants for Cu(I) and Cu(II) as a function of temperature, with comparisons to those for HCl and NaOH, where the solid curves for the copper species should be compared as their equations have equivalent forms.

4.4 Applications

The solubilities of CuO and Cu_2O are compared in Figures 4-1 and 4-7 at the extremes of the temperature range investigated in this research project clearly demonstrating that at the range of pH_t values encountered in fossil-fired power plants, Cu_2O is significantly less soluble at start up conditions, but is almost equally more soluble at normal operating temperatures. However, it is insightful to compare the relative solubilities for pH_t values that correspond to fixed $pH_{25°C}$ values typical of those referenced in EPRI guidelines, for example. Figure 4-13 illustrates the results of such a comparison where the solubilities of both oxides in water are given in ppb units as a function of temperature, at two fixed values of $pH_t°$ (t = 25°C), namely 9.0 and 9.5. Clearly if these two reference $pH_{25°C}$ were maintained during startup or if these temperature gradients are

encountered in the feed-water preheaters, then large solubility variations would occur that could lead to dissolution and re-precipitation, or the reverse. Moreover, higher $pH_{25°C}$ values favor lower solubilities across the whole spectrum of temperatures with $pH_{25°C}$ values of 10 giving close to the minimum copper levels. In addition it is clear that Cu_2O is far more soluble and its temperature dependence is more extreme than that of CuO. Other scenarios would be interesting to consider, such as considering fixed $pH_{25°C}$ values at 350°C as determined by an NH_4^+/NH_3 buffer under typical AVT conditions and calculating the equilibrium copper concentrations as this solution is cooled to 25°C. Other buffers and buffer mixtures used under various chemistries at normal and action-level conditions could also be treated in this manner. Finally, it must be emphasized that these predictions are all based on equilibrium conditions, whereas in actual operating plants solutions are likely to be undersaturated where dissolution occurs and possibly oversaturated where precipitation takes place. Moreover other mixed oxide phases may influence the copper concentration in the water/steam cycle and surface adsorption of dissolved copper onto plant internals may further affect the levels of copper in the system.

The effect of added water treatment chemicals (*e.g.*, NH_3) or contaminants (phosphate, acetate, and chloride) on the solubilities of CuO and Cu2O are measurable in experiments, but can generally be ignored in the water – steam cycles of fossil-fired plants (see section 4.3.2).

The solubility of CuO in steam appears to be virtually constant up to high temperatures (*ca*. 350°C) at pressures close to the saturation pressure of water. However, this constant amount of *ca*. 1.5ppb is much higher than for many treatment chemicals and impurities with the exception of ammonia and other volatile chemicals. This can lead to a constant flow of copper from the boiler as vaporous carry over. The more marked effect of pressure on the solubility at supercritical conditions can lead to precipitation and re-dissolution onto and from the superheater walls to the high-pressure turbine if the plant is operated under a variable load.

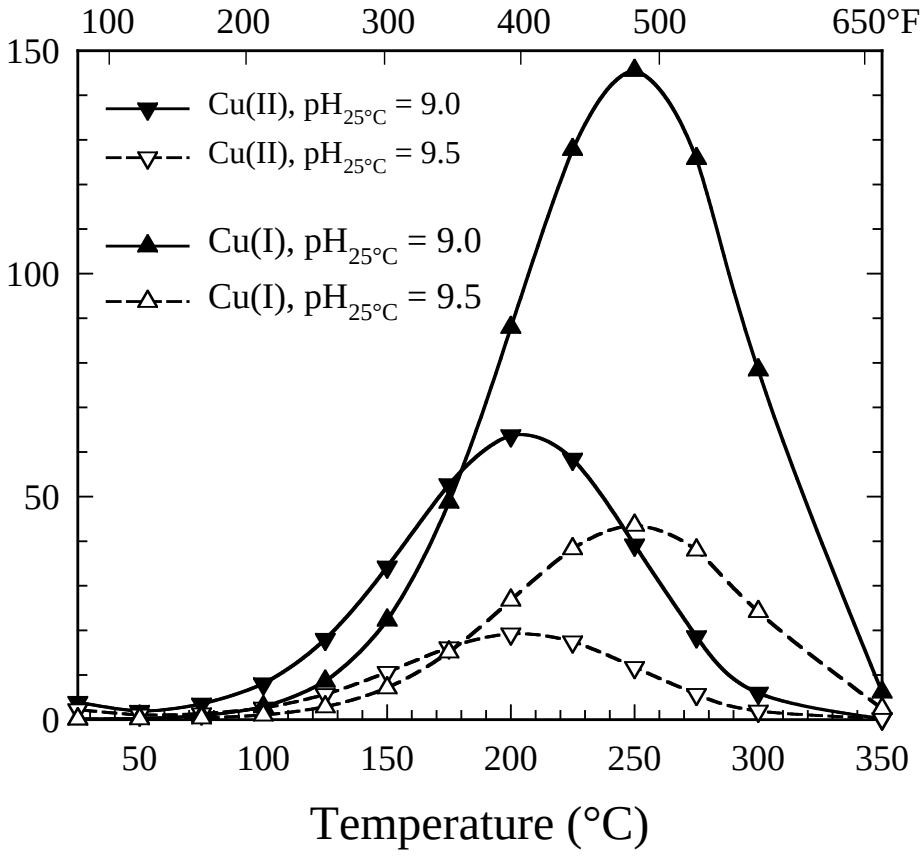

Figure 4-13
The temperature dependence of the solubilities of CuO and Cu_2O in water at two fixed $pH_{25°C}$ values, *viz.* 9.0 and 9.5.

4.5 References

1. D.A. Palmer, P. Bénézeth, A.Y. Petrov, L.M. Anovitz, and J.M. Simonson. *Behavior of Aqueous Electrolytes in Steam Cycles, The Solubility and Volatility of Cupric Oxide*, EPRI, Palo Alto, CA: November 2000. TR-1000455.

2. D.A. Palmer, P. Bénézeth, A.Y. Petrov, L.M. Anovitz, and J.M. Simonson. *Behavior of Aqueous Electrolytes in Steam Cycles, The Solubility and Volatility of Copper(I) and Copper(II) Oxides*, EPRI, Palo Alto, CA: December 2001. TR-1003993.

3. W.T. Lindsay, Jr., "Chemistry of Steam Cycle Solutions: Principles", in "*The ASME Handbook on Water Technology for Thermal Power Plants*", P. Cohen, Ed., The American Society of Mechanical Engineers, Chapter 7, p. 483 (1989).

4. W. Wagner and A. Pruss, "The IAPWS Formulation 1995 for the Thermodynamic Properties of Ordinary Water Substance for General and Scientific Use." *Journal of Chemical Reference Data*, Vol. 31, No. 2, 387–535 (2002).

5. D.A. Palmer, P. Bénézeth and D.J. Wesolowski, "Boric Acid Hydrolysis: A New Look at the Available Data." *PowerPlant Chemistry*, Vol. 2, No. 5, pp. 261-264 (2000).

6. R.E. Mesmer and C.F. Baes, Jr., "Phosphoric Acid Dissociation Equilibria in Aqueous Solutions to 300°C." *Journal of Solution Chemistry*, Vol. 3, No. 4, pp. 307-322 (1974).

7. R.E. Mesmer, C.S. Patterson, R.H. Busey and H.F. Holmes, "Ionization of Acetic Acid in NaCl(aq) Media: A Potentiometric Study to 573 K and 130 bar." *Journal of Physical Chemistry*, Vol. 93, pp. 7483-7490 (1989).

8. D.A. Palmer and D. Wesolowski, "Acid Association Quotients of Tris(hydroxymethyl)-aminomethane in Aqueous NaCl Media to 200°C." *Journal of Solution Chemistry*, Vol. 16, No. 7, pp. 571-581 (1987).

9. D.J. Wesolowski and D.A. Palmer, "Acid Association Quotients of Bis-Tris in Aqueous Sodium Chloride Media to 125°C." *Journal of Solution Chemistry*, Vol. 18, No. 6, pp. 545-559 (1989).

10. W.R.Busing and H.A.Levy, "ORGLS, A General Fortran Least Squares Program." Oak Ridge National Laboratory Report, ORNL-TM-271 (1962).

11. P. Bénézeth, D.A. Palmer and D.J. Wesolowski, "*Overcoming Solubility Limitations to Zinc Addition in Pressurized Water Reactors*." EPRI, Palo Alto, CA: December 2001. TR-1003156.

12. D.A. Palmer, Bénézeth, D.J. Wesolowski and L.M. Anovitz, "Impact of Nickel Oxide Solubility on PWR Fuel Deposition Chemistry." EPRI, Palo Alto, CA: in press, TR-1003155.

13. C.F. Baes, Jr. and R.E. Mesmer, "*The Hydrolysis of Cations*." John Wiley and Sons, 1976.

14. S.E. Ziemniak, M.E. Jones and K.E.S. Combs, "Copper(II) Oxide Solubility Behavior in Aqueous Sodium Phosphate Solutions at Elevated Temperatures." *Journal of Solution Chemistry*. Vol. 29, pp. 179-200 (1992).

15. T.H. Giordano and S.E. Drummond, "The Potentiometric Determination of Stability Constants for Zinc Acetate Complexes in Aqueous Solutions to 295°C." *Geochimica et Cosmochimica Acta*. Vol. 55, pp. 2401-2415 (1991).

16. D.J. Wesolowski, D.A. Palmer and G.M. Begun, "Complexation of Aluminate by Bis-Tris Aqueous Media at 25-50°C." *Journal of Solution Chemistry*. Vol. 19, pp.159-173 (1990).

17. J. Stodola, P. Tremaine, V. Binette, and L. Trevani, "Volatility of Copper Corrosion Products in Reactor Primary Conditions." *PowerPlant Chemistry*. Vol. 2, pp. 9-13 (2000).

18. J.S. Solis, G. Hefter and P.M. May, "Chemical Speciation in the Copper(I)-Ammonia-Chloride System." *Australian Journal of Chemistry*. Vol. 48, pp. 1283-1292 (1995).

19. F.J. Pocock and J.F. Stewart, "The Solubility of Copper and Its Oxides in Supercritical Steam." *Journal of Engineering for Power*. pp. 33-45 (1963).

20. B. Hearn, M.R. Hunt, and A. Hayward, "Solubility of Cupric Oxide in Pure Subcritical and Supercritical Water," *Journal of Chemical and Engineering Data.* Vol. 14, pp. 442-447 (1969).

A
SOLUBILITY DATA FOR CUPROUS OXIDE OBTAINED WITH THE HIGH-TEMPERATURE CELL

The samples are listed in chronological order within each table, which are divided according to the nature of the feed solution used. As indicated in the schematic of the apparatus in Figure 2-1, the two pressures listed in the following tables refer to the inlet pressure immediately upstream from the pre-heater and the pressure of the gas ballast reservoir. The concentrations and flow rates given in the next column refer to the feed solution and in all cases a post reactor solution was injected into the flow just after it exits the reaction vessel or column. The analytical techniques employed are symbolized as: flame atomic absorption spectrophotometry (AA), graphite furnace atomic absorption spectrophotometry (GFAA) and inductively-coupled plasma mass spectrometry (ICPMS).

Table A-1
Cuprous oxide solubility data in trifluoromethanesulfonic acid solutions

Sample ID	Temperature °C	Inlet pressure bar	Outlet pressure bar	CF_3SO_3H, m Flow rate mL· min^{-1}	Cu (AA) ppm
Cu_2O-250-4-1	250.1	54.2	54.0	0.0003104 0.1	11.7
Cu_2O-250-4-2	250.1	54.7	54.3	0.0003104 0.1	11.9
Cu_2O-250-4-3	250.1	54.7	54.5	0.0003104 0.1	13.1
Cu_2O-250-4-4	250.0	54.6	54.5	0.0003104 0.1	13.0
Cu_2O-250-4-5	250.2	54.8	54.6	0.0003104 0.1	14.2
Cu_2O-250-4-6	250.2	54.8	54.6	0.0003104 0.1	13.4
Cu_2O-250-4-7	250.0	54.9	54.7	0.0003104 0.1	14.2
Cu_2O-250-4-8	250.1	55.0	54.7	0.0003104 0.1	16.3
Cu_2O-250-4-9	250.1	54.8	54.6	0.0003104 0.1	16.3
Cu_2O-250-4-10	250.1	54.9	54.7	0.0003104 0.1	17.8
Cu_2O-250-8-2	300.2	92.8	91.9	0.0009769 0.1	49.4
Cu_2O-250-8-3	300.0	93.2	92.4	0.0009769 0.1	49.7
Cu_2O-250-8-4	300.1	94.1	91.5	0.0009769 0.1	49.2
Cu_2O-250-8-5	300.0	94.1	93.2	0.0009769 0.1	50.1
Cu_2O-250-8-6	300.0	94.2	93.2	0.0009769 0.1	49.7
Cu_2O-250-8-7	300.1	93.9	92.6	0.0009769 0.1	48.9
Cu_2O-250-8-8	300.0	94.0	92.6	0.0009769 0.1	49.3
Cu_2O-300-9-1	300.1	96.1	91.6	0.0001958 0.1	9.1
Cu_2O-300-9-2	300.2	97.3	91.4	0.0001958 0.1	7.8
Cu_2O-250-9-3	300.2	93.9	85.2	0.0001958 0.1	8.5

Table A-1
Continued

Sample ID	Temperature °C	Inlet pressure bar	Outlet pressure bar	CF_3SO_3H, m Flow rate mL· min^{-1}	Cu (AA) ppm
Cu_2O-250-9-4	300.1	94.6	94.3	0.0001958 0.1	8.4
Cu_2O-250-9-5	300.0	94.5	91.1	0.0001958 0.1	8.5
Cu_2O-300-12-2	300.0	121.7	121.5	0.0009595 0.1	47.2
Cu_2O-300-12-3	300.0	119.9	119.7	0.0009595 0.1	47.0
Cu_2O-300-12-4	300.0	121.5	121.4	0.0009595 0.1	46.9
Cu_2O-300-12-5	300.0	118.4	118.3	0.0009595 0.1	46.9
Cu_2O-300-12-6	300.0	118.8	118.7	0.0009595 0.1	47.0
Cu_2O-300-12-7	300.0	118.5	118.3	0.0009595 0.1	47.2
Cu_2O-300-12-8	300.0	115.1	115.0	0.0009595 0.1	47.1
Cu_2O-300-12-9	300.0	119.5	119.4	0.0009595 0.1	47.2
Cu_2O-300-12-10	300.0	119.6	119.5	0.0009595 0.1	47.2
Cu_2O-300-12-11	300.0	119.6	119.5	0.0009595 0.1	47.3

Table A-2
Cuprous oxide solubility data in sodium hydroxide solutions

Sample ID	Temperature °C	Inlet pressure bar	Outlet pressure bar	NaOH, m Flow rate mL· min^{-1}	Cu (GFAA) ppb
Cu_2O-250-9-1*	250.0	41.3	41.3	0.001089 0.1	~~18.0~~
Cu_2O-250-9-2*	250.0	41.3	41.3	0.001089 0.1	~~8.0~~
Cu_2O-250-9-3*	250.1	41.0	41.1	0.001089 0.1	7.1
Cu_2O-250-9-4*	250.1	41.2	41.3	0.001089 0.1	7.3
Cu_2O-250-9-5*	250.0	41.2	41.3	0.001089 0.1	5.1
Cu_2O-250-9-6*	250.1	41.1	41.1	0.001089 0.1	4.8
Cu_2O-250-9-7*	250.0	41.3	41.3	0.001089 0.1	4.2
Cu_2O-250-9-8*	250.0	40.7	40.8	0.001089 0.1	3.3
Cu_2O-250-9-9*	250.0	41.0	41.1	0.001089 0.1	2.1
Cu_2O-250-1-2	200.1	54.0	52.1	0.000996 0.1	9.8
Cu_2O-250-1-3	200.1	50.6	47.3	0.000996 0.1	12.1
Cu_2O-250-1-4	200.0	54.1	51.4	0.000996 0.1	11.1
Cu_2O-250-1-5	200.1	55.4	53.6	0.000996 0.1	9.5
Cu_2O-250-1-6	200.0	55.6	53.8	0.000996 0.1	11.1
Cu_2O-250-1-7	200.2	56.5	53.8	0.000996 0.1	11.9
Cu_2O-250-1-8	200.2	55.3	53.6	0.000996 0.1	8.3
Cu_2O-250-1-9	200.2	58.7	53.0	0.000996 0.1	12.9
Cu_2O-250-1-10	200.2	89.7	53.2	0.000996 0.1	8.0
Cu_2O-200-2-1	200.2	51.2	51.0	0.000125 0.1	29.9

Cu_2O-200-2-2	200.0	51.3	51.1	0.000125 0.1	35.9

Table A-2
Continued

Sample ID	Temperature °C	Inlet pressure bar	Outlet pressure bar	NaOH, m Flow rate mL· min^{-1}	Cu (GFAA) ppb
Cu_2O-200-2-3	200.2	51.2	51.0	0.000125 0.1	27.6
Cu_2O-200-2-4	200.0	51.1	50.9	0.000125 0.1	30.0
Cu_2O-200-2-5	200.1	51.0	50.8	0.000125 0.1	26.2
Cu_2O-200-2-6	200.0	47.3	47.1	0.000125 0.1	32.8
Cu_2O-200-2-7	200.2	51.3	51.1	0.000125 0.1	27.3
Cu_2O-200-2-8	200.1	53.6	53.4	0.000125 0.1	23.9
Cu_2O-200-2-9	200.2	56.6	56.5	0.000125 0.1	23.9
Cu_2O-250-3-1	250.1	53.8	53.7	0.001205 0.1	13.4
Cu_2O-250-3-2	250.2	53.9	53.8	0.001205 0.1	13.4
Cu_2O-250-3-3	250.2	54.4	54.3	0.001205 0.1	16.2
Cu_2O-250-3-4	250.1	54.6	54.4	0.001205 0.1	~~24.5~~
Cu_2O-250-3-5	250.1	54.6	54.5	0.001205 0.1	~~61.8~~
Cu_2O-250-3-6	250.0	54.5	54.4	0.001205 0.1	11.1
Cu_2O-250-3-7	250.1	54.7	54.5	0.001205 0.1	12.1
Cu_2O-250-3-8	250.1	54.4	54.3	0.001205 0.1	11.7
Cu_2O-250-3-9	250.1	54.5	54.4	0.001205 0.1	10.1
Cu_2O-250-3-10	250.2	54.6	54.5	0.001205 0.1	11.1
Cu_2O-250-3-11	250.0	54.6	54.5	0.001205 0.1	12.4
Cu_2O-250-3-12	250.2	54.0	53.9	0.001205 0.1	12.2
Cu_2O-250-3-13	250.0	53.5	53.4	0.001205 0.1	11.7

Cu_2O-250-3-14	250.1	52.2	52.0	0.001205 0.1	11.1

Table A-2
Continued

Sample ID	Temperature °C	Inlet pressure bar	Outlet pressure bar	NaOH, m Flow rate mL· min^{-1}	Cu (GFAA) ppb
Cu_2O-250-3-15	250.1	54.3	54.1	0.001205 0.1	11.4
Cu_2O-250-6-2	250.0	54.7	54.5	0.001118 0.1	~~22.1~~
Cu_2O-250-6-3	250.1	54.9	54.8	0.001118 0.1	12.7
Cu_2O-250-6-4	250.0	54.9	54.7	0.001118 0.1	12.2
Cu_2O-250-6-5	250.1	54.5	54.4	0.001118 0.1	11.4
Cu_2O-250-6-6	250.2	53.2	53.0	0.001118 0.1	11.3
Cu_2O-250-6-7	250.0	53.8	53.7	0.001118 0.1	15.0
Cu_2O-250-6-8	250.0	54.1	54.0	0.001118 0.1	11.8
Cu_2O-250-6-9	250.2	53.1	53.0	0.001118 0.1	11.9
Cu_2O-250-6-10	250.1	53.8	53.7	0.001118 0.1	11.9
Cu_2O-250-6-11	250.1	54.1	54.0	0.001118 0.1	11.4
Cu_2O-250-6-12	250.1	53.1	52.9	0.001118 0.1	10.0
Cu_2O-250-6-13	250.1	54.1	53.9	0.001118 0.1	10.0
Cu_2O-250-7-2	250.1	52.1	51.2	0.01002 0.1	224
Cu_2O-250-7-3	250.0	53.7	53.6	0.01002 0.1	227
Cu_2O-250-7-4	250.2	52.1	51.2	0.01002 0.1	222
Cu_2O-250-7-5	250.2	52.7	51.5	0.01002 0.1	220
Cu_2O-250-7-6	250.1	53.5	53.4	0.01002 0.1	221
Cu_2O-250-7-7	250.0	53.3	53.2	0.01002 0.1	220

Cu_2O-250-7-8	250.0	56.5	54.1	0.01002 0.1	244

Table A-2
Continued

Sample ID	Temperature °C	Inlet pressure bar	Outlet pressure bar	NaOH, m Flow rate mL· min^{-1}	Cu (GFAA) ppb
Cu_2O-250-7-9	250.1	55.4	53.5	0.01002 0.1	~~300~~
Cu_2O-250-7-10	250.1	60.1	53.7	0.01002 0.1	~~274~~
Cu_2O-350-13-7	350.0	80.9**	80.8**	0.000099 0.2	1.8
Cu_2O-350-13-8	350.0	81.0**	80.9**	0.000099 0.2	0.9
Cu_2O-350-13-9	350.0	80.4**	80.3**	0.000099 0.2	0.8
Cu_2O-350-13-10	350.0	81.0**	80.9**	0.000099 0.2	0.6
Cu_2O-350-13-11	350.0	80.9**	80.8**	0.000099 0.2	1.6
Cu_2O-350-13-12	350.0	80.6**	80.5**	0.000099 0.2	0.6
Cu_2O-350-14-1	350.0	144.7**	144.6**	0.000193 0.2	1.8
Cu_2O-350-14-2	350.0	144.4**	144.1**	0.000193 0.2	1.6
Cu_2O-350-14-3	350.0	142.9**	142.8**	0.000193 0.2	1.6
Cu_2O-350-14-4	350.0	144.9**	144.8**	0.000193 0.2	1.9
Cu_2O-350-14-5	350.0	144.0**	143.9**	0.000193 0.2	1.7
Cu_2O-350-14-6	350.0	143.3**	143.2**	0.000193 0.2	1.2
Cu_2O-350-14-7	350.0	144.1**	144.0**	0.000193 0.2	1.6
Cu_2O-350-14-8	350.0	143.9**	143.8**	0.000193 0.2	1.6
Cu_2O-350-14-9	350.0	143.5**	143.3**	0.000193 0.2	1.5
Cu_2O-350-14-10	350.0	144.2**	144.1**	0.000193 0.2	1.2
Cu_2O-350-14-11	350.0	145.2**	145.2**	0.000193 0.2	1.4
Cu_2O-350-14-12	350.0	144.8**	144.7**	0.000193 0.2	0.4

Table A-2
Continued

Sample ID	Temperature °C	Inlet pressure bar	Outlet pressure bar	NaOH, m Flow rate mL· min^{-1}	Cu (GFAA) ppb
Cu_2O-350-15-1	350.0	182.3	182.2	0.001124 0.2	48.8
Cu_2O-350-15-2	350.0	183.1	182.4	0.001124 0.2	41.8
Cu_2O-350-15-3	350.0	183.1	182.1	0.001124 0.2	35.6
Cu_2O-350-15-4	350.0	187.9	182.8	0.001124 0.2	47.1
Cu_2O-350-15-5	350.0	201.0	182.7	0.001124 0.2	46.1
Cu_2O-350-15'-1	350.0	183.0	182.9	0.01261 0.1	522
Cu_2O-350-15'-2	350.1	183.3	183.1	0.01261 0.1	536
Cu_2O-350-15'-3	350.0	183.6	183.4	0.01261 0.1	500
Cu_2O-350-15'-4	350.0	183.2	183.0	0.01261 0.1	522
Cu_2O-350-15'-5	350.0	183.0	182.8	0.01261 0.1	611
Cu_2O-350-15'-6	349.9	183.2	182.9	0.01261 0.1	513
Cu_2O-350-15'-7	350.0	183.5	183.3	0.01261 0.1	522
Cu_2O-400-18-1	400.0	157.3**	157.1**	0.000137 0.15	8.0
Cu_2O-400-18-2	400.0	156.4**	156.3**	0.000137 0.15	~~12.8~~
Cu_2O-400-18-3	400.0	159.6**	159.4**	0.000137 0.15	7.9
Cu_2O-400-18-4	400.0	159.7**	159.5**	0.000137 0.15	8.2
Cu_2O-400-18-5	400.0	159.6**	159.5**	0.000137 0.15	8.5
Cu_2O-400-18-6	400.0	159.0**	158.8**	0.000137 0.15	8.5
Cu_2O-400-18-7	400.0	159.8**	159.6**	0.000137 0.15	7.7

Cu_2O-400-18-8	400.0	160.0**	159.8**	0.000137 0.15	6.9
Cu_2O-400-18-9	400.0	160.1**	160.0**	0.000137 0.15	7.3

Table A-2
Continued

Sample ID	Temperature °C	Inlet pressure bar	Outlet pressure bar	NaOH, m Flow rate mL· min^{-1}	Cu (GFAA) ppb
Cu_2O-400-18-10	400.0	159.8**	159.6**	0.000137 0.15	6.9
Cu_2O-400-18-11	400.0	159.4**	159.3**	0.000137 0.15	6.8
Cu_2O-400-18-12	400.0	159.4**	159.3**	0.000137 0.15	8.9
Cu_2O-400-19-1	400.0	198.4**	198.2**	0.000137 0.15	~~59.1~~
Cu_2O-400-19-2	400.0	198.2**	198.1**	0.000137 0.15	~~46.0~~
Cu_2O-400-19-3	400.0	198.4**	198.3**	0.000137 0.15	~~39.1~~
Cu_2O-400-19-4	400.0	197.3**	197.2**	0.000137 0.15	29.9
Cu_2O-400-19-5	400.0	197.5**	197.4**	0.000137 0.15	28.2
Cu_2O-400-19-6	400.0	198.6**	198.5**	0.000137 0.15	27.9
Cu_2O-400-19-7	400.0	198.4**	198.2**	0.000137 0.15	24.6
Cu_2O-400-20-2	400.0	93.1**	92.9**	0.000172 0.15	0.49
Cu_2O-400-20-3	400.0	93.4**	93.2**	0.000172 0.15	0.53
Cu_2O-400-20-4	400.0	94.5**	94.3**	0.000172 0.15	0.15
Cu_2O-400-20-5	400.0	93.1**	92.9**	0.000172 0.15	0.11
Cu_2O-400-20-6	400.0	92.9**	92.7**	0.000172 0.15	0.20
Cu_2O-400-20-10	400.0	93.9**	93.6**	0.000172 0.15	0.12
Cu_2O-400-20-11	400.0	93.6**	93.4**	0.000172 0.15	0.25
Cu_2O-400-20-12	400.0	95.1**	94.9**	0.000172 0.15	0.36

Cu_2O-400-21-1	400.0	119.0**	118.8**	0.000172 0.15	0.39
Cu_2O-400-21-2	400.0	118.6**	118.4**	0.000172 0.15	0.11
Cu_2O-400-21-3	400.0	117.5**	117.3**	0.000172 0.15	0.57

Table A-2
Continued

Sample ID	Temperature °C	Inlet pressure bar	Outlet pressure bar	NaOH, m Flow rate mL· min^{-1}	Cu (GFAA) ppb
Cu_2O-400-21-4	400.0	118.0**	117.8**	0.000172 0.15	0.34
Cu_2O-400-21-5	400.0	119.1**	119.0**	0.000172 0.15	0.73
Cu_2O-400-21-6	400.0	119.9**	119.7**	0.000172 0.15	0.64
Cu_2O-400-21-7	400.0	118.9**	118.8**	0.000172 0.15	1.29
Cu_2O-400-21-8	400.0	119.7**	119.6**	0.000172 0.15	3.13
Cu_2O-400-21-9	400.0	120.7**	120.6**	0.000172 0.15	1.16
Cu_2O-400-21-10	400.0	120.7**	120.6**	0.000172 0.15	1.09
Cu_2O-400-21-11	400.0	120.9**	120.7**	0.000172 0.15	0.13
Cu_2O-400-21-12	400.0	120.6**	120.4**	0.000172 0.15	0.26
Cu_2O-400-21-13	400.0	120.9**	120.7**	0.000172 0.15	0.95
Cu_2O-400-21-14	400.0	120.4**	120.2**	0.000172 0.15	0.38
Cu_2O-400-21-15	400.0	120.8**	120.6**	0.000172 0.15	0.85

** pressure below the saturation vapor pressure of water (*i.e.*, steam phase)

Table A-3
Cuprous oxide solubility data in ammonia solutions

Sample ID	Temperature °C	Inlet pressure bar	Outlet pressure bar	$\underline{NH_3}$ m Flow rate mL· min^{-1}	Cu (GFAA) ppb
Cu_2O-250-10-1*	250.0	40.4	40.4	0.002671 0.1	282
Cu_2O-250-10-2*	250.0	41.4	41.4	0.002671 0.1	162
Cu_2O-250-10-3*	250.0	41.1	41.2	0.002671 0.1	299
Cu_2O-250-10-4*	250.1	40.8	40.9	0.002671 0.1	271
Cu_2O-250-10-5*	250.1	39.8	39.9	0.002671 0.1	230
Cu_2O-250-10-6*	250.0	40.9	40.9	0.002671 0.1	186
Cu_2O-250-10-7*	250.0	40.7	40.7	0.002671 0.1	179
Cu_2O-250-10-8*	250.0	41.3	41.3	0.002671 0.1	165
Cu_2O-250-10-9*	250.0	40.4	40.4	0.002671 0.1	153
Cu_2O-250-10-10*	250.0	41.2	41.2	0.002671 0.1	149
Cu_2O-250-10-11*	250.0	41.2	41.2	0.002671 0.1	164
Cu_2O-300-10-9	300.0	94.2	94.0	0.000994 0.1	10.1
Cu_2O-300-10-10	300.0	95.5	95.4	0.000994 0.1	10.8
Cu_2O-300-10-11	300.0	97.4	97.3	0.000994 0.1	11.2
Cu_2O-300-10-12	300.0	97.4	97.3	0.000994 0.1	11.1
Cu_2O-300-11-7	300.0	72.7**	72.5**	0.000994 0.1	3.0
Cu_2O-300-11-8	300.0	80.7**	80.4**	0.000994 0.1	3.3
Cu_2O-300-11-9	300.0	80.0**	79.9**	0.000994 0.1	2.8
Cu_2O-300-11-10	300.0	81.6**	80.1**	0.000994 0.1	2.7
Cu_2O-300-11-11	300.0	80.6**	80.5**	0.000994 0.1	2.4
Cu_2O-300-11-12	300.0	80.8**	80.7**	0.000994 0.1	2.4

Table A-3
Continued

Sample ID	Temperature °C	Inlet pressure bar	Outlet pressure bar	$\underline{NH_3}$ m Flow rate mL· min^{-1}	Cu (GFAA) ppb
Cu_2O-300-11-13	300.0	80.8**	80.7**	0.000994 0.1	2.2
Cu_2O-300-11-14	300.0	80.6**	80.5**	0.000994 0.1	2.1
Cu_2O-300-11-15	300.0	80.9**	80.8**	0.000994 0.1	1.9
Cu_2O-350-12-17	350.0	156.9**	156.8**	0.000994 0.1	1.4
Cu_2O-350-12-18	350.0	157.2**	157.1**	0.000994 0.1	1.3
Cu_2O-350-12-19	350.0	157.1**	157.0**	0.000994 0.1	1.3
Cu_2O-350-12-20	350.0	155.2**	155.0**	0.000994 0.1	1.2
Cu_2O-350-12-21	350.0	155.3**	155.1**	0.000994 0.1	1.2
Cu_2O-350-12-22	350.0	154.4**	154.2**	0.000994 0.1	1.1
Cu_2O-350-12-23	350.0	154.3**	154.2**	0.000994 0.1	1.1
Cu_2O-350-12-24	350.0	155.5**	154.5**	0.000994 0.1	1.1

* number system from the previous report : EPRI-1003993
** pressure below the saturation vapor pressure of water (i.e., steam phase)

Table A-4
Cuprous oxide solubility data in ammonia, trifluoromethanesulfonic acid solutions

Sample ID	Temperature °C	Inlet pressure bar	Outlet pressure bar	$\underline{NH_3}$ m $\underline{CF_3SO_3H}$, m Flow rate mL· min^{-1}	Cu (AA) ppm
Cu_2O-250-5-1	250.2	56.6	56.2	0.002106 0.1 0.001072	2.7
Cu_2O-250-5-2	250.2	57.2	52.9	0.002106 0.1 0.001072	2.5
Cu_2O-250-5-3	250.1	57.8	52.7	0.002106 0.1 0.001072	2.0
Cu_2O-250-5-4	250.2	69.7	54.0	0.002106 0.1 0.001072	2.7
Cu_2O-250-5-5	250.1	78.5	52.2	0.002106 0.1 0.001072	1.7
Cu_2O-250-5-6	250.2	53.4	52.9	0.002106 0.1 0.001072	2.6
Cu_2O-250-5-7	250.2	53.0	52.9	0.002106 0.1 0.001072	2.9
Cu_2O-250-5-8	250.0	58.3	53.5	0.002106 0.1 0.001072	2.2
Cu_2O-250-5-9	250.0	52.9	52.8	0.002106 0.1 0.001072	2.0
Cu_2O-250-5-10	250.1	54.4	54.3	0.002106 0.1 0.001072	2.1
Cu_2O-250-5-12	250.1	52.1	51.7	0.002106 0.1 0.001072	1.5
Cu_2O-250-5-13	250.1	54.8	51.7	0.002106 0.1 0.001072	1.5
Cu_2O-250-5-15	250.0	58.7	53.7	0.002106 0.1	2.4

				0.001072	

Table A-4
Continued

Sample ID	Temperature °C	Inlet pressure bar	Outlet pressure bar	$\underline{NH_3}$ m $\underline{CF_3SO_3H}$, m Flow rate mL· min^{-1}	Cu (GFAA) ppm
Cu_2O-350-16-1	350.0	181.6	181.4	0.005529 0.1 0.0005278	1.34
Cu_2O-350-16-2	350.0	181.4	181.2	0.005529 0.1 0.0005278	1.36
Cu_2O-350-16-3	350.0	183.7	183.6	0.005529 0.1 0.0005278	1.48
Cu_2O-350-16-4	350.0	183.0	182.9	0.005529 0.1 0.0005278	1.41
Cu_2O-350-16-5	350.0	182.8	182.6	0.005529 0.1 0.0005278	1.45
Cu_2O-350-16-6	350.0	182.3	182.2	0.005529 0.1 0.0005278	1.34
Cu_2O-350-16-7	350.0	182.6	182.4	0.005529 0.1 0.0005278	1.25
Cu_2O-350-16-8	350.0	182.2	182.1	0.005529 0.1 0.0005278	1.38
Cu_2O-350-16-9	350.0	183.2	183.1	0.005529 0.1 0.0005278	1.18
Cu_2O-350-17-1	350.0	182.1	182.0	0.001954 0.1 0.001950	~~40.6~~
Cu_2O-350-17-2	350.0	182.2	182.1	0.001954 0.1 0.001950	37.5
Cu_2O-350-17-3	350.0	183.2	183.1	0.001954 0.1 0.001950	37.0

Cu_2O-350-17-3'	350.0	183.5	183.4	0.001954 0.1 0.001950	36.1

Table A-4
Continued

Sample ID	Temperature °C	Inlet pressure bar	Outlet pressure bar	$\underline{NH_3}$ m $\underline{CF_3SO_3H}$, m Flow rate mL· min^{-1}	Cu (GFAA) ppm
Cu_2O-350-17-4	350.0	182.8	182.7	0.001954 0.1 0.001950	36.7
Cu_2O-350-17-5	350.0	183.7	183.5	0.001954 0.1 0.001950	37.5
Cu_2O-350-17-6	350.0	182.8	182.7	0.001954 0.1 0.001950	35.6
Cu_2O-350-17-7	350.0	182.9	182.7	0.001954 0.1 0.001950	35.8
Cu_2O-350-17-8	350.0	183.5	183.4	0.001954 0.1 0.001950	35.7
Cu_2O-350-17-9	350.0	182.9	182.8	0.001954 0.1 0.001950	36.9
Cu_2O-350-13-1	300.0	120.5*	120.3*	0.001949 0.15 0.000946	0.112
Cu_2O-350-13-2	300.0	119.5*	119.3*	0.001949 0.15 0.000946	0.122
Cu_2O-350-13-3	300.0	120.5*	120.2*	0.001949 0.15 0.000946	0.129
Cu_2O-350-13-4	300.0	121.1*	121.0*	0.001949 0.15 0.000946	0.138
Cu_2O-350-13-5	300.0	121.1*	121.0*	0.001949 0.15 0.000946	0.137
Cu_2O-350-13-6	300.1	121.2*	121.1*	0.001949 0.15	0.137

				0.000946	
Cu_2O-350-13-7	300.0	121.8*	121.7*	0.001949 0.15 0.000946	0.140

Table A-4
Continued

Sample ID	Temperature °C	Inlet pressure bar	Outlet pressure bar	$\underline{NH_3}$ m $\underline{CF_3SO_3H}$, m Flow rate mL· min^{-1}	Cu (GFAA) ppm
Cu_2O-350-13-8	300.0	122.3*	122.1*	0.001949 0.15 0.000946	0.149
Cu_2O-350-13-9	300.0	121.0*	120.9*	0.001949 0.15 0.000946	0.158
Cu_2O-350-13-10	300.0	122.6*	122.4*	0.001949 0.15 0.000946	0.159
Cu_2O-350-13-11	300.0	122.2*	122.0*	0.001949 0.15 0.000946	0.154
Cu_2O-350-13-12	300.0	120.1*	119.8*	0.001949 0.15 0.000946	0.141

* the feed solution was saturated with a mixture of 5,000 ppm H_2 in Ar with an over pressure of 0.5 bar (7 psi).

B

SOLUBILITY DATA FOR CUPROUS OXIDE OBTAINED WITH THE LOW-TEMPERATURE CELL

The tables are grouped according to the make-up of the feed solution and are therefore not listed in chronological order. Pressure on the system was one atmosphere (*c*a. 1 bar) although a positive helium pressure (10 psi) was maintained over the feed solution. The flow rate of the feed solution was maintained at 0.02 $mL \cdot min^{-1}$. The analytical technique employed was either conventional flame atomic adsorption spectrophotometry (AA) or graphite furnace atomic absorption spectrophotometry (GFAA).

Table B-1
Cuprous oxide solubility data in trifluoromethanesulfonic acid solutions

Sample ID	Temperature °C	CF_3SO_3H, m Flow rate mL· min^{-1}	Cu (AA) ppm
Cu_2O-25-1-1*	25.0	0.001013 0.02	233
Cu_2O-25-1-2*	25.1	0.001013 0.02	233
Cu_2O-25-1-3*	25.1	0.001013 0.02	225
Cu_2O-25-1-4*	25.0	0.001013 0.02	228
Cu_2O-25-1-5*	25.1	0.001013 0.02	226
Cu_2O-25-1-6*	25.1	0.001013 0.02	221
Cu_2O-25-1-8*	25.0	0.001013 0.02	224
Cu_2O-25-1-9*	25.0	0.001013 0.02	219
Cu_2O-25-1-10*	25.1	0.001013 0.02	202
Cu_2O-25-1-11*	25.0	0.001013 0.02	224
Cu_2O-25-1-12*	25.1	0.001013 0.02	224
Cu_2O-25-2-1§	24.9	0.001013 0.02	9.1
Cu_2O-25-2-2§	25.0	0.001013 0.02	0.83
Cu_2O-25-2-3§	25.0	0.001013 0.02	4.1
Cu_2O-25-2-4§	25.0	0.001013 0.02	13.2
Cu_2O-25-2-5§	25.0	0.001013 0.02	2.5
Cu_2O-25-2-6§	25.0	0.001013 0.02	5.2
Cu_2O-25-2-7§	25.0	0.001013 0.02	1.11**
Cu_2O-25-2-8§	25.0	0.001013 0.02	0.84**
Cu_2O-25-2-9§	25.0	0.001013 0.02	0.41**

Cu_2O-25-2-10§	25.0	0.001013 0.02	0.53**

Table B-1
Continued

Sample ID	Temperature °C	$\underline{CF_3SO_3H}$ m Flow rate mL· min^{-1}	Cu (AA) ppm
Cu_2O-25-2-11§	25.0	0.001013 0.02	0.64**
Cu_2O-25-2-12§	25.0	0.001013 0.02	0.31**
Cu_2O-25-2-13§	25.0	0.001013 0.02	0.65**
Cu_2O-25-3-1	24.9	0.001213 0.02	35.8
Cu_2O-25-3-2	25.0	0.001213 0.02	35.6
Cu_2O-25-3-3	25.0	0.001213 0.02	35.7
Cu_2O-25-3-5	25.0	0.001213 0.02	35.5
Cu_2O-25-3-6	25.0	0.001213 0.02	35.5
Cu_2O-25-3-7	25.0	0.001213 0.02	35.6
Cu_2O-25-3-8	25.0	0.001213 0.02	35.4
Cu_2O-25-3-9	25.0	0.001213 0.02	35.8
Cu_2O-25-4-1	25.0	0.0001504 0.02	3.80 3.87
Cu_2O-25-4-2	25.0	0.0001504 0.02	3.73 3.82
Cu_2O-25-4-3	25.0	0.0001504 0.02	3.72 3.78
Cu_2O-25-4-4	25.0	0.0001504 0.02	3.73 3.75
Cu_2O-25-4-5	25.0	0.0001504 0.02	3.73 3.82
Cu_2O-25-4-6	25.0	0.0001504 0.02	3.65
Cu_2O-50-1-1	50.1	0.001213 0.02	32.1
Cu_2O-50-1-2	50.0	0.001213 0.02	31.2

solubility data for cuprous oxide obtained with the low-temperature cell

Cu_2O-50-1-3	50.0	0.001213 0.02	31.2
Cu_2O-50-1-4	50.0	0.001213 0.02	31.3

Table B-1
Continued

Sample ID	Temperature °C	CF_3SO_3H m Flow rate mL· min^{-1}	Cu (AA) ppm
Cu_2O-75-8-1	74.8	0.001025 0.04	24.8
Cu_2O-75-8-2	74.8	0.001025 0.04	24.7
Cu_2O-75-8-3	75.0	0.001025 0.04	25.8
Cu_2O-75-8-4	74.9	0.001025 0.04	24.9
Cu_2O-75-8-5	74.9	0.001025 0.04	25.0
Cu_2O-75-8-6	75.0	0.001025 0.04	25.2
Cu_2O-75-8-7	75.0	0.001025 0.04	~~21.7~~
Cu_2O-75-8-8	74.8	0.001025 0.04	25.9
Cu_2O-75-9-2	74.6	0.000341 0.04	5.3
Cu_2O-75-9-3	74.6	0.000341 0.04	5.1
Cu_2O-75-9-4	74.6	0.000341 0.04	5.2
Cu_2O-75-9-5	75.0	0.000341 0.04	5.4
Cu_2O-75-9-6	75.0	0.000341 0.04	5.2
Cu_2O-75-9-7	75.0	0.000341 0.04	5.1
Cu_2O-75-9-8	75.0	0.000341 0.04	5.0
Cu_2O-75-9-9	75.0	0.000341 0.04	5.5
Cu_2O-75-10-1	75.0	0.004783 0.04	151
Cu_2O-75-10-2	74.9	0.004783 0.04	105
Cu_2O-75-10-3	75.1	0.004783 0.04	148
Cu_2O-75-10-4	75.1	0.004783 0.04	141
Cu_2O-75-10-5	75.0	0.004783 0.03	105

Table B-1
Continued

Sample ID	Temperature °C	$\underline{CF_3SO_3H}$ m Flow rate mL· min^{-1}	Cu (AA) ppm
Cu_2O-75-10-6	74.9	0.004783 0.03	121
Cu_2O-75-10-7	75.0	0.004783 0.03	115
Cu_2O-75-10-8	75.0	0.004783 0.03	129
Cu_2O-75-10-9	75.0	0.004783 0.03	131
Cu_2O-75-10-10	75.0	0.004783 0.03	135
Cu_2O-75-12-3	75.0	0.002412 0.03	64.6
Cu_2O-75-12-4	75.0	0.002412 0.03	62.4
Cu_2O-75-12-5	75.0	0.002412 0.03	61.9
Cu_2O-75-12-6	74.9	0.002412 0.03	63.0
Cu_2O-75-12-7	74.9	0.002412 0.03	62.1
Cu_2O-75-12-8	75.0	0.002412 0.03	63.1

* The solid "Cu_2O" charge in the flow-through columns must have contained an impurity of CuCl, which could neither be detected by XRD nor purged with the acidic feed solution, and led to high copper concentrations Therefore these data were discarded.
§ This freshly-prepared charge of Cu_2O contained a minor amount of basic impurity which led to neutralization of the feed solution and low copper concentrations. Following the Cu_2O-25-2 series, the feed solution was pumped through the three columns in series for five days at a flow rate of 0.2 mL· min^{-1} until the pH of the exiting solution reached a constant value, at which time the flow rate was reduced back to 0.2 mL· min^{-1} and maintained at this rate for two days until sampling was resumed.
** GFAA

Table B-2
Cuprous oxide solubility data in sodium hydroxide solutions

Sample ID	Temperature °C	NaOH, m Flow rate mL· min^{-1}	Cu (GFAA) ppb
Cu_2O-25-5-1	25.0	0.01201 0.02	~~110.8~~
Cu_2O-25-5-2	25.0	0.01201 0.02	32.3
Cu_2O-25-5-3	25.0	0.01201 0.02	35.5
Cu_2O-25-5-4	25.0	0.01201 0.02	35.5
Cu_2O-25-5-5	25.0	0.01201 0.02	33.0
Cu_2O-25-5-6	25.0	0.01201 0.02	40.5
Cu_2O-25-5-7	25.0	0.01201 0.02	28.6
Cu_2O-25-5-8	25.0	0.01201 0.02	28.9
Cu_2O-25-5-9	25.0	0.01201 0.02	27.0
Cu_2O-25-6-1	25.0	0.001339 0.02	~~7.5~~ ~~7.5~~
Cu_2O-25-6-2	25.0	0.001339 0.02	3.5
Cu_2O-25-6-3	25.0	0.001339 0.02	3.0
Cu_2O-25-6-4	25.0	0.001339 0.02	2.5
Cu_2O-25-6-5	25.0	0.001339 0.02	3.6
Cu_2O-25-6-6	25.1	0.001339 0.02	2.7
Cu_2O-25-6-7	25.0	0.001339 0.02	2.7
Cu_2O-25-6-9	25.1	0.001339 0.02	~~4.9~~
Cu_2O-25-6-10	25.0	0.001339 0.02	3.0
Cu_2O-25-6-11	25.0	0.001339 0.02	2.1
Cu_2O-25-6-12	25.0	0.001339 0.02	2.9
Cu_2O-25-6-13	2510	0.001339 0.02	1.9

Table B-2
Continued

Sample ID	Temperature °C	NaOH, m Flow rate mL· min^{-1}	Cu (GFAA) ppb
Cu_2O-25-6-14	25.0	0.001339 0.02	2.2
Cu_2O-25-6-15	25.1	0.001339 0.02	2.3
Cu_2O-25-7-1	24.9	0.1085 0.02	207
Cu_2O-25-7-2	24.9	0.1085 0.02	222
Cu_2O-25-7-3	25.0	0.1085 0.02	164
Cu_2O-25-7-4	24.9	0.1085 0.02	190
Cu_2O-25-7-5	24.9	0.1085 0.02	201
Cu_2O-25-7-6	24.9	0.1085 0.02	201
Cu_2O-25-7-7	24.9	0.1085 0.02	250
Cu_2O-25-8-1	24.9	0.0001349 0.02	~~3.9 3.5~~
Cu_2O-25-8-2	25.0	0.0001349 0.02	~~3.8 3.4~~
Cu_2O-25-8-3	24.9	0.0001349 0.02	~~1.9 1.4~~
Cu_2O-25-8-4	25.0	0.0001349 0.02	~~3.0 2.9~~
Cu_2O-25-8-5	25.0	0.0001349 0.02	~~5.8 3.9~~
Cu_2O-25-8-6	25.0	0.0001349 0.02	~~3.5 3.2~~
Cu_2O-25-8-7	25.0	0.0001349 0.02	~~2.3 1.9~~
Cu_2O-25-8-8	25.0	0.0001349 0.02	1.2
Cu_2O-25-8-9	25.0	0.0001349 0.02	1.5 1.5 1.5
Cu_2O-25-8-10	25.0	0.0001349 0.02	1.1 1.2 1.2
Cu_2O-25-8-11	25.0	0.0001349 0.02	1.06 0.92 0.89

Cu_2O-25-8-12	25.0	0.0001349 0.02	1.03

Table B-2
Continued

Sample ID	Temperature °C	NaOH, m Flow rate mL· min^{-1}	Cu (GFAA) ppb
Cu_2O-25-8-13	25.0	0.0001349 0.02	1.5
Cu_2O-25-8-14	25.0	0.0001349 0.02	1.07
Cu_2O-25-8-15	25.0	0.0001349 0.02	1.3
Cu_2O-25-8-16	25.0	0.0001349 0.02	1.04
Cu_2O-25-8-17	25.0	0.0001349 0.02	0.82 0.69
Cu_2O-25-8-18	25.0	0.0001349 0.02	0.70
Cu_2O-25-8-19	25.0	0.0001349 0.02	0.94
Cu_2O-50-2-8	50.0	0.001004 0.02	4.8
Cu_2O-50-2-9	50.0	0.001004 0.02	4.8
Cu_2O-50-2-10	50.0	0.001004 0.02	5.9
Cu_2O-50-2-11	50.0	0.001004 0.02	4.9
Cu_2O-50-2-12	50.0	0.001004 0.02	4.5
Cu_2O-50-2-13	50.0	0.001004 0.02	4.4
Cu_2O-50-2-14	50.0	0.001004 0.02	4.2
Cu_2O-50-3-1	49.9	0.01098 0.02	10.8
Cu_2O-50-3-2	49.9	0.01098 0.02	9.8
Cu_2O-50-3-3	49.9	0.01098 0.02	9.3
Cu_2O-50-3-4	50.0	0.01098 0.02	8.8
Cu_2O-50-3-5	50.0	0.01098 0.02	6.7

Cu_2O-50-3-6	50.0	0.01098 0.02	7.2
Cu_2O-50-3-7	50.0	0.01098 0.02	6.9

Table B-2
Continued

Sample ID	Temperature °C	NaOH, m Flow rate mL· min^{-1}	Cu (GFAA) ppb
Cu_2O-50-3-8	50.0	0.01098 0.02	13.3
Cu_2O-50-4-3	50.0	0.09625 0.02	125.5
Cu_2O-50-4-4	50.0	0.09625 0.02	99.2
Cu_2O-50-4-5	50.0	0.09625 0.02	106.3
Cu_2O-50-4-6	50.0	0.09625 0.02	110.0
Cu_2O-50-4-7	50.0	0.09625 0.02	110.6
Cu_2O-50-4-8	50.0	0.09625 0.02	115.3
Cu_2O-50-4-9	50.0	0.09625 0.02	109.4
Cu_2O-50-4-10	50.0	0.09625 0.02	105.3
Cu_2O-50-6-1	50.0	0.03215 0.02	18.7
Cu_2O-50-6-2	50.0	0.03215 0.02	20.5
Cu_2O-50-6-3	50.0	0.03215 0.02	15.8
Cu_2O-50-6-4	50.0	0.03215 0.02	16.8
Cu_2O-50-6-5	50.0	0.03215 0.02	16.0
Cu_2O-50-6-6	50.0	0.03215 0.02	14.4
Cu_2O-50-6-7	50.1	0.03215 0.02	16.2
Cu_2O-50-6-8	50.1	0.03215 0.02	13.5
Cu_2O-50-6-9	50.1	0.03215 0.02	21.1
Cu_2O-50-7-1	49.9	0.000111 0.02	1.69

Cu_2O-50-7-2	49.9	0.000111 0.02	1.57
Cu_2O-50-7-3	50.0	0.000111 0.02	1.24

Table B-2
Continued

Sample ID	Temperature °C	NaOH, m Flow rate mL· min^{-1}	Cu (GFAA) ppb
Cu_2O-50-7-4	50.0	0.000111 0.02	0.81
Cu_2O-50-7-5	50.0	0.000111 0.02	0.78
Cu_2O-50-7-6	50.0	0.000111 0.02	0.79
Cu_2O-50-7-7	50.0	0.000111 0.02	~~11.6~~
Cu_2O-50-7-8	50.0	0.000111 0.02	1.56
Cu_2O-50-7-9	50.0	0.000111 0.02	0.85
Cu_2O-50-7-10	50.0	0.000111 0.02	0.65
Cu_2O-50-7-11	50.0	0.000111 0.02	1.05
Cu_2O-50-7-12	50.0	0.000111 0.02	0.64
Cu_2O-50-8-1	50.1	0.000965 0.02	1.38
Cu_2O-50-8-2	50.1	0.000965 0.02	1.37
Cu_2O-50-8-3	50.1	0.000965 0.02	1.50
Cu_2O-50-8-4	50.1	0.000965 0.02	1.39
Cu_2O-50-8-5	50.1	0.000965 0.02	1.16
Cu_2O-50-8-6	50.1	0.000965 0.02	1.57
Cu_2O-50-8-7	50.0	0.000965 0.02	1.71
Cu_2O-50-8-8	50.1	0.000965 0.02	1.52
Cu_2O-50-8-9	50.1	0.000965 0.02	1.54

Cu_2O-50-8-10	50.1	0.000965 0.02	1.18
Cu_2O-75-2-2	75.0	0.000109 0.04	2.10
Cu_2O-75-2-3	75.0	0.000109 0.04	2.25

Table B-2
Continued

Sample ID	Temperature °C	NaOH, m Flow rate mL· min^{-1}	Cu (GFAA) ppb
Cu_2O-75-2-4	75.0	0.000109 0.04	2.72
Cu_2O-75-2-5	75.0	0.000109 0.04	~~6.56~~
Cu_2O-75-2-6	75.0	0.000109 0.04	2.07
Cu_2O-75-2-7	74.9	0.000109 0.04	2.14
Cu_2O-75-2-8	75.0	0.000109 0.04	2.36
Cu_2O-75-2-9	74.9	0.000109 0.04	2.32
Cu_2O-75-3-2	75.0	0.001090 0.04	3.2
Cu_2O-75-3-3	75.1	0.001090 0.04	2.6
Cu_2O-75-3-4	75.0	0.001090 0.04	3.1
Cu_2O-75-3-5	75.0	0.001090 0.04	2.5
Cu_2O-75-3-6	75.0	0.001090 0.04	5.2,4.9
Cu_2O-75-3-7	75.0	0.001090 0.04	3.1
Cu_2O-75-3-8	75.0	0.001090 0.04	3.1
Cu_2O-75-3-9	75.0	0.001090 0.04	3.0
Cu_2O-75-4-2	74.9	0.01066 0.04	9.1
Cu_2O-75-4-3	75.0	0.01066 0.04	8.9
Cu_2O-75-4-4	74.9	0.01066 0.04	9.0

Cu_2O-75-4-5	75.0	0.01066 0.04	8.2
Cu_2O-75-4-6	75.0	0.01066 0.04	8.0,8.8
Cu_2O-75-4-7	75.0	0.01066 0.04	7.6

Table B-2
Continued

Sample ID	**Temperature °C**	**NaOH, m Flow rate mL· min^{-1}**	**Cu (GFAA) ppb**
Cu_2O-75-5-2	75.0	0.07621 0.04	119
Cu_2O-75-5-3	74.8	0.07621 0.04	115
Cu_2O-75-5-4	75.0	0.07621 0.04	111
Cu_2O-75-5-5	75.0	0.07621 0.04	72
Cu_2O-75-5-6	75.1	0.07621 0.04	131
Cu_2O-75-5-7	75.1	0.07621 0.04	76
Cu_2O-75-5-8	75.1	0.07621 0.04	74
Cu_2O-75-5-9	75.2	0.07621 0.04	100
Cu_2O-75-5-10	75.1	0.07621 0.04	100
Cu_2O-75-6-3	74.9	0.03608 0.04	55
Cu_2O-75-6-4	74.9	0.03608 0.04	~~113~~
Cu_2O-75-6-5	74.9	0.03608 0.04	55
Cu_2O-75-6-6	74.9	0.03608 0.04	57
Cu_2O-75-6-7	75.0	0.03608 0.04	49,45
Cu_2O-75-6-8	75.0	0.03608 0.04	68
Cu_2O-75-6-9	75.0	0.03608 0.04	40
Cu_2O-75-6-10	75.0	0.03608 0.04	37

Table B-3
Cuprous oxide solubility data in boric acid, sodium hydroxide solutions

Sample ID	Temperature °C	$\underline{B(OH)_3}$ $\underline{NaOH}$, m Flow rate $mL \cdot min^{-1}$	Cu (GFAA) ppb
Cu_2O-50-9-1	50.0	<u>0.002381 0.000149</u> 0.02	1.52,1.76*
Cu_2O-50-9-2	49.9	<u>0.002381 0.000149</u> 0.02	1.10,1.76*
Cu_2O-50-9-3	50.0	<u>0.002381 0.000149</u> 0.02	0.93,0.99*
Cu_2O-50-9-4	49.9	<u>0.002381 0.000149</u> 0.02	0.82,0.97*
Cu_2O-50-9-5	49.9	<u>0.002381 0.000149</u> 0.02	0.91,1.06*
Cu_2O-50-9-6	49.9	<u>0.002381 0.000149</u> 0.02	0.75,0.87*
Cu_2O-50-9-7	49.9	<u>0.002381 0.000149</u> 0.02	0.76,1.25*
Cu_2O-50-9-8	50.0	<u>0.002381 0.000149</u> 0.02	0.85,1.01*
Cu_2O-50-9-9	50.0	<u>0.002381 0.000149</u> 0.02	0.98,~~5.85*~~
Cu_2O-25-10-1	25.0	<u>0.002381 0.000149</u> 0.02	1.17,1.14
Cu_2O-25-10-2	25.0	<u>0.002381 0.000149</u> 0.02	1.00
Cu_2O-25-10-3	25.0	<u>0.002381 0.000149</u> 0.02	1.02
Cu_2O-25-10-4	25.0	<u>0.002381 0.000149</u> 0.02	0.94
Cu_2O-25-10-5	25.0	<u>0.002381 0.000149</u> 0.02	1.02
Cu_2O-25-10-7	25.0	<u>0.002381 0.000149</u> 0.02	1.06
Cu_2O-25-10-8	25.0	<u>0.002381 0.000149</u> 0.02	0.99
Cu_2O-25-11-1	25.2	<u>0.002307 0.001656</u> 0.02	0.70*
Cu_2O-25-11-2	25.2	<u>0.002307 0.001656</u> 0.02	0.70*
Cu_2O-25-11-3	25.1	<u>0.002307 0.001656</u> 0.02	0.68*
Cu_2O-25-11-4	25.1	<u>0.002307 0.001656</u> 0.02	~~3.93~~*

Table B-3
Continued

Sample ID	Temperature °C	$\underline{B(OH)_3}$ NaOH, m Flow rate $mL \cdot min^{-1}$	Cu (GFAA) ppb
Cu_2O-25-11-5	25.1	0.002307 0.001656 0.02	0.33*
Cu_2O-25-11-6	25.1	0.002307 0.001656 0.02	0.33*
Cu_2O-25-11-7	25.1	0.002307 0.001656 0.02	0.26*
Cu_2O-25-11-8	25.0	0.002307 0.001656 0.02	0.29*
Cu_2O-25-16-1	25.0	0.001950 0.001014 0.02	0.53
Cu_2O-25-16-2	25.0	0.001950 0.001014 0.02	1.10
Cu_2O-25-16-3	25.0	0.001950 0.001014 0.02	0.30
Cu_2O-25-16-4	25.0	0.001950 0.001014 0.02	1.33
Cu_2O-25-16-5	25.0	0.001950 0.001014 0.02	1.30
Cu_2O-25-16-7	25.0	0.001950 0.001014 0.02	1.63
Cu_2O-25-16-8	24.9	0.001950 0.001014 0.02	0.47
Cu_2O-25-16-9	25.0	0.001950 0.001014 0.02	0.50
Cu_2O-25-17-1	25.0	0.001950 0.001014** 0.02	0.30
Cu_2O-25-17-2	25.0	0.001950 0.001014** 0.02	0.33
Cu_2O-25-17-3	25.0	0.001950 0.001014** 0.02	0.37
Cu_2O-25-17-4	25.0	0.001950 0.001014** 0.02	0.35
Cu_2O-25-17-5	25.0	0.001950 0.001014** 0.02	0.36
Cu_2O-25-17-6	25.0	0.001950 0.001014** 0.02	0.57
Cu_2O-25-17-7	25.0	0.001950 0.001014** 0.02	0.30
Cu_2O-25-17-8	25.0	0.001950 0.001014** 0.02	0.93

Table B-3
Continued

Sample ID	Temperature °C	$\underline{B(OH)_3}$ $\underline{NaOH}$, m Flow rate $mL \cdot min^{-1}$	Cu (GFAA) ppb
Cu_2O-75-1-1	74.6	<u>0.001950</u> <u>0.001014</u> 0.04	~~3.55~~
Cu_2O-75-1-2	75.0	<u>0.001950</u> <u>0.001014</u> 0.04	2.93
Cu_2O-75-1-3	74.9	<u>0.001950</u> <u>0.001014</u> 0.04	2.52
Cu_2O-75-1-4	75.1	<u>0.001950</u> <u>0.001014</u> 0.04	2.58
Cu_2O-75-1-5	75.1	<u>0.001950</u> <u>0.001014</u> 0.04	2.33
Cu_2O-75-1-6	75.0	<u>0.001950</u> <u>0.001014</u> 0.04	2.64
Cu_2O-75-7-4	75.0	<u>0.002124</u> <u>0.000232</u> 0.04	3.3
Cu_2O-75-7-5	75.0	<u>0.002124</u> <u>0.000232</u> 0.04	4.1
Cu_2O-75-7-6	75.0	<u>0.002124</u> <u>0.000232</u> 0.04	1.8
Cu_2O-75-7-7	75.0	<u>0.002124</u> <u>0.000232</u> 0.04	2.8
Cu_2O-75-7-8	75.0	<u>0.002124</u> <u>0.000232</u> 0.04	1.9
Cu_2O-75-7-10	75.0	<u>0.002124</u> <u>0.000232</u> 0.04	2.5
Cu_2O-75-7-11	75.0	<u>0.002124</u> <u>0.000232</u> 0.04	2.8

* Samples were concentrated under vacuum;
** The feed solution was saturated with CO_2-free air

Table B-4
Cuprous oxide solubility data in sodium dihydrogenphosphate, sodium hydroxide solutions

Sample ID	Temperature °C	NaH_2PO_4 $NaOH$, m Flow rate $mL \cdot min^{-1}$	Cu (GFAA) ppb
Cu_2O-25-9-4	25.0	0.000955 0.000472 0.02	6.2
Cu_2O-25-9-5	25.0	0.000955 0.000472 0.02	5.6
Cu_2O-25-9-6	25.0	0.000955 0.000472 0.02	6.2
Cu_2O-25-9-7	25.0	0.000955 0.000472 0.02	4.0
Cu_2O-25-9-8	25.0	0.000955 0.000472 0.02	4.1
Cu_2O-25-9-9	25.0	0.000955 0.000472 0.02	3.9
Cu_2O-25-9-10	25.0	0.000955 0.000472 0.02	4.0
Cu_2O-25-9-12	25.0	0.000955 0.000472 0.02	5.1
Cu_2O-25-9-13	25.0	0.000955 0.000472 0.02	5.0
Cu_2O-75-11-2	75.1	0.001035 0.000521 0.03	86.2
Cu_2O-75-11-3	75.0	0.001035 0.000521 0.03	75.0
Cu_2O-75-11-4	75.1	0.001035 0.000521 0.03	68.4
Cu_2O-75-11-5	75.1	0.001035 0.000521 0.03	59.3
Cu_2O-75-11-6	75.0	0.001035 0.000521 0.03	40.2
Cu_2O-75-11-7	75.0	0.001035 0.000521 0.03	37.1
Cu_2O-75-11-8	75.0	0.001035 0.000521 0.03	92.0
Cu_2O-75-11-9	75.0	0.001035 0.000521 0.03	31.4
Cu_2O-75-11-10	75.0	0.001035 0.000521 0.03	44.4
Cu_2O-75-11-11	75.0	0.001035 0.000521 0.03	60.4

Table B-5
Cuprous oxide solubility data in acetic acid, sodium hydroxide solutions

Sample ID	Temperature °C	$\underline{CH_3COOH\ NaOH,}$ m Flow rate $mL \cdot min^{-1}$	Cu (AA) ppb
Cu_2O-25-12-4	25.0	0.001103 0.000565 0.02	597
Cu_2O-25-12-5	25.0	0.001103 0.000565 0.02	602
Cu_2O-25-12-6	25.0	0.001103 0.000565 0.02	658
Cu_2O-25-12-7	25.0	0.001103 0.000565 0.02	627
Cu_2O-25-12-8	25.0	0.001103 0.000565 0.02	600
Cu_2O-25-12-9	25.0	0.001103 0.000565 0.02	603
Cu_2O-25-12-10	25.0	0.001103 0.000565 0.02	569

Table B-6
Cuprous oxide solubility data in ammonia, sodium hydroxide solutions

Sample ID	Temperature °C	$\underline{NH_3\ NaOH,}$ m Flow rate $mL \cdot min^{-1}$	Cu (AA) ppb
Cu_2O-25-13-5	25.0	0.001082 0.001017 0.02	5.4
Cu_2O-25-13-6	25.0	0.001082 0.001017 0.02	5.1
Cu_2O-25-13-7	25.0	0.001082 0.001017 0.02	4.2
Cu_2O-25-13-8	25.0	0.001082 0.001017 0.02	4.0
Cu_2O-25-13-9	25.0	0.001082 0.001017 0.02	4.0
Cu_2O-25-13-10	25.0	0.001082 0.001017 0.02	4.6
Cu_2O-25-13-11	25.0	0.001082 0.001017 0.02	4.8

Table B-7
Cuprous oxide solubility data in ammonia, trifluoromethanesulfonic acid solutions

Sample ID	Temperature °C	NH_3 F_3SO_3H, m Flow rate $mL \cdot min^{-1}$	Cu (AA) ppb
Cu_2O-25-14-1	25.0	0.002005 0.001863 0.02	26.4
Cu_2O-25-14-2	25.0	0.002005 0.001863 0.02	26.4
Cu_2O-25-14-3	25.0	0.002005 0.001863 0.02	26.2
Cu_2O-25-14-4	25.0	0.002005 0.001863 0.02	25.5
Cu_2O-25-14-5	25.0	0.002005 0.001863 0.02	28.0
Cu_2O-25-14-6	25.0	0.002005 0.001863 0.02	25.4,25.9
Cu_2O-25-14-7	25.0	0.002005 0.001863 0.02	25.6
Cu_2O-25-14-8	25.0	0.002005 0.001863 0.02	27.4
Cu_2O-25-15-1	25.0	0.006371 0.005799 0.02	293
Cu_2O-25-15-2	25.0	0.006371 0.005799 0.02	299
Cu_2O-25-15-3	24.9	0.006371 0.005799 0.02	319
Cu_2O-25-15-4	24.9	0.006371 0.005799 0.02	298
Cu_2O-25-15-5	25.0	0.006371 0.005799 0.02	291
Cu_2O-25-15-6	25.0	0.006371 0.005799 0.02	277,280
Cu_2O-25-15-7	25.0	0.006371 0.005799 0.02	280
Cu_2O-25-18-1	25.0	0.000918 0.000853 0.02	7.2
Cu_2O-25-18-2	25.0	0.000918 0.000853 0.02	6.8
Cu_2O-25-18-3	24.9	0.000918 0.000853 0.02	6.7
Cu_2O-25-18-4	24.7	0.000918 0.000853 0.02	6.6
Cu_2O-25-18-5	25.0	0.000918 0.000853 0.02	6.7

Table B-7
Continued

Sample ID	Temperature °C	$\underline{NH_3\ F_3SO_3H,}$ m Flow rate $mL \cdot min^{-1}$	Cu (AA) ppb
Cu_2O-25-18-6	25.0	0.000918 0.000853 0.02	6.2
Cu_2O-25-18-7	25.0	0.000918 0.000853 0.02	7.0
Cu_2O-50-13-1	50.0	0.000918 0.000853 0.02	12.7
Cu_2O-50-13-2	50.0	0.000918 0.000853 0.02	11.7
Cu_2O-50-13-3	50.4	0.000918 0.000853 0.02	12.5
Cu_2O-50-13-4	49.9	0.000918 0.000853 0.02	11.5
Cu_2O-50-13-5	50.1	0.000918 0.000853 0.02	10.7
Cu_2O-50-13-6	50.0	0.000918 0.000853 0.02	10.9
Cu_2O-50-13-7	50.0	0.000918 0.000853 0.02	11.7

C
SOLUBILITY DATA FOR CUPRIC OXIDE OBTAINED WITH THE HIGH-TEMPERATURE CELL

The samples are listed in chronological order within each table, which are divided according to the nature of the feed solution used. As indicated in the schematic of the apparatus in Figure 2-1, the two pressures listed in the following tables refer to the inlet pressure immediately upstream from the pre-heater and the pressure of the gas ballast reservoir. The concentrations and flow rates given in the next column refer to the feed solution and in all cases a post reactor solution was injected into the flow just after it exits the reaction vessel or column. The analytical techniques employed are symbolized as: flame atomic absorption spectrophotometry (AA) and graphite furnace atomic absorption spectrophotometry (GFAA).

Table C-1
Cupric oxide solubility data in trifluoromethanesulfonic acid solutions

Sample ID	Temperature °C	Inlet pressure bar	Outlet pressure bar	CF_3SO_3H, m Flow rate mL· min^{-1}	Cu (AA) ppm
CuO-100-16-1	100.0	11.1	10.1	0.0009617 0.1	32.5
CuO-100-16-2	100.0	11.1	11.2	0.0009617 0.1	31.8
CuO-100-16-3	100.2	11.4	11.4	0.0009617 0.1	31.9
CuO-100-16-4	100.1	11.3	11.3	0.0009617 0.1	31.9
CuO-100-16-5	100.0	12.6	12.6	0.0009617 0.1	32.2
CuO-100-16-6	100.1	11.6	11.6	0.0009617 0.1	32.2
CuO-100-16-7	100.2	12.4	12.4	0.0009617 0.1	32.2
CuO-100-16-8	100.1	11.8	11.8	0.0009617 0.1	32.2
CuO-100-16-9	100.1	12.2	12.2	0.0009617 0.1	32.5
CuO-100-17-1	100.0	12.1	12.1	0.0002070 0.1	9.4
CuO-100-17-2	100.1	12.3	12.3	0.0002070 0.1	8.7
CuO-100-17-3	100.0	12.1	12.1	0.0002070 0.1	8.7
CuO-100-17-4	100.0	12.6	12.6	0.0002070 0.1	8.7
CuO-100-17-5	100.1	11.4	11.3	0.0002070 0.1	8.7
CuO-100-17-6	100.1	12.3	12.3	0.0002070 0.1	8.7
CuO-100-17-7	100.0	12.9	12.9	0.0002070 0.1	8.7
CuO-100-17-8	100.2	13.3	13.3	0.0002070 0.1	8.9
CuO-100-17-9	100.0	12.8	12.7	0.0002070 0.1	8.7
CuO-100-17-10	100.2	12.6	12.6	0.0002070 0.1	8.7
CuO-100-17-11	100.2	12.3	12.3	0.0002070 0.1	8.7
CuO-100-17-12	100.2	12.3	12.3	0.0002070 0.1	8.8

Table C-1
Continued

Sample ID	Temperature °C	Inlet pressure bar	Outlet pressure bar	$\underline{CF_3SO_3H}$, m Flow rate mL· min^{-1}	Cu (AA) ppm
CuO-100-17-13	100.2	12.2	12.2	0.0002070 0.1	8.7
CuO-100-17-14	100.2	13.2	13.2	0.0002070 0.1	9.7
CuO-200-2-1	200.0	22.6	22.6	0.0002070 0.1	~~88.8~~
CuO-200-2-2	200.0	22.7	22.6	0.0002070 0.1	~~80.3~~
CuO-200-2-3	200.1	21.5	21.5	0.0002070 0.1	~~62.9~~
CuO-200-2-4	200.2	22.2	22.2	0.0002070 0.1	~~58.1~~
CuO-200-2-5	200.2	22.9	22.9	0.0002070 0.1	~~45.5~~
CuO-200-2-6	200.0	22.0	22.00	0.0002070 0.1	18.3
CuO-200-2-7	200.0	22.3	22.3	0.0002070 0.1	17.1
CuO-200-2-8	200.0	20.6	20.6	0.0002070 0.1	16.4
CuO-200-2-9	200.0	19.9	19.9	0.0002070 0.1	16.5
CuO-200-3-1	200.0	20.7	20.8	0.0003103 0.1	18.6
CuO-200-3-2	200.2	21.7	21.7	0.0003103 0.1	19.2
CuO-200-3-3	200.2	21.2	21.2	0.0003103 0.1	18.2
CuO-200-3-4	200.2	22.1	22.1	0.0003103 0.1	18.2
CuO-200-3-5	200.2	22.1	22.1	0.0003103 0.1	18.2
CuO-200-3-6	200.0	21.9	21.9	0.0003103 0.1	18.7
CuO-200-3-7	200.1	21.9	21.9	0.0003103 0.1	18.5
CuO-200-3-8	200.2	22.0	22.0	0.0003103 0.1	18.6
CuO-200-3-9	200.0	21.8	21.8	0.0003103 0.1	19.1

CuO-200-3-10	200.2	21.9	21.9	0.0003103 0.1	20.0

Table C-1
Continued

Sample ID	Temperature °C	Inlet pressure bar	Outlet pressure bar	$\underline{CF_3SO_3H}$, m Flow rate mL· min^{-1}	Cu (AA) ppm
CuO-200-3-11	200.0	22.1	22.1	0.0003103 0.1	18.7
CuO-350-6-1	349.9	176.0	174.1	0.0005269 0.1	3.9
CuO-350-6-2	350.0	176.8	174.0	0.0005269 0.1	3.8
CuO-350-6-3	350.1	178.5	173.5	0.0005269 0.1	3.6
CuO-350-6-4	350.0	176.1	173.4	0.0005269 0.1	4.0
CuO-350-6-5	350.1	177.3	173.6	0.0005269 0.1	3.8
CuO-350-6-6	349.9	180.9	173.3	0.0005269 0.1	3.9
CuO-350-6-7	350.0	181.0	175.8	0.0005269 0.1	3.8
CuO-350-6-8	349.9	182.3	174.8	0.0005269 0.1	4.0
CuO-350-6-9	350.1	182.6	174.2	0.0005269 0.1	3.9
CuO-350-6-10	350.0	182.9	174.9	0.0005269 0.1	3.7

Table C-2
Cupric oxide solubility data in ammonia –trifluoromethanesulfonic acid solutions

Sample ID	Temperature °C	Inlet pressure bar	Outlet pressure bar	Σ $\underline{NH_3}$, m Σ $\underline{CF_3SO_3H}$, m Flow rate mL· min^{-1}	Cu (AA) ppb
CuO-350-7-1	350.0	172.5	172.3	0.002060 0.1 0.001015	~~900~~
CuO-350-7-2	350.1	173.0	172.7	0.002060 0.1 0.001015	402
CuO-350-7-3	350.1	172.9	172.8	0.002060 0.1 0.001015	400
CuO-350-7-4	350.1	172.9	172.9	0.002060 0.1 0.001015	491
CuO-350-7-5	350.1	170.3	170.3	0.002060 0.1 0.001015	406
CuO-350-7-6	350.1	174.0	173.0	0.002060 0.1 0.001015	410
CuO-350-7-7	350.1	173.4	173.3	0.002060 0.1 0.001015	480
CuO-350-7-8	350.1	173.8	173.0	0.002060 0.1 0.001015	470
CuO-350-7-9	350.1	179.8	173.5	0.002060 0.1 0.001015	465
CuO-350-7-10	350.0	176.9	171.4	0.002060 0.1 0.001015	450
CuO-350-8-1	350.1	176.7	174.3	0.002721 0.1 0.0002467	~~3630~~* §
CuO-350-8-2	350.0	174.1	173.9	0.002721 0.1 0.0002467	~~4610~~* §

Table C-2
Continued

Sample ID	Temperature °C	Inlet pressure bar	Outlet pressure bar	Σ NH_3, m Σ CF_3SO_3H, m Flow rate mL· min^{-1}	Cu (AA) ppb
CuO-350-8-3	350.1	174.4	174.3	0.002721 0.1 0.0002467	~~3730~~* §
CuO-350-8-4	350.1	174.6	174.5	0.002721 0.1 0.0002467	~~3010~~* §
CuO-350-8-5	350.0	175.2	175.2	0.002721 0.1 0.0002467	2550* §
CuO-350-8-6	349.9	175.8	175.6	0.002721 0.1 0.0002467	2570* §
CuO-350-8-7	350.0	175.8	175.7	0.002721 0.1 0.0002467	2460* §
CuO-350-8-8	350.1	176.2	176.1	0.002721 0.1 0.0002467	2320* §
CuO-350-8-9	350.1	172.5	172.4	0.002721 0.1 0.0002467	2740* §
CuO-350-8-10	350.1	174.3	174.0	0.002721 0.1 0.0002467	2580* §
CuO-350-8-11	350.0	175.0	174.6	0.002721 0.1 0.0002467	2680* §
CuO-350-8-12	350.0	175.6	175.4	0.002721 0.1 0.0002467	2840* §
CuO-350-8-13	350.0	175.8	175.7	0.002721 0.1 0.0002467	2640* §
CuO-350-8-14	350.0	175.8	175.7	0.002721 0.1 0.0002467	2900* §

CuO-350-8-15	350.0	176.5	176.4	0.002721 0.1 0.0002467	2780* §

Table C-2
Continued

Sample ID	Temperature °C	Inlet pressure bar	Outlet pressure bar	Σ $\underline{NH_3}$, m Σ $\underline{CF_3SO_3H}$, m Flow rate mL· min^{-1}	Cu (AA) ppb
CuO-350-8-16	350.1	177.3	177.3	0.002721 0.1 0.0002467	2610* §
CuO-350-9-1	350.2	175.0	174.9	0.006046 0.1 0.0001299	~~1340*~~
CuO-350-9-2	350.1	174.4	174.4	0.006046 0.1 0.0001299	~~85.8*~~
CuO-350-9-3	350.0	174.5	174.4	0.006046 0.1 0.0001299	23.2*
CuO-350-9-4	350.2	174.2	174.2	0.006046 0.1 0.0001299	14.1*
CuO-350-9-5	350.2	175.0	174.9	0.006046 0.1 0.0001299	20.2*
CuO-350-9-6	350.2	175.5	175.5	0.006046 0.1 0.0001299	20.1*
CuO-350-9-7	350.1	175.6	175.6	0.006046 0.1 0.0001299	17.1* 17.3*
CuO-350-9-8	350.2	175.7	175.6	0.006046 0.1 0.0001299	18.0
CuO-350-9-9	350.1	176.0	176.0	0.006046 0.1 0.0001299	17.1*
CuO-350-9-10	350.0	176.0	176.0	0.006046 0.1 0.0001299	15.5*
CuO-350-9-11	350.1	174.0	173.9	0.006046 0.1	21.8*

				0.0001299	
CuO-350-9-12	350.0	176.1	176.1	0.006046 0.1 0.0001299	16.7*

Table C-2
Continued

Sample ID	Temperature °C	Inlet pressure bar	Outlet pressure bar	Σ $\underline{NH_3}$, m Σ $\underline{CF_3SO_3H}$, m Flow rate mL· min^{-1}	Cu (AA) ppb
CuO-350-9-13	350.1	176.2	176.2	0.006046 0.1 0.0001299	18.7*

* analyzed by GFAA
§ see discussion – results are compatible with Cu_2O solubility

Table C-3
Cupric oxide solubility data in sodium hydroxide solutions

Sample ID	Temperature °C	Inlet pressure bar	Outlet pressure bar	NaOH, m Flow rate $mL \cdot min^{-1}$	Cu (GFAA) ppb
CuO-350-10-1	350.1	175.3	175.3	0.001963 0.1	~~1340~~
CuO-350-10-2	350.0	175.4	175.4	0.001963 0.1	~~85.8~~
CuO-350-10-3	350.0	175.4	175.3	0.001963 0.1	~~36.0~~
CuO-350-10-4	350.1	175.5	175.5	0.001963 0.1	7.3
CuO-350-10-5	349.9	175.7	175.6	0.001963 0.1	6.5
CuO-350-10-6	350.0	175.7	175.7	0.001963 0.1	10.1
CuO-350-10-7	350.0	175.8	175.8	0.001963 0.1	7.1
CuO-350-10-8	349.9	176.0	175.9	0.001963 0.1	8.0
CuO-350-10-9	350.1	176.0	175.9	0.001963 0.1	10.0
CuO-350-15-1	350.0	175.4	175.4	0.002044 0.1	0.68
CuO-350-16-1*	350.0	175.5	175.5	0.0001112 0.15	18.6
CuO-350-16-2*	350.1	175.1	174.9	0.0001112 0.15	19.9
CuO-350-16-3*	350.0	174.9	174.8	0.0001112 0.15	17.1
CuO-350-16-4*	350.0	175.0	1745.3	0.0001112 0.15	22.6
CuO-350-16-5*	350.0	172.5	172.4	0.0001112 0.15	20.9
CuO-350-16-6*	349.9	172.8	172.7	0.0001112 0.15	17.9
CuO-350-16-7*	349.9	170.8	170.7	0.0001112 0.15	18.6
CuO-350-16-8*	350.1	170.3	170.2	0.0001112 0.15	19.8
CuO-350-16-9*	350.0	171.7	171.6	0.0001112 0.15	21.9
CuO-350-16-10*	350.0	170.4	170.4	0.0001112 0.15	27.0

Table C-3
Continued

Sample ID	Temperature °C	Inlet pressure bar	Outlet pressure bar	NaOH, Flow rate mL·min^{-1}	Cu (GFAA) ppb
CuO-350-5-1	350.0	174.3	174.3	0.0001902 0.1	3.9
CuO-350-5-2	350.0	177.2	177.3	0.0001902 0.1	1.5
CuO-350-5-3	350.0	177.3	177.4	0.0001902 0.1	1.8
CuO-350-5-4	350.0	178.7	178.8	0.0001902 0.1	2.4
CuO-350-5-5	350.0	179.0	179.0	0.0001902 0.1	1.3
CuO-350-5-6	350.0	177.1	177.0	0.0001902 0.1	1.1
CuO-350-5-7	350.0	177.6	177.7	0.0001902 0.1	1.5
CuO-350-5-8	350.0	177.4	177.5	0.0001902 0.1	3.2
CuO-350-5-9	350.0	177.7	177.8	0.0001902 0.1	1.5
CuO-350-5-10	350.0	177.5	177.6	0.0001902 0.1	1.9
CuO-350-5-11	350.0	175.7	175.7	0.0001902 0.1	1.0
CuO-350-11-1	350.1	191.5	191.5	0.0001128 0.1	~~21.4~~
CuO-350-11-2	350.0	174.8	174.7	0.0001128 0.1	~~6.9~~
CuO-350-11-3	350.0	174.8	174.87	0.0001128 0.1	3.8
CuO-350-11-4	349.9	174.7	174.6	0.0001128 0.1	3.3
CuO-350-11-5	350.0	174.6	174.6	0.0001128 0.1	2.8
CuO-350-11-6	350.2	174.6	174.6	0.0001128 0.1	2.6
CuO-350-11-7	349.9	174.8	174.8	0.0001128 0.1	2.4
CuO-350-11-8	350.1	174.8	174.8	0.0001128 0.1	2.4
CuO-350-11-9	350.0	174.9	174.9	0.0001128 0.1	2.0

CuO-350-11-10	350.0	174.8	174.8	0.0001128 0.1	2.0

Table C-3
Continued

Sample ID	Temperature °C	Inlet pressure bar	Outlet pressure bar	NaOH, Flow rate $mL \cdot min^{-1}$	Cu (GFAA) ppb
CuO-350-11-11	350.0	175.6	175.6	0.0001128 0.1	1.8
CuO-350-11-12	350.1	175.6	175.6	0.0001128 0.1	2.3
CuO-350-11-13	350.0	175.8	175.8	0.0001128 0.1	2.9
CuO-350-11-14	350.1	175.9	175.9	0.0001128 0.1	2.7
CuO-350-11-15	350.1	176.0	175.9	0.0001128 0.1	3.5

* feed ammonia solution pressurized with 0.7 bar (10 psi) O_2

Table C-4
Cupric oxide solubility data in nitric acid solutions

Sample ID	Temperature °C	Inlet pressure bar	Outlet pressure bar	$\underline{HNO_3}$, m Flow rate mL· min^{-1}	Cu (AA) ppm
CuO-350-12-1	350.0	175.0	174.9	0.0007611 0.15	1.13
CuO-350-12-2	349.9	175.0	175.0	0.0007611 0.15	1.13
CuO-350-12-3	350.1	176.2	176.2	0.0007611 0.15	1.14
CuO-350-12-4	350.0	176.1	176.1	0.0007611 0.15	1.18
CuO-350-12-5	350.0	176.1	176.2	0.0007611 0.15	1.16
CuO-350-12-6	350.1	175.8	175.7	0.0007611 0.15	1.19
CuO-350-12-7	350.1	175.6	175.5	0.0007611 0.15	1.21
CuO-350-12-8	350.1	176.0	175.9	0.0007611 0.15	1.22
CuO-350-12-9	350.0	175.5	175.5	0.0007611 0.15	1.25
CuO-350-12-10	350.0	175.5	175.5	0.0007611 0.15	1.24
CuO-350-12-11	350.1	173.7	173.4	0.0007611 0.15	1.28
CuO-350-13-1	350.0	173.5	173.5	0.0004685 0.15	1.55
CuO-350-13-2	350.0	174.5	174.4	0.0004685 0.15	1.22
CuO-350-13-3	350.1	174.9	174.9	0.0004685 0.15	1.21
CuO-350-13-4	350.0	176.0	175.9	0.0004685 0.15	1.20
CuO-350-13-5	350.1	176.1	176.1	0.0004685 0.15	1.21
CuO-350-13-6	350.0	176.1	176.1	0.0004685 0.15	1.21
CuO-350-13-7	350.1	176.2	176.2	0.0004685 0.15	1.22
CuO-350-13-8	350.1	176.2	176.1	0.0004685 0.15	1.22

Table C-4
Continued

Sample ID	Temperature °C	Inlet pressure bar	Outlet pressure bar	$\underline{HNO_3}$, m Flow rate mL· min^{-1}	Cu (GFAA) ppm
CuO-350-17-7	350.1	154.8	154.8	0.001096 0.1	4.4
CuO-350-17-8	350.0	156.7	156.6	0.001096 0.1	4.6
CuO-350-17-9	350.0	155.3	155.2	0.001096 0.1	4.5
CuO-350-18-1	350.0	158.7	158.7	0.0000000 0.1	4.2
CuO-350-18-2	350.2	159.0	158.9	0.0000000 0.1	3.4
CuO-350-18-3	350.1	157.4	157.4	0.0000000 0.1	2.9
CuO-350-18-4	350.1	154.3	154.3	0.0000000 0.1	2.8
CuO-350-18-5	350.0	160.4	160.3	0.0000000 0.1	2.8

Table C-5
Cupric oxide solubility data in ammonia, nitric acid solutions

Sample ID	Temperature °C	Inlet pressure bar	Outlet pressure bar	Σ NH_3, m Σ HNO_3, m Flow rate mL· min^{-1}	Cu (AA) ppm
CuO-350-14-1	350.1	174.4	174.4	0.002044 0.1 0.0001779	9.0
CuO-350-14-2	349.9	174.9	174.8	0.002044 0.1 0.0001779	8.3
CuO-350-14-3	350.1	176.3	176.3	0.002044 0.1 0.0001779	7.5
CuO-350-14-4	350.0	176.3	176.3	0.002044 0.1 0.0001779	7.4
CuO-350-14-5	350.1	176.1	176.1	0.002044 0.1 0.0001779	7.3
CuO-350-14-6	349.9	176.1	176.1	0.002044 0.1 0.0001779	7.0
CuO-350-14-7	350.0	176.2	176.2	0.002044 0.1 0.0001779	6.8
CuO-350-14-8	350.1	176.0	176.0	0.002044 0.1 0.0001779	7.0
CuO-350-15-3	350.0	175.5	175.5	0.001956 0.1 0.0002013	6.6
CuO-350-15-4	350.1	175.6	175.6	0.001956 0.1 0.0002013	6.6
CuO-350-15-5	350.1	175.4	175.4	0.001956 0.1 0.0002013	6.6
CuO-350-15-6	350.1	175.4	175.3	0.001956 0.1 0.0002013	6.8
CuO-350-15-7	350.1	175.4	175.3	0.001956 0.1	6.9

				0.0002013	

Table C-5
Continued

Sample ID	Temperature °C	Inlet pressure bar	Outlet pressure bar	Σ $\underline{NH_3}$, m Σ $HN\underline{O_3}$, m Flow rate mL· min^{-1}	Cu (AA) ppm
CuO-350-15-8	350.0	175.5	175.5	0.001956 0.1 0.0002013	7.1
CuO-350-15-9	350.0	174.8	174.7	0.001956 0.1 0.0002013	7.3
CuO-350-15-10	350.0	175.3	175.3	0.001956 0.1 0.0002013	7.7
CuO-350-15-11	350.0	175.5	175.5	0.001956 0.1 0.0002013	7.4
CuO-350-15-12	350.1	175.4	175.4	0.001956 0.1 0.0002013	7.2
CuO-350-15-13	3549.9	175.6	175.6	0.001956 0.1 0.0002013	7.1

D

SOLUBILITY DATA FOR CUPRIC OXIDE OBTAINED WITH THE LOW-TEMPERATURE CELL

The samples are listed in chronological order within each table, which are divided according to the nature of the feed solution used. The flow rate of the feed solution was varied initially and the concentration of copper was found to be independent of flow rate from 0.01 to 0.05 $mL \cdot min^{-1}$ and hence the flow rate of 0.02 $mL \cdot min^{-1}$ was adopted for all the measurements tabulated here. Copper concentrations that are struck-out were not used further in the data analysis. The analytical techniques employed are symbolized as: flame atomic absorption spectrophotometry (AA), graphite furnace atomic absorption spectrophotometry (GFAA), and inductively-coupled plasma mass spectrometry (ICPMS).

Table D-1
Cupric oxide solubility data in trifluoromethanesulfonic acid solutions

Sample ID	Temperature °C	CF_3SO_3H, m Flow rate mL min^{-1}	Cu (AA) ppm
CuO-25-1-1	25.0	0.002005 0.06	63.0
CuO-25-1-2	25.0	0.002005 0.06	62.6
CuO-25-1-3	25.0	0.002005 0.07	62.2
CuO-25-1-4	25.0	0.002005 0.07	62.7
CuO-25-1-5	25.0	0.002005 0.04	63.0
CuO-25-1-6	25.0	0.002005 0.04	62.9
CuO-25-1-7	25.0	0.002005 0.02	63.6
CuO-25-1-8	25.0	0.002005 0.02	63.3
CuO-25-1-9	25.0	0.002005 0.009	63.5
CuO-25-1-10	25.0	0.002005 0.009	63.6
CuO-25-1-11	25.0	0.002005 0.009	63.9
CuO-25-1-12	25.0	0.002005 0.009	63.3
CuO-25-1-13	25.0	0.002005 0.009	62.9
CuO-25-2-1	25.0	0.000590 0.02	~~26.1~~
CuO-25-2-2	25.0	0.000590 0.02	~~22.2~~
CuO-25-2-3	25.0	0.000590 0.02	~~20.1~~
CuO-25-2-4	25.0	0.000590 0.02	~~19.0~~
CuO-25-2-5	25.0	0.000590 0.02	~~18.7~~
CuO-25-2-6	25.0	0.000590 0.02	18.4
CuO-25-2-7	25.0	0.000590 0.02	18.3

CuO-25-2-8	25.0	0.000590 0.02	18.4

Table D-1 continued

Sample ID	Temperature °C	CF_3SO_3H, m Flow rate mL min^{-1}	Cu (AA) ppm
CuO-25-2-9	25.0	0.000590 0.02	18.3
CuO-25-3-1	25.0	0.000213 0.02	~~9.18~~
CuO-25-3-2	25.0	0.000213 0.02	~~8.03~~
CuO-25-3-3	25.0	0.000213 0.009	~~7.37~~
CuO-25-3-4	25.0	0.000213 0.009	~~7.05~~
CuO-25-3-5	25.0	0.000213 0.009	~~6.90~~
CuO-25-3-6	25.0	0.000213 0.01	~~6.82~~
CuO-25-3-7	25.0	0.000213 0.01	~~6.77~~
CuO-25-3-8	25.0	0.000213 0.02	~~9.19~~
CuO-25-3-9	25.0	0.000213 0.02	~~6.83 6.90~~
CuO-25-3-10	25.0	0.000213 0.02	~~6.82~~
CuO-50-7-1	50.0	0.002005 0.02	~~51.0~~
CuO-50-7-2	50.0	0.002005 0.02	63.2
CuO-50-7-3	50.0	0.002005 0.02	64.0
CuO-50-7-5	50.1	0.002005 0.02	64.5
CuO-50-7-6	50.2	0.002005 0.02	64.4
CuO-50-7-7	50.1	0.002005 0.02	65.1
CuO-50-7-8	50.1	0.002005 0.02	66.3

Table D-2
Cupric oxide solubility data in Bis-Tris*, trifluoromethanesulfonic acid solutions

Sample ID	Temperature °C	Bis-Tris F_3CSO_3H, m Flow rate mL min^{-1}	Cu (AA) ppm
CuO-25-4-1	25.0	0.001944 0.000951 0.02	50.7
CuO-25-4-2	25.0	0.001944 0.000951 0.02	50.5
CuO-25-4-3	25.0	0.001944 0.000951 0.02	51.0

* Bis-Tris = 2,2-bis(hydroxymethyl)-2,2',2"-nitrilotriethanol

Table D-3
Cupric oxide solubility data in sodium hydroxide solutions

Sample ID	Temperature °C	NaOH, m Flow rate mL min^{-1}	Cu (GFAA) ppb	Cu (ICPMS) ppb
CuO-25-5-1	25.0	0.001034 0.02	~~577~~	
CuO-25-5-2	25.0	0.001034 0.02	~~231~~	
CuO-25-5-3	25.0	0.001034 0.02	~~256~~	
CuO-25-5-4	25.0	0.001034 0.02	~~136~~	
CuO-25-5-5	25.0	0.001034 0.02	~~84.5~~	
CuO-25-5-6	25.0	0.001034 0.02	~~40.0~~	
CuO-25-5-7	25.0	0.001034 0.02	~~19.4~~	
CuO-25-5-8	25.0	0.001034 0.02	~~9.1~~	
CuO-25-5-9	25.0	0.001034 0.02	~~9.1~~	
CuO-25-5-10	25.0	0.001034 0.02	~~4.2 6.1~~	
CuO-25-5-11	25.0	0.001034 0.02	~~3.3 3.8~~	
CuO-25-5-12	25.0	0.001034 0.02	2.1 3.5 3.3	
CuO-25-5-13	25.0	0.001034 0.02	1.5 3.4 2.7	~~9.5~~
CuO-25-5-14	25.0	0.001034 0.02	1.2 3.1 2.1	~~8.2~~
CuO-25-5-15	25.0	0.001034 0.02	2.1 2.1	
CuO-25-6-1	25.0	0.009901 0.02	~~34.9~~	
CuO-25-6-2	25.0	0.009901 0.02	~~26.9~~	
CuO-25-6-3	25.0	0.009901 0.02	~~20.3~~	11.2
CuO-25-6-4	25.0	0.009901 0.02	~~16.9~~	
CuO-25-6-5	25.0	0.009901 0.02	11.8	
CuO-25-6-6	25.0	0.009901 0.02	9.2	

Table D-3
Continued

Sample ID	Temperature °C	NaOH, m Flow rate mL min^{-1}	Cu (GFAA) ppb	Cu (ICPMS) ppb
CuO-25-6-7	25.0	0.009901 0.02	8.4	4.6
CuO-25-6-8	25.0	0.009901 0.02	8.0	3.9
CuO-25-6-9	25.0	0.009901 0.02	5.2	1.1 1.2
CuO-25-6-10	25.0	0.009901 0.02	4.8	1.1 1.2
CuO-25-6-11	25.0	0.009901 0.02	12.6 12.2	
CuO-25-6-12	25.0	0.009901 0.02	5.8	
CuO-25-6-13	25.0	0.009901 0.02	9.0 4.4	
CuO-25-6-14	25.0	0.009901 0.02	7.2 3.7	
CuO-25-6-15	25.0	0.009901 0.02	7.4 5.9	5.4
CuO-25-9-1	25.0	0.000101 0.02	5.8	2.30
CuO-25-9-2	25.0	0.000101 0.02	2.9	1.9
CuO-25-9-3	25.0	0.000101 0.02	~~8.6~~	1.6
CuO-25-9-4	25.0	0.000101 0.02	2.0	1.7
CuO-25-9-5	25.0	0.000101 0.02	~~14.1~~	
CuO-25-9-6	25.0	0.000101 0.02	1.9 1.2	1.0 1.2
CuO-25-9-7	25.0	0.001034 0.02	1.0	1.1 1.3
CuO-25-9-8	25.0	0.000101 0.02	2.7	1.0 1.2
CuO-25-9-9	25.0	0.000101 0.02	1.4	
CuO-25-9-10	25.0	0.000101 0.02	2.1	
CuO-25-9-11	25.0	0.000101 0.02	1.1	

Table D-3
Continued

Sample ID	Temperature °C	NaOH, m Flow rate mL min^{-1}	Cu (GFAA) ppb
CuO-25-9-12	25.0	0.000101 0.02	1.0
CuO-25-9-13	25.0	0.000101 0.02	3.4
CuO-25-9-14	25.0	0.000101 0.02	1.2
CuO-25-12-1	25.0	0.000966 0.02	2.7
CuO-25-12-2	25.0	0.000966 0.02	1.2
CuO-25-12-3	25.0	0.000966 0.02	1.2
CuO-25-12-4	25.0	0.000966 0.02	1.5
CuO-25-12-5	25.0	0.000966 0.02	1.4
CuO-25-12-6	25.0	0.000966 0.02	1.3
CuO-25-12-7	25.0	0.000966 0.02	1.5
CuO-25-12-8	25.0	0.000966 0.02	2.7
CuO-25-12-9	25.0	0.000966 0.02	1.4
CuO-25-12-10	25.1	0.000966 0.02	1.8
CuO-25-12-11	25.2	0.000966 0.02	2.3 1.4
CuO-25-12-12	25.0	0.000966 0.02	1.4
CuO-25-12-13	25.0	0.000966 0.02	1.0
CuO-25-13-1	25.0	0.09736 0.02	56.2
CuO-25-13-2	25.0	0.09736 0.02	56.1
CuO-25-13-3	25.0	0.09736 0.02	47.4
CuO-25-13-4	25.0	0.09736 0.02	47.5

CuO-25-13-5	25.0	0.09736 0.02	43.4

Table D-3
Continued

Sample ID	Temperature °C	NaOH, m Flow rate mL min^{-1}	Cu (GFAA) ppb
CuO-25-13-6	25.0	0.09736 0.02	40.9
CuO-25-13-7	25.0	0.09736 0.02	47.8
CuO-25-13-8	25.0	0.09736 0.02	40.9
CuO-25-13-9	25.0	0.09736 0.02	33.0
CuO-25-13-10	25.0	0.09736 0.02	40.2
CuO-25-13-11	25.0	0.09736 0.02	33.2
CuO-25-13-12	25.0	0.09736 0.02	33.1
CuO-25-13-13	25.0	0.09736 0.02	~~29.5~~
CuO-25-13-14	25.0	0.09736 0.02	34.1
CuO-25-13-15	25.0	0.09736 0.02	39.3
CuO-50-3-1	49.9	0.0001761 0.02	~~5.7~~
CuO-50-3-2	49.9	0.0001761 0.02	1.8
CuO-50-3-3	50.0	0.0001761 0.02	~~4.1 3.2~~
CuO-50-3-4	50.0	0.0001761 0.02	0.8 0.6
CuO-50-3-5	50.0	0.0001761 0.02	1.7
CuO-50-3-6	50.0	0.0001761 0.02	0.6 0.4
CuO-50-3-7	50.1	0.0001761 0.02	0.6 0.5
CuO-50-3-8	50.0	0.0001761 0.02	0.7 0.5
CuO-50-3-9	50.1	0.0001761 0.02	1.7 0.4

CuO-50-3-10	50.1	0.0001761 0.02	1.3 1.4
CuO-50-3-11	50.1	0.0001761 0.02	0.9

Table D-3
Continued

Sample ID	Temperature °C	NaOH, m Flow rate mL min^{-1}	Cu (GFAA) ppb
CuO-50-4-1	50.0	0.001077 0.02	1.9
CuO-50-4-2	50.0	0.001077 0.02	1.0
CuO-50-4-3	50.0	0.001077 0.02	1.8
CuO-50-4-4	50.0	0.001077 0.02	0.8
CuO-50-4-5	50.1	0.001077 0.02	1.3
CuO-50-4-6	50.1	0.001077 0.02	0.8
CuO-50-4-7	50.0	0.001077 0.02	0.7
CuO-50-4-8	50.0	0.001077 0.02	0.5
CuO-50-4-9	50.1	0.001077 0.02	0.4
CuO-50-4-10	50.0	0.001077 0.02	0.8
CuO-50-4-11	50.1	0.001077 0.02	0.5 0.5
CuO-50-4-12	50.1	0.001077 0.02	0.5
CuO-50-5-1	50.0	0.01156 0.02	2.4
CuO-50-5-2	49.9	0.01156 0.02	2.2
CuO-50-5-5	50.1	0.01156 0.02	2.0
CuO-50-5-6	50.0	0.01156 0.02	2.2
CuO-50-5-7	50.0	0.01156 0.02	2.0
CuO-50-5-8	50.0	0.01156 0.02	1.7

CuO-50-5-9	50.0	0.01156	0.02	1.7
CuO-50-5-10	50.0	0.01156	0.02	1.6
CuO-50-5-11	49.9	0.01156	0.02	1.9

Table D-3
Continued

Sample ID	Temperature °C	NaOH, m Flow rate mL min^{-1}		Cu (GFAA) ppb
CuO-50-5-12	49.9	0.01156	0.02	1.4
CuO-50-5-13	49.9	0.01156	0.02	1.5
CuO-50-6-1	50.0	0.1022	0.02	~~18.5~~
CuO-50-6-2	50.0	0.1022	0.02	28.9
CuO-50-6-3	50.0	0.1022	0.02	30.4
CuO-50-6-4	50.0	0.1022	0.02	29.6
CuO-50-6-5	50.0	0.1022	0.02	28.9
CuO-50-6-7	50.0	0.1022	0.02	25.4
CuO-50-6-8	50.0	0.1022	0.02	27.9
CuO-50-6-9	50.0	0.1022	0.02	28.2
CuO-50-6-10	49.9	0.1022	0.02	28.7
CuO-50-6-11	49.9	0.1022	0.02	26.7
CuO-50-6-12	50.1	0.1022	0.02	27.3

Table D-4
Cupric oxide solubility data in Tris*, trifluoromethanesulfonic acid solutions

Sample ID	Temperature °C	Tris F_3CSO_3H, m Flow rate mL min^{-1}	Cu (AA) ppb
CuO-25-7-1	25.0	0.001798 0.001986 0.02	723
CuO-25-7-2	25.0	0.001798 0.001986 0.02	625
CuO-25-7-3	25.0	0.001798 0.001986 0.02	650
CuO-25-7-4	25.0	0.001798 0.001986 0.02	642
CuO-25-7-5	25.0	0.001798 0.001986 0.02	627
CuO-25-7-6	25.0	0.001798 0.001986 0.02	621
CuO-25-7-7	25.0	0.001798 0.001986 0.02	618
CuO-25-8-1	25.0	0.000191 0.000140 0.02	10700
CuO-25-8-2	25.0	0.000191 0.000140 0.02	8430
CuO-25-8-3	25.0	0.000191 0.000140 0.02	7900
CuO-25-8-4	25.0	0.000191 0.000140 0.02	8130
CuO-25-8-5	25.0	0.000191 0.000140 0.02	13100
CuO-25-8-6	25.0	0.000191 0.000140 0.02	8250
CuO-25-8-7	25.0	0.000191 0.000140 0.02	8130

* Tris = tris(hydroxymethyl)aminomethane

Table D-5
Cupric oxide solubility data in boric acid, sodium hydroxide solutions

Sample ID	Temperature °C	$\underline{B(OH)_3}$ $\underline{NaOH}$, m Flow rate mL min^{-1}	Cu (GFAA) ppb	Cu (ICPMS) ppb
CuO-25-10-1	25.0	0.002153 0.000943 0.02	1.8	
CuO-25-10-2	25.0	0.002153 0.000943 0.02	1.7	
CuO-25-10-3	25.0	0.002153 0.000943 0.02	5.9	5.8
CuO-25-10-4	25.0	0.002153 0.000943 0.02	1.8	
CuO-25-10-5	25.1	0.002153 0.000943 0.02	1.5	1.5
CuO-25-10-6	25.2	0.002153 0.000943 0.02	2.1 1.4	1.9
CuO-25-10-7	25.1	0.002153 0.000943 0.02	1.4	1.6
CuO-25-10-8	24.9	0.002153 0.000943 0.02	1.8	1.4
CuO-25-10-9	24.9	0.002153 0.000943 0.02	1.7	
CuO-25-10-10	25.0	0.002153 0.000943 0.02	1.5	1.4
CuO-25-11-1	24.9	0.002083 0.0001204 0.02	5.6	
CuO-25-11-2	25.0	0.002083 0.0001204 0.02	10.8	
CuO-25-11-3	24.9	0.002083 0.0001204 0.02	6.0	
CuO-25-11-4	24.9	0.002083 0.0001204 0.02	8.0	
CuO-25-11-5	25.0	0.002083 0.0001204 0.02	5.0	

CuO-25-11-6	25.0	0.002083 0.0001204 0.02	22.1	
CuO-25-11-7	25.0	0.002083 0.0001204 0.02	4.5	4.0
CuO-25-11-8	25.0	0.002083 0.0001204 0.02	5.9	
CuO-25-11-9	25.0	0.002083 0.0001204 0.02	5.0	4.2
CuO-25-11-10	25.0	0.002083 0.0001204 0.02	4.0 5.2	4.1

Table D-5
Continued

Sample ID	**Temperature °C**	**$B(OH)_3$ NaOH, m Flow rate mL min^{-1}**	**Cu (GFAA) ppb**	**Cu (ICPMS) ppb**
CuO-25-11-11	24.9	0.002083 0.0001204 0.02	5.2	4.3
CuO-25-11-12	24.9	0.002083 0.0001204 0.02	4.4	4.1
CuO-50-2-1	49.9	0.002083 0.0001204 0.02	4.2	
CuO-50-2-3	50.0	0.002083 0.0001204 0.02	4.2	
CuO-50-2-4	50.3	0.002083 0.0001204 0.02	4.4	
CuO-50-2-5	50.0	0.002083 0.0001204 0.02	3.5	
CuO-50-2-6	50.2	0.002083 0.0001204 0.02	3.4	
CuO-50-2-7	49.9	0.002083 0.0001204 0.02	3.1	
CuO-50-2-8	50.0	0.002083 0.0001204 0.02	5.1	
CuO-50-2-9	50.0	0.002083 0.0001204 0.02	2.5	
CuO-50-2-10	50.0	0.002083 0.0001204 0.02	2.2	
CuO-50-2-11	50.0	0.002083 0.0001204 0.02	2.0	
CuO-50-2-12	50.0	0.002083 0.0001204 0.02	1.9	
CuO-50-2-13	50.0	0.002083 0.0001204 0.02	1.7	

CuO-50-2-14	50.0	0.002083 0.0001204 0.02	1.7	
CuO-50-2-15	50.0	0.002083 0.0001204 0.02	1.8	
CuO-50-2-16	50.0	0.002083 0.0001204 0.02	~~12.4~~	
CuO-50-2-18	50.0	0.002083 0.0001204 0.02	2.2	
CuO-50-2-19	50.0	0.002083 0.0001204 0.02	2.0	
CuO-50-2-20	50.0	0.002083 0.0001204 0.02	1.9	

Table D-5
Continued

Sample ID	Temperature °C	$B(OH)_3$ NaOH, m Flow rate mL min^{-1}	Cu (GFAA) ppb
CuO-50-12-1	50.0	0.002402 0.000000 0.02	~~489~~
CuO-50-12-2	50.0	0.002402 0.000000 0.02	~~444~~
CuO-50-12-3	50.1	0.002402 0.000000 0.02	387
CuO-50-12-4	50.0	0.002402 0.000000 0.02	358
CuO-50-12-5	50.0	0.002402 0.000000 0.02	348
CuO-50-12-6	50.0	0.002402 0.000000 0.02	353 378
CuO-50-12-7	50.0	0.002402 0.000000 0.02	337
CuO-50-12-8	50.0	0.002402 0.000000 0.02	333

Table D-6
Cupric oxide solubility data in sodium dihydrogenphosphate, sodium hydroxide solutions

Sample ID	Temperature °C	NaOH, m NaH_2PO_4, m Flow rate mL· min^{-1}	Cu (GFAA) ppb
CuO-25-14-1	25.0	0.0004977 0.02 0.0004712	18.6
CuO-25-14-2	25.0	0.0004977 0.02 0.0004712	18.6
CuO-25-14-3	25.0	0.0004977 0.02 0.0004712	17.0
CuO-25-14-4	25.0	0.0004977 0.02 0.0004712	25.2
CuO-25-14-5	25.0	0.0004977 0.02 0.0004712	27.0
CuO-25-14-6	25.0	0.0004977 0.02 0.0004712	29.4
CuO-25-14-7	25.0	0.0004977 0.02 0.0004712	35.4
CuO-25-14-8	25.0	0.0004977 0.02 0.0004712	43.5
CuO-25-14-9	25.0	0.0004977 0.02 0.0004712	53.0

CuO-25-14-10	25.0	0.0004977 0.02 0.0004712	50.2
CuO-25-14-11	25.0	0.0004977 0.02 0.0004712	58.7
CuO-25-14-12	25.0	0.0004977 0.02 0.0004712	57.4
CuO-25-14-13	25.0	0.0004977 0.02 0.0004712	59.6

Table D-6
Continued

Sample ID	**Temperature °C**	**NaOH, m NaH_2PO_4, m Flow rate mL· min^{-1}**	**Cu (GFAA) ppb**
CuO-25-14-14	25.0	0.0004977 0.02 0.0004712	73.6
CuO-25-14-15	25.0	0.0004977 0.02 0.0004712	51.9
CuO-25-15-1	25.1	0.0000782 0.02 0.0001522	47.9
CuO-25-15-2	25.1	0.0000782 0.02 0.0001522	45.4
CuO-25-15-3	25.0	0.0000782 0.02 0.0001522	51.1
CuO-25-15-4	25.0	0.0000782 0.02 0.0001522	50.5
CuO-25-15-5	25.0	0.0000782 0.02 0.0001522	48.7
CuO-25-15-6	25.0	0.0000782 0.02 0.0001522	50.0
CuO-25-15-7	25.0	0.0000782 0.02 0.0001522	47.4

CuO-25-15-8	24.9	0.0000782 0.02 0.0001522	50.9
CuO-25-15-9	24.9	0.0000782 0.02 0.0001522	49.4
CuO-25-15-10	24.9	0.0000782 0.02 0.0001522	46.6

Table D-6
Continued

Sample ID	Temperature °C	NaOH, m NaH_2PO_4, m Flow rate mL· min^{-1}	Cu (GFAA) ppb
CuO-50-1-1	49.9	0.0000782 0.02 0.0001522	54.5
CuO-50-1-2	50.0	0.0000782 0.02 0.0001522	46.9
CuO-50-1-3	50.0	0.0000782 0.02 0.0001522	49.3
CuO-50-1-4	50.0	0.0000782 0.02 0.0001522	39.8
CuO-50-1-5	50.0	0.0000782 0.02 0.0001522	41.4
CuO-50-1-6	50.0	0.0000782 0.02 0.0001522	36.7
CuO-50-1-7	50.0	0.0000782 0.02 0.0001522	36.1
CuO-50-8-1	50.0	0.0004977 0.02 0.0009689	~~11.2~~
CuO-50-8-2	50.1	0.0004977 0.02	~~14.9~~

		0.0009689	
CuO-50-8-3	50.1	0.0004977 0.02 0.0009689	~~24.8~~
CuO-50-8-4	50.1	0.0004977 0.02 0.0009689	30.6 31.6
CuO-50-8-5	50.1	0.0004977 0.02 0.0009689	34.2
CuO-50-8-6	50.1	0.0004977 0.02 0.0009689	35.8

Table D-6
Continued

Sample ID	**Temperature °C**	**NaOH, m NaH_2PO_4, m Flow rate mL· min^{-1}**	**Cu (GFAA) ppb**
CuO-50-8-7	50.1	0.0004977 0.02 0.0009689	38.7
CuO-50-8-8	50.0	0.0004977 0.02 0.0009689	37.0
CuO-50-8-9	50.1	0.0004977 0.02 0.0009689	34.5
CuO-50-8-10	50.0	0.0004977 0.02 0.0009689	33.9

Table D-7
Cupric oxide solubility data in acetic acid, sodium hydroxide solutions

Sample ID	Temperature °C	NaOH, m CH_3OOH, m Flow rate mL· min^{-1}	Cu (AA) ppm
CuO-50-9-1	50.0	0.0000991 0.02 0.001016	18.4
CuO-50-9-2	50.0	0.0000991 0.02 0.001016	20.6
CuO-50-9-3	50.0	0.0000991 0.02 0.001016	20.9
CuO-50-9-4	50.1	0.0000991 0.02 0.001016	20.6
CuO-50-9-5	50.0	0.0000991 0.02 0.001016	20.6
CuO-50-9-6	50.0	0.0000991 0.02 0.001016	20.2
CuO-50-9-7	50.0	0.0000991 0.02 0.001016	20.6
CuO-50-10-1	50.0	0.0003056 0.02 0.003128	63.1
CuO-50-10-2	50.0	0.0003056 0.02 0.003128	56.4
CuO-50-10-3	50.0	0.0003056 0.02 0.003128	56.3
CuO-50-10-4	50.1	0.0003056 0.02 0.003128	56.0
CuO-50-10-5	50.0	0.0003056 0.02 0.003128	56.8
CuO-50-10-6	50.1	0.0003056 0.02 0.003128	56.1

Table D-7
Continued

Sample ID	Temperature °C	NaOH, m CH_3OOH, m Flow rate $mL \cdot min^{-1}$	Cu (AA) ppm
CuO-50-10-7	50.0	0.0003056 0.02 0.003128	56.9
CuO-50-10-8	50.0	0.0003056 0.02 0.003128	56.6
CuO-50-10-9	50.1	0.0003056 0.02 0.003128	57.4
CuO-50-10-10	50.0	0.0003056 0.02 0.003128	56.6
CuO-50-10-11	50.0	0.0003056 0.02 0.003128	56.9
CuO-50-11-12	49.8	0.0001058 0.02 0.0002091	2.49
CuO-50-11-2	49.8	0.0001058 0.02 0.0002091	2.46 2.37
CuO-50-11-3	50.2	0.0001058 0.02 0.0002091	2.27 2.33
CuO-50-11-4	50.1	0.0001058 0.02 0.0002091	2.25 2.31
CuO-50-11-5	50.1	0.0001058 0.02 0.0002091	2.30
CuO-50-11-6	49.9	0.0001058 0.02 0.0002091	2.31
CuO-50-11-7	50.0	0.0001058 0.02 0.0002091	2.32
CuO-50-11-8	49.9	0.0001058 0.02	2.30

		0.0002091	

E
SOLUBILITY DATA FOR COPPER METAL OXIDE OBTAINED WITH THE HIGH-TEMPERATURE CELL

The samples are listed in chronological order within each table, which are divided according to the nature of the feed solution used. The flow rate of the feed solution was varied from 0.10 to 0.20 $mL \cdot min^{-1}$. Copper concentrations that are struck-out were not used further in the data analysis. The analytical technique employed is symbolized as: graphite furnace atomic absorption spectrophotometry (GFAA)

Table E-1
Copper metal solubility data in sodium hydroxide solutions

Sample ID	Temperature °C	Inlet pressure bar	Outlet pressure bar	NaOH, m Flow rate mL· min^{-1}	Cu (GFAA) ppb
Cu-100-1-1	100.0	49.6	49.3	0.001047* 0.2	~~341~~
Cu-100-1-2	100.0	52.7	52.6	0.001047* 0.2	~~49~~
Cu-100-1-3	100.0	52.8	52.7	0.001047* 0.2	17
Cu-100-1-4	100.0	52.5	52.4	0.001047* 0.2	18
Cu-100-1-5	100.0	52.8	52.6	0.001047* 0.2	17
Cu-100-1-6	100.0	52.9	52.8	0.001047* 0.2	17
Cu-100-1-7	100.0	52.5	52.4	0.001047* 0.2	17
Cu-100-1-8	100.0	53.0	52.9	0.001047* 0.2	37
Cu-100-1-9	100.0	53.4	53.3	0.001047* 0.2	26
Cu-100-1-10	100.0	53.4	53.3	0.001047* 0.2	20
Cu-100-1-11	100.0	54.1	54.1	0.001033* 0.2	~~106~~
Cu-100-1-12	100.0	53.9	53.8	0.001033* 0.2	19
Cu-100-1-13	100.0	54.2	54.2	0.001033* 0.2	14
Cu-100-1-14	100.0	54.0	54.0	0.001033* 0.2	22
Cu-100-1-15	100.0	54.8	54.7	0.001033* 0.2	16
Cu-100-1-16	100.0	54.8	54.8	0.001033* 0.2	12
Cu-100-1-17	100.0	54.6	54.6	0.001033* 0.2	11
Cu-100-1-18	100.0	54.7	54.7	0.001033* 0.2	27
Cu-100-1-19	100.0	54.7	54.7	0.001033* 0.2	12
Cu-100-1-20	100.0	54.6	54.5	0.001033* 0.2	13

Table E-1
Continued

Sample ID	Temperature °C	Inlet pressure bar	Outlet pressure bar	NaOH, m Flow rate mL· min^{-1}	Cu (GFAA) ppb
Cu-100-1-21	100.0	54.5	54.5	0.001033* 0.1	9
Cu-100-1-22	100.0	54.3	54.3	0.001033* 0.1	9
Cu-100-1-23	100.0	54.6	54.7	0.001033* 0.1	~~29~~
Cu-100-1-24	100.0	54.7	54.7	0.001033* 0.1	9
Cu-100-1-25	100.0	54.6	54.6	0.001033* 0.1	11
Cu-100-1-26	100.0	54.6	54.6	0.001033* 0.1	14
Cu-100-1-27	100.0	54.7	54.7	0.000999* 0.1	21
Cu-100-1-28	100.0	54.7	54.7	0.000999* 0.1	7
Cu-100-1-29	100.0	54.7	54.6	0.000999* 0.1	8
Cu-100-1-30	100.1	54.4	54.4	0.000999* 0.1	7
Cu-100-1-31	100.0	54.7	54.7	0.000999* 0.2	10
Cu-100-1-32	100.0	54.4	54.5	0.000999* 0.1	19
Cu-100-1-33	100.0	54.5	54.5	0.001143* 0.1	2
Cu-100-1-34	100.0	54.2	54.2	0.001143* 0.1	1
Cu-100-1-35	100.0	54.7	54.7	0.001143* 0.1	1
Cu-100-1-36	100.0	54.1	54.1	0.001143* 0.1	5
Cu-100-1-42	100.0	54.4	54.4	0.001143* 0.1	18
Cu-100-1-43	100.0	54.6	54.6	0.001143* 0.1	18
Cu-100-1-44	100.0	54.4	54.4	0.001143* 0.1	17
Cu-100-1-45	100.0	54.4	54.4	0.001143* 0.1	23

Table E-1
Continued

Sample ID	Temperature °C	Inlet pressure bar	Outlet pressure bar	NaOH, m Flow rate mL· min^{-1}	Cu (GFAA) ppb
Cu-100-1-46	100.1	54.1	54.1	0.001016[§] 0.1	15
Cu-100-1-47	100.1	53.8	53.8	0.001016[§] 0.1	16
Cu-100-1-48	100.0	53.7	53.6	0.001016[§] 0.1	16
Cu-100-1-49	100.1	54.5	54.5	0.001016[§] 0.1	18
Cu-100-1-50	100.1	54.8	54.8	0.001016[§] 0.1	16
Cu-100-1-51	100.1	54.4	54.3	0.001016[§] 0.1	17
Cu-100-1-52	100.1	54.8	54.7	0.001016[§] 0.1	17
Cu-100-1-53	100.1	54.8	54.8	0.001016[§] 0.1	22
Cu-100-1-54	100.1	54.6	54.5	0.001016[§] 0.1	17
Cu-100-1-55	100.0	54.9	54.8	0.001016[§] 0.1	17
Cu-100-1-56	100.1	54.9	54.8	0.001016[§] 0.1	18
Cu-100-1-57	100.1	54.6	54.6	0.001016[§] 0.1	18
Cu-100-1-58	100.0	54.5	54.5	0.001016[§] 0.1	17
Cu-100-1-59	100.0	54.6	54.5	0.001016[§] 0.1	16

* Feed solution was pre-saturated and pressurized with 5 psi CO_2-free air

[§] Feed solution was pre-saturated and pressurized with 5 psi gas mixture (4990 ppm H_2 in Ar)